

Titre: Chaos Theory Applied to Analyze Tool Wear During Machining of
Title: Titanium Metal Matrix Composite (TiMMCs)

Auteur: Xuan Truong Duong
Author:

Date: 2015

Type: Mémoire ou thèse / Dissertation or Thesis

Référence: Duong, X. T. (2015). Chaos Theory Applied to Analyze Tool Wear During Machining
Citation: of Titanium Metal Matrix Composite (TiMMCs) [Ph.D. thesis, École Polytechnique
de Montréal]. PolyPublie. <https://publications.polymtl.ca/1758/>

 **Document en libre accès dans PolyPublie**
Open Access document in PolyPublie

URL de PolyPublie: <https://publications.polymtl.ca/1758/>
PolyPublie URL:

**Directeurs de
recherche:** Marek Balazinski, & J. R. René Mayer
Advisors:

Programme: Génie mécanique
Program:

UNIVERSITÉ DE MONTRÉAL

CHAOS THEORY APPLIED TO ANALYZE TOOL WEAR DURING MACHINING
OF TITANIUM METAL MATRIX COMPOSITE (TiMMC_s)

XUAN TRUONG DUONG

DÉPARTEMENT DE GÉNIE MÉCANIQUE
ÉCOLE POLYTECHNIQUE DE MONTRÉAL

THÈSE PRÉSENTÉE EN VUE DE L'OBTENTION
DU DIPLÔME DE PHILOSOPHIAE DOCTOR
(GÉNIE MÉCANIQUE)

JUIN 2015

UNIVERSITÉ DE MONTRÉAL

ÉCOLE POLYTECHNIQUE DE MONTRÉAL

Cette thèse intitulée :

CHAOS THEORY APPLIED TO ANALYZE TOOL WEAR DURING MACHINING
OF TITANIUM METAL MATRIX COMPOSITE (TiMMCs)

présenté par : DUONG Xuan Truong

en vue de l'obtention du diplôme de : Philosophiae Doctor

a été dûment acceptée par le jury d'examen constitué de :

M. LAKIS Aouni A., Ph.D., président

M. BALAZINSKI Marek, Docteur ès sciences, membre et directeur de recherche

M. MAYER René, Ph.D., membre et codirecteur de recherche

M. VADEAN Aurelian, Doct., membre

M. KOSHY Philip, Ph.D., membre externe

DEDICATION

This PhD dissertation is dedicated to my family friends and my colleagues. I would like to express my deep gratitude to my parents, Duong Thanh Quang and Duong Thi Loc whose words of encouragement give me tenacity for working harder; my wife Le Thi Thu Hien and my son Duong Binh Minh have never left my side, for your love and are very special. I also dedicate this dissertation to my brother Duong Van Doanh, my sisters Duong Thi Oanh and Duong Van Anh, to many friends as well as to my colleagues; all they have done is appreciated.

Luận án Tiến sĩ này là để dành tặng cho gia đình, các bạn thân và đồng nghiệp. Con cảm ơn Bố Mẹ, anh Doanh, Vợ Hiền, con trai Bình Minh, chị Oanh và chị Vân Anh. Tình yêu thương, sự giúp đỡ và luôn động viên chia sẻ của cả gia đình đã giúp con hoàn thành luận án này.

ACKNOWLEDGEMENTS

During the course of my PhD study at Polytechnique Montreal, Canada I received support and help from several people, research institutes, companies, my family and friends.

I would like to thank my advisors Prof. B.Eng., M.Sc., Ph.D. Marek Balazinski and my co-advisor Prof., B.Eng., Ph.D. Rene Mayer for their guidance and support throughout my studies, as well as for their encouragement. I truly believe that the main reason my Ph.D. studies have been more successful and make so many contribute to the science than I ever hoped for is the fact that I was able to learn so much from them. I would also like to thank for the assistance from Polytechnique Montreal, in particular, the Virtual Manufacturing Research Laboratory (LRFV) for their support; I especially want to thank Mr. Guy Gironne, Mr. Vincent Mayer and Mr Francois Menard for all my experimentations and collect the data analysis. Mrs. Carole Fraser, Mrs. Martine B  nard, Mrs. Jos  e Dugas and Mrs. Rachel Godin I really appreciate all the help you gave me. I am glad to have met all of you and so lucky to work with you in Polytechnique.

I would like to express deep gratitude to my family and my friends for their support, love, believe and always beside me; especially my parents, who have been bringing me up in the greatest love and care as well as get me back since I did something wrong at high school; I deeply appreciate your support and teaching me the values of education. My appreciation goes to my wife and my son, Le Thi Thu Hien and Duong Binh Minh; whose have supported me and equally shared my success as well as failures with me through the years. Their loves gave me more motivation for study harder during my school years.

I would like to acknowledge to LISI Aerospace Canada, Finncraft Design Inc for their supports and give me a great opportunities working as an internship. So I had a good chance to apply my knowledge to the industrial manufacturing and validate the obtained results from my studies here. Special acknowledgements go to my colleagues at Thai Nguyen University of Technology; I would like to thank them so much for the supports, time and energy they expended on me, during my research studies performed abroad.

Finally, I would like to gratefully acknowledge the financial supported from Government of Vietnam - Ministry of Education and Training (scholarship scheme - Project 322); the Natural Sciences and Engineering Research Council of Canada (NSERC) and Canadian Network for Research & Innovation in Machining Technology (CANRIMT).

RÉSUMÉ

Ma thèse de doctorat a porté sur le développement d'une nouvelle méthode pour étudier l'usure de l'outil et de la vie de l'outil lors de l'usinage d'un composite à matrice métallique de titane (TiMMCs). Ce nouveau matériau offre de nombreux autres avantages par rapport aux alliages de titane conventionnels et les matériaux composites à matrice métallique. Grâce à haute résistance, rigidité au fluage à des températures élevées, TiMMCs est considéré comme un matériau de choix pour des applications dans l'aérospatiale et de l'automobile dans un avenir proche. Toutefois, la combinaison de toutes ces caractéristiques d'usinage d'alliages de titane et des matériaux composites à matrice métallique rend les TiMMCs extrêmement difficile à usiner tandis que leur usinabilité n'est pas complètement comprise dans la littérature.

Dans des diverses études sur l'usure de l'outil trois régions différentes de l'usure des outils ont été distingués en fonction de l'augmentation de l'outil usure rapport au temps de coupe. Ils sont successivement l'usure initiale, l'usure régulière et la période d'usure accélérée. Cependant, le phénomène d'usure initiale de l'outil et ainsi que son impact sur la vie de l'outil pendant le processus d'usinage n'est pas clairement compris. Ce fait peut être expliqué en notant que la plupart de ces études ont été focalisées sur la période de l'usure régulière qui semble intuitivement être une bonne méthode pour estimer la vie de l'outil.

Par conséquence, dans le but de mieux comprendre le phénomène de l'usure de l'outil initiale et ses influences sur la vie de l'outil, le comportement initial de l'usure de l'outil pendant l'usinage de TiMMCs a été considéré dans le cadre de ma thèse. Les résultats obtenus nous ont montré que l'usure se produit dès le premier instant de l'usinage. Cette usure spéciale se prolonge jusqu'à seulement dix secondes au maximum. Tel usure initiale est le résultat de plusieurs procédés compliqués tels que les dommages de la couche du revêtement, la friction – tribologique, la diffusion et l'adhérence. La basse conductivité thermique et une grande réactivité des alliages de titane conduisent à la déformation plastique et à la formation d'un built-up-edge (BUE) à des températures élevées dans toutes les conditions expérimentales effectuées dans la première (ou initiale) zone d'usure. Ce mécanisme d'usure est en effet opposé à celui de l'abrasion de la période de l'usure régulière.

Il est également important de montrer que les analyses du mécanisme d'usure lors de la première période sur l'usure de transition nous amènent à une nouvelle forme d'usure. L'effet de

contraintes chimiques sous la force de coupe accélérée et des températures élevées était la raison principale de l'usure de diffusion. Les sous-produits de ce procédé peuvent spontanément réagir avec l'oxygène atmosphérique pour former les matériaux à base de titane et d'aluminium oxydés qui, par la suite, se diffusent à partir de la couche de revêtement et les TiMMCs sous l'influence de haute pression et température élevée. Ces mécanismes en association avec la couche de revêtement (Ti,Al) N de l'outil de coupe et la présence du matériau de renforcement (TiC) de la pièce à couper ont généré une nouvelle couche mince dans son ensemble impliquant dans le processus d'usinage. Cette nouvelle couche d'usure qui a souvent été appelé le “wear shield” se trouve notamment sur la face de dépouille à la première période de l'usure de transition. Cette formulation de la couche d'usure de bouclier nous permet une meilleure explication pourquoi les taux d'usure augmente très rapidement lors de l'usure initiale, puis diminue brusquement au point de transition à la période de l'usure stationnaire; et aussi nous permet d'interpréter de manière significative comment l'usure d'outil initiale et de conditions de coupe initiales affectent l'évolution de l'usure des outils et ainsi que toute la vie de l'outil.

Un autre point important à souligner est que la théorie du chaos est appliquée pour la première fois au à notre connaissance afin d'étudier l'effet des conditions initiales de l'usure de l'outil. L'efficacité de cette théorie mathématique a été prouvée pour décrire comment quelque chose change avec le temps en fonction de la dépendance sensible aux conditions initiales. Plus important encore, des études scientifiques ont prouvé que la théorie du chaos s'applique aux systèmes dynamiques les plus simples, démontrant que le chaos est la règle. Cette nouvelle philosophie pourrait changer considérablement les méthodes de recherche en théorie d'usinage. Les analyses de la dynamique d'usinage et de l'usure des outils d'un point de vue de la théorie du chaos peuvent donc se révéler très intéressante. Cela implique une analyse approfondie des paramètres initiaux des processus d'usinage. Nous avons donc concentré la recherche sur ces caractéristiques de chaos pour démontrer la dépendance de la vie de l'outil des conditions de coupe initiales. En fait, presque toutes les applications de chaos ont concerné un système dynamique non-linéaire tandis que son application n'a jamais été rapportée dans des études sur l'usure de l'outil. Par conséquent, un nouveau concept, l'usure chaotique de l'outil, doit être numériquement envisagé pour étudier les influences des conditions de coupe initiales sur la vie de l'outil. Dans notre cas, l'évolution des courbes d'usure au cours du processus d'usinage qui

vont démontrer utilisés pour calculer les exposants de Lyapunov requise une caractérisation par une fonction continue.

Deux nouveaux modèles mathématiques sont donc proposés dans ce travail. Premièrement, un nouveau modèle mathématique dit «chaotic tool wear» a été développé pour quantifier correctement une usure chaotique de l'outil pendant un processus d'usinage. Ce modèle est basé sur l'exposant de Lyapunov et de la dimension fractale. Afin de résoudre les phénomènes d'usure chaotiques, un autre modèle mathématique pour caractériser la variation de la courbe d'usure sous différents paramètres initiaux est également développé. En particulier, les méthodes de B-splines cubique de collocation et de plusieurs étapes sont utilisées pour résoudre une équation différentielle ordinaire d'un modèle chaotique de l'usure de l'outil.

Notre nouveau modèle usure chaotique d'outil fournit, pour la première fois, une explication entière du comportement du taux de l'usure à la période d'usure initiale et apporte plus de perceptibilité concernant la dépendance significative de la vie de l'outil sur les conditions de coupe initiales. En outre, l'application de tel modèle chaotique d'usure de l'outil pour varier les conditions initiales de coupe lors de l'usinage TiMMCs nous permet une amélioration de la vie de l'outil jusqu'à 24,5%.

ABSTRACT

This research work focused on developing a new method to investigate the tool wear and tool life during machining of titanium metal matrix composite (TiMMCs). That novel generation material offers many other advantages compared to titanium alloys and metal matrix composites. Due to high strength, high stiffness, and creep resistance at high temperatures, TiMMCs is considered as a material of choice for applications in aerospace and automotive industries in the near future. However, the combination of all the hard machining characteristics of titanium alloys and metal matrix composites makes the TiMMCs an extremely difficult to cut material while their machinability is still not fully understood in the open literature.

In various studies on tool wear and tool life, three distinctive regions of tool wear have widely been classified according to the increase of tool wear versus cutting time. They are the initial wear, steady wear and accelerated wear periods. However, the initial tool wear phenomenon and its influence on the tool life are not yet clearly understood. This fact can be explained by noting that most of these studies have been performed within the steady wear period which intuitively seems to be the right method to handle tool life problem.

Accordingly, with the aim of contributing to a better understanding of the initial tool wear phenomenon as well as how it affects to the tool life, an investigation on initial tool wear behavior during machining of TiMMCs has been conducted in this thesis. The results have shown that the initial wear occurs at the first instant and extends to only ten seconds at the most; it is a result of complicated mechanisms such as coating layer damage, friction - tribological wear diffusion and adhesion. The low thermal conductivity and high reactivity of titanium alloys lead to plastic deformation and forming of a built-up-edge (BUE) at elevated temperatures under all experimental cutting conditions in the first or initial, wear zone. This wear mechanism is indeed opposite to the wear mechanism of abrasion found in the steady wear period.

More importantly, by analyzing the wear mechanism at the first transition wear period we report herein a new wear form. The effect of chemical stresses under high cutting force and high temperatures was the main reason for the resulting diffusion wear; the by-products of that cutting process can spontaneously react with atmospheric oxygen. These oxidized titanium and aluminum based materials then diffuse from the coating layer and the TiMMCs at high pressure and elevated temperature. All together, these mechanisms in association with the coating layer

(Ti,Al)N of the cutting tool and TiC reinforcement of the workpiece material generated a new hard thin layer involved in the machining process. This new wear layer which authors have coined “wear shield” is mostly found on the flank face at the first transition wear period. The formulation of the wear shield layer allows a better explanation why the wear rate increases very fast during initial wear and then decreases abruptly at the transition point to the steady wear period on one hand; and interpreting how significantly the initial tool wear and initial cutting conditions affect the tool wear evolution and the entire tool life on the other.

In this work, chaos theory is applied, for the first time to the best of our knowledge, to investigate the effect of initial conditions on the tool wear. The mathematic of chaos theory has been proved efficient in describing how something changes in time based on its sensitive dependence on initial conditions. More importantly, it is reported that chaos theory can apply to a simple dynamical system. This new philosophy can notably change the methodologies for the studies of machining technology. Analyzing dynamical cutting and tool wear during machining process based on the chaos theory is thus of interest. This implies a thorough analysis of the initial parameters of the machining process. We therefore considered these characteristics of chaos to demonstrate the dependence of the tool life on the initial cutting conditions. In fact, almost all applications of chaos have concerned a nonlinear dynamical system while its application in the tool wear investigation has not been reported in the literature so far. Hence to investigate how sensitively the tool life is affected by the initial cutting conditions the chaotic tool wear should be quantified numerically. In this case, the wear curves evolution during the machining processes that are being used to calculate Lyapunov exponents need to be modeled by a continuous function.

Accordingly, two new mathematical models are proposed in this thesis. First, a new mathematical model so called “chaotic tool wear” is proposed to quantify a chaotic tool wear during machining based on the Lyapunov exponent and fractal dimension. In order to solve the chaotic wear phenomena, another mathematical model is developed to characterize the variation in wear curves under different initial parameters. In the present work, the multistep method and cubic B-splines collocation methods are used to solve an ordinary differential equation of a chaotic tool wear model.

As a result, a new concept of tool wear, “chaotic tool wear”, is proposed in the study of tool wear. The chaotic tool wear model provides for the first time with a full explanation of the wear rate behavior at the first initial wear period and brings more insight on how the tool life depends significantly on the initial cutting conditions. More importantly, application of the chaotic tool wear model to change initial cutting conditions when machining TiMMCs improved the tool life by up to 24.5%.

TABLE OF CONTENTS

DEDICATION	iii
ACKNOWLEDGEMENTS	iv
RÉSUMÉ.....	v
ABSTRACT	viii
TABLE OF CONTENTS	xi
LIST OF TABLES	xiv
LIST OF FIGURES	xv
LIST OF SYMBOLS AND ABBREVIATIONS.....	xviii
CHAPTER 1 INTRODUCTION	1
1.1 Motivation.....	1
1.2 Research objectives	3
1.3 Hypothesis statements.....	4
1.4 Research approach	4
1.5 Outline of the dissertation	5
CHAPTER 2 LITERATURE REVIEW	7
2.1 Machinability of titanium metal matrix composites (TiMMCs).....	7
2.2 Initial wear phenomenon.....	8
2.3 Overview of the chaos theory	9
2.4 Fractal dimension	15
CHAPTER 3 ARTICLE 1: INITIAL TOOL WEAR BEHAVIOR DURING MACHINING OF TITANIUM METAL MATRIX COMPOSITE (TiMMCs)	24
3.1 Introduction.....	24
3.2 Experimental procedure	27

3.3 Results and Discussion.....	28
3.3.1 Initial wear determination.....	28
3.3.2 Initial wear mechanism.....	30
3.3.3 Initial tool wear at the transition period.....	34
3.4 Conclusions	37
CHAPTER 4 ARTICLE 2: CHAOTIC TOOL WEAR DURING MACHINING OF TITANIUM METAL MATRIX COMPOSITE (TiMMCs)	39
4.1 Introduction.....	39
4.2 Modelling of Chaotic tool wear	41
4.2.1 Quantitative measures of Chaotic tool wear.....	41
4.2.2 Chaotic tool wear modeling.....	44
4.3 Experimentation	46
4.4 Results and discussion	47
4.4.1 Initial tool wear during machining process	47
4.4.2 Chaotic tool wear during machining of TiMMCs	50
4.5 Conclusions	54
CHAPTER 5 ARTICLE 3: A NEW CONCEPT FOR TOOL WEAR DURING MACHINING PROCESS BASED ON CHARACTERISTICS OF CHAOS THEORY	55
5.1 Introduction.....	56
5.2 Chaotic tool wear modelling	58
5.2.1 Chaotic wear curve definition.....	59
5.2.2 Sensitive dependence on initial conditions.....	66
5.2.3 Fractal dimension analysis.....	69
5.3 Experimental procedure	71
5.4 Results and discussion	73

5.4.1	Tool wear evolution during machining of TiMMCs	73
5.4.2	Effect of initial condition on the tool life	77
5.4.3	Chaotic tool wear phenomenon during machining process.....	80
5.5	Conclusions.....	84
CHAPTER 6 GENERAL DISSCUSSION AND CONCLUSIONS		86
6.1	Summary of Research Accomplishments	86
6.1.1.	Conclusions on initial tool wear behavior during machining TiMMCs	86
6.1.2.	Conclusions on chaotic tool wear during a machining process.....	87
6.2	Originality of the work and contribution to knowledge.....	88
REFERENCES.....		91
APPENDIX		103

LIST OF TABLES

Table 2-1: The length of a coastline [73]	19
Table 3-1: Chemical composition of the TiMMCs	31
Table 4-1: Physical properties of TiMMCs [15]	47
Table 4-2: Experiment for the different initial condition strategies	51
Table 4-3: Scatter wear dimension during machining of TiMMCs	52
Table 5-1: Different initial cutting parameters for experiments	77
Table 5-2: B-spline polynomials of chaotic wear curve when machining TiMMCs	78
Table 5-3: Lyapunov exponents λ_i and fractal dimension (D_i)	82

LIST OF FIGURES

Figure 2-1: Three wear period of the tool wear vs. cutting time.....	8
Figure 2-2: Lorenz attractor generated from Eq. (2-1); (a) 2D animated, (b) 3D animated, (c) evolution in the space time; (sourced from: http://www.mathworks.com)	11
Figure 2-3: Two trajectories evolution in a phase space [44]	12
Figure 2-4: Bifurcation diagram and Lyapunov exponent [44]	13
Figure 2-5: Cantor set fractal dimensions [71].....	16
Figure 2-6: Koch curve generation of fractal dimension, expressed from [71]	16
Figure 2-7: Sierpinski triangle generation of fractal dimension, expressed from [71]	17
Figure 2-8: Fractal Box-dimensional [44].....	18
Figure 2-9: Three different size grids for Great Britain [71]	19
Figure 2-10: Fractal calculation of profiles [76]	20
Figure 2-11: Fractal calculation of surfaces [76]	20
Figure 2-12: 3-D Fractal surface generated from Eq.3.20 [81].....	22
Figure 2-13: 2D profile of a truncated rough (fractal) surface [82]	22
Figure 3-1: Tool wear curves evolution versus cutting time.....	26
Figure 3-2: Experimental set-up.....	27
Figure 3-3: Tool wears during machining TiMMCs under different cutting speeds	29
Figure 3-4: The initial wear period during machining of TiMMCs	30
Figure 3-5: TiC particles in the machined surface of TiMMC and EDX analysis.....	31
Figure 3-6: Initial tool wear mechanism at the first moment cutting (0.05 sec); (a) $V=20$ m/min; (b) $V=40$ m/min; (c) $V=60$ m/min, (d & e) EDX analysis	32
Figure 3-7: The BUE occurs within initial wear period when machining TiMMCs; (a) $V=20$ m/min-1.0sec; (b) $V=40$ m/min-1.5sec; (c) $V=50$ m/min-2.0sec; (d) $V=60$ m/min-5.0sec	33

Figure 3-8: Tool wear mechanism close to the location of the transition point; (a) $V=20\text{m/min}$; (b) $V=60\text{m/min}$; (c and d) EDX analysis	35
Figure 3-9: Brace wear at the location of transition wear period; (a) $V=20\text{m/min}$; (b) $V=40\text{m/min}$; (c) $V=50\text{m/min}$; (d) EDX analysis	36
Figure 4-1: Dimensional projections of Lorenz attractor [42]	42
Figure 4-2: Two trajectories evolution in a phase space	44
Figure 4-3: Chaotic tool wear modeling	46
Figure 4-4: Initial tool wear mechanism on the clearance face during machining of TiMMCs	49
Figure 4-5: Cutting tool life for different initial conditions	51
Figure 4-6: Scatter wear dimension; (a) after 20s, (b) - 30s, (c) - 60s and (d) after 90s	53
Figure 5-1: Chaotic tool wear modeling [93]	58
Figure 5-2: Scatter wear dimension and chaotic wear curve definition	62
Figure 5-3: Sensitive dependency on initial conditions of two wear curve trajectories	68
Figure 5-4: Fractal dimension analysis of a chaotic wear curve	70
Figure 5-5: Chaos theory characterized tool wear during machining process	71
Figure 5-6: Experimental set-up	72
Figure 5-7: Tool wear during machining TiMMCs under different cutting speeds [110]	73
Figure 5-8: Cubic B-spline functions describe tool wear curves	75
Figure 5-9: Initial tool wear during machining TiMMCs; (a) $V=20\text{m/min}$ after 2s; (b) $V=40\text{m/min}$ after 5s; (c) $V=50\text{m/min}$ after 6s; (d) EDX analysis [110]	76
Figure 5-10: Chaotic wear curves in three initial condition strategies	80
Figure 5-11: Scatter wear dimensions under different initial cutting conditions;	81
Figure 5-12: Relationship between λ and D and cutting time	83
Figure 5-13: Relationship between λ and D and tool wear; (No.1 - Initial speed)	83
Figure 5-14: Relationship between λ and D and tool wear; (No.2 – Initial feed rate)	83

Figure 5-15: Relationship between λ and D and tool wear; (No.3 – Initial depth of cut).....83

LIST OF SYMBOLS AND ABBREVIATIONS

TiMMCs	Titanium metal matrix composites
MMCs	Metal matrix composites
TiC	Titanium carbide
SiC	Silicon carbide
TiB	Titanium boride
HRC	Rockwell hardness of material
CNC	Computer-Aided Manufacturing
SEM	Scanning Electron Microscope
EDX	Energy Dispersive X-ray
PCD	Polycrystalline Diamond
CBN	Cubic Boron Nitride
PVD	Physical Vapor Deposition
BUE	Built-Up-Edge
λ	Lyapunov exponent
∂_{VB_0}	Initial conditions
∂_{VB_k}	Scatter wear dimension at cutting time t_k
D	Fractal dimension
D_s	Fractal dimension determined by scatter wear function
T_c	Tool life
B-spline	Basic spline
NURBS	Non-Uniform Rational Basis Spline
η	Mesh-size for determine a wear curve

Δ	Empirical coefficient
RSM	Response Surface Methodology
CCD	Central Composite Design
ANOVA	Statistical Analysis of Variables
γ_0	rake angl
γ_p	back rake angle
r_ϵ	nose radius
ϵ_r	tool included angle
κ_r	tool cutting angle
μ	coefficient factors
$F_C(N)$	cutting force
$F_R(N)$	thrust force
$F_F(N)$	feed force
V_W	Tool wear volume removed
h_0 and h_x	Limitation values of the integral equations

CHAPTER 1 INTRODUCTION

This chapter presents the research plan for this study. First discussion will deal with the state-of-the-art of chaos theory, initial wear phenomenon and the problem of machining titanium metal matrix composites (TiMMCs). The research questions and motivation for the research project are revealed. In order to bring out the problem statements our research objectives, hypothesis statements and research approach are then discussed. Finally outlines of the remaining contents are provided.

1.1 Motivation

Chaos theory is a field of study in mathematics that primarily refers to the behavior of nonlinear dynamical systems. Chaos is considered as an aperiodic long-term behavior in a deterministic system and exhibits sensitive dependence on initial conditions [1]. Therefore, it has been widely used to explain how something changes over time and predicting the behavioral change in a system based on the initial conditions. The prediction based on the characteristics of chaos was recently applied not only to the short term but also the long-term behavior of numerous technical systems [2]; eventually chaos can be used to predict something deemed unpredictable [3]. More importantly, the work of X. Buff and A. Cheritat [4] have demonstrated that chaos theory can be applied to a simple dynamical systems, as well as such the chaos is the rule. This new philosophy can change dramatically on the theoretical research method of machining. Analyses of tool wear and tool life during a machining process based on the chaos theory, therefore, being interested. This involves a thorough analysis of the initial cutting parameters during machining process.

Notwithstanding the efficiency of chaos in the many different fields mentioned above, in the literature no research study is related to the application of chaos to investigate tool wear during a machining process. Additionally, the effect of initial conditions and initial tool wear mechanism on the tool life has not been clearly expressed in all the studies of tool wear. During a machining process, the tool life is determined based on a wear curve evolution over time; this curve normally consists of three distinctive regions [5] according to the increase of tool wear versus cutting time: the initial wear or running-in period, steady wear stage and accelerated wear period. However, most researchers in the field have studied the steady wear period [6-8] which

intuitively seems to be the right method to handle tool life problem. Therefore, the tool wear mechanisms at the first instant of machining and its evolution within the first, or initial wear, period are not clearly understood. It is reported that, the initial wear or break-in period plays a very important role in the working life of a vehicle engine [9-11]. In this case, the initial wear period or running-in period occurs rapidly with extremely high wear rate; its wear behavior determines performance capability of the system [12] and therefore control of the running-in process within the first or initial wear zone can extend the working life of engineering tribosystems [11, 13, 14].

Indeed, the nature of the tool wear mechanism in the case of machining differ from the wear in cylinder-engine systems discussed above; but their initial wear behavior in regards to the initial conditions could be related. Therefore, studying the initial tool wear and the effect of the initial conditions on the tool life during a machining process is of interest.

Studying the tool wear during a machining process is even more crucial with respect to the new materials such as titanium metal matrix composites (TiMMCs) in the present work. The latter is considered as a new generation material owning many advantages compared to the conventional titanium alloys and metal matrix composites. Therefore, the TiMMCs are increasingly attractive for a wide range of applications in the aerospace and automotive industries [15, 16]; however, due to the combination of all the machining problems of the titanium alloys and metal matrix composites the TiMMCs is a very difficult to cut material causing relatively very short tool life while the studies their machinability is still very limited in the open literature [15, 17].

All the facts mentioned above leave open fundamental questions which require further investigation:

1. The first question deals with the initial tool wear behavior, such as what exactly the initial tool wear phenomenon during machining TiMMCs is? What is the mechanism of wear at the first moment of cutting as well as when does it occur, how long does it take and why its wear rate increases so fast within the first wear period and then decreases abruptly to the steady period?

2. The second question is as follows: what is relationship between the initial conditions or initial tool wear behavior and the tool life? In the case study, we focus on investigating how much the tool life changes with the different initial conditions.
3. The final question is devoted finding a chaotic signal in the relatively simple system of the tool wear during machining.

We thus focus our attention on the initial tool wear behavior and the effect of initial cutting conditions on the tool life during machining of TiMMCs. Part of the work is to develop a novel methodology on the basis of chaos theory to demonstrate the relationship between the initial conditions and tool life.

1.2 Research objectives

In order to express the research questions this dissertation concentrates on 2 main objectives. The first objective is to study the initial tool wear mechanism during machining TiMMCs material, and in particular, the effect of cutting parameters on the wear mechanism within the first wear period is analyzed. The second objective is to investigate how the initial cutting conditions as well as initial wear mechanism influence the tool life. In this case, characteristics of chaos are being used to demonstrate the significant dependence of the tool life on the initial cutting parameters. That second objective consists of two parts: first, a wear curve evolution in time that is used to model a chaotic wear function and model by a continuous equation; hence a new mathematical model to characterize the variation in wear curves under different initial parameters is developed. The second part is linked to a development of a new mathematical model to quantify a chaotic tool wear based on the Lyapunov exponent. To achieve the research goals, here are the specific objectives:

1. Investigate experimentally initial tool wear and its evolution over time during machining TiMMCs. The analysis of tool wear mechanism is specially taken into consideration at the first moment of cutting and at the first wear transition moment;
2. Study the effect of cutting parameters on the initial wear mechanism to find the most significant factor towards the initial tool wear;

3. Study the influence of initial cutting conditions on the tool life when machining TiMMCs; this is aimed at exhibiting the chaotic signal in accordance with the positive values of the Lyapunov exponent within the tool wear system.
4. Develop a new mathematical model to quantify a chaotic behavior in the tool wear system based on Lyapunov exponent and fractal dimension. Calculation and quantification of a chaotic signal in the wear system require developing a new mathematical equation to characterize a wear curve evolution over time under different initial conditions. If the sensitive dependence of the tool life on the initial conditions is exhibited within the proposed model, a new concept of tool wear, a “chaotic tool wear” would then be discussed.

1.3 Hypothesis statements

1. It is reported that the abrasion is the dominant wear mechanism in almost all investigated cutting conditions when machining MMCs and TiMMCs. We expect that the initial tool wear mechanism at the first moment of cutting differs to the wear mechanism at the steady wear region.
2. Chaos theory has never been applied to the case of tool wear. It is expected that initial cutting parameters influence significantly the tool life during a machining process. In this case a chaotic motion can be found within a simple tool wear system.
3. Controlling the initial cutting conditions would improve the tool life during machining process.

1.4 Research approach

The first step in accomplishing the objectives of this work is to investigate experimentally the initial tool wear during machining of TiMMCs. The experimental design is taken into consideration to find which cutting tool and cutting condition as well as what experimental model would fit the special case in this thesis. We focus this work attention on the tool wear mechanism at the first moment cutting and wear behavior at the first transition, between the initial and steady wear by a scanning electron microscope (SEM) and an energy dispersive X-ray (EDX). The first experimental work is conducted under different cutting speeds with the purpose of studying tool

wear evolution in time and tool life when machining the TiMMCs. In order to investigate the impact of cutting parameters on the initial wear mechanism the second experiment stage is performed using the response surface methodology (RSM) in accordance with central composite design (CCD).

In order to investigate how significant is the tool life affected by the initial cutting conditions the characteristics of chaos theory was used to bring out an existence of a relationship between the tool life and the initial cutting conditions. First, we focus on developing a new mathematical model to characterize a wear curve's evolution over time under different cutting conditions. This curve is then used to calculate the scatter wear dimension and the Lyapunov exponents to find any sensitive dependence of the tool life on the initial conditions. A new mathematical model so called "chaotic tool wear" was therefore proposed in the second phase based on the Lyapunov exponent in accordance with the ordinary differential equation to quantify both empirically and numerically the chaotic tool wear behavior during a machining process. The multistep and Cubic B-splines collocation methods were used to solve the ordinary differential equation of chaotic tool wear. In addition, the variations in tool wear curves under different initial cutting parameters are quantified by a fractal dimension. The chaotic tool wear model was then applied to change initial cutting conditions during machining of TiMMCs. The obtained results are discussed in detail and validated on the basis of the Chaos theory.

1.5 Outline of the dissertation

- Chapter 2 provides knowledge background of the chaos theory and fractal geometry. It also contains a literature review related to the machinability of the titanium metal matrix composites and the initial wear problems.
- Chapter 3 deals with the initial tool wear behavior during machining of TiMMCs. This work focus on the study of initial tool wears mechanism at the first moment of cutting and at the transition between the first initial and second steady wear zones. The effect of cutting parameters on the initial wear mechanism will be discussed.
- Chapter 4 presents an experimental study of chaotic phenomenon in a tool wear system. A chaotic tool wear model based on the scatter wear dimension during a machining process is proposed in this section.

- In chapter 5 we propose a new method to investigate tool wear during a machining process based on chaos theory. A new mathematical model to characterize tool wear curve evolution in time is first developed by using multistep and Cubic B-splines collocation methods. A novel mathematical model to quantify a chaotic tool wear behavior is proposed based on Lyapunov exponent and fractal dimension. Accordingly, a new concept of tool wear so called “chaotic tool wear” is then discussed.
- Chapter 6 is a general conclusion and recommendations for future work.

CHAPTER 2 LITERATURE REVIEW

2.1 Machinability of titanium metal matrix composites (TiMMCs)

Titanium metal matrix composites (TiMMCs) have appeared as a new generation material. They are generally distinguished by the characteristics of the reinforcement, such as particles of titanium carbide (TiC) and titanium boride (TiB) [18-21], whiskers and continuous or discontinuous fibers of silicon carbide (SiC) [16, 22, 23]. Among them, reinforcing with the hardest refractory metal carbides such the TiC particles provides superior properties at elevated temperature and exceptional wear resistance [18, 21, 24]. Thanks to their high strength, stiffness, and creep resistance at high temperatures the TiMMCs has been tackled by different research groups for applications in areas such as aerospace and automotive industries [15, 16, 18]. However, the combination of machining problems associated with metal matrix composites (MMCs) and titanium alloys into the (TiMMCs) renders the machining of this material a real challenge in the field [15, 17].

The difficult machining characteristics of titanium alloys are high reactivity, low thermal conductivity, relatively low modulus, and maintaining their high strength and hardness at elevated temperatures [25, 26]. The low thermal conductivity of titanium leads to a significant increase in cutting temperature at the tool-workpiece interface during machining. As a result, the cutting tool material tends to react chemically with titanium at high temperature and causes adhesion of the workpiece material to the cutting edge [7]. Consequently, the adhesive wear through plastic deformation and welding rapidly develops [27, 28]. In addition, the high tensile strength in combination with the low Young's modulus of titanium alloys cause high temperature and high mechanical stresses at the cutting edge which lead to a particularly fast tool wear [29].

Furthermore, metal matrix composites (MMCs) are also considered as a difficult to cut material due to the abrasive properties of hard particle reinforcement [21, 30, 31]. The MMCs reinforced with ceramic particulates provide a number of advantages compared to their base metals such as higher specific strengths and moduli, higher wear resistance at elevated temperature and lower coefficients of thermal expansion [32]. As a result, machining of MMCs lead to poor tool life and inconsistent machined surface quality [33]. Hence, abrasion is found to be the dominant wear mechanism in almost all investigated cutting conditions [17, 34, 35]. The

abrasive wear is accelerated and depends on the percentage of reinforcement in the MMCs due to the interference between the reinforcement particles [36].

2.2 Initial wear phenomenon

Cutting tool life depends on the combined effect of several factors occurring during the machining process; where the tool wear evolution over time is the result of complicated physical, chemical, and thermo-mechanical phenomena forming through the different mechanisms such as adhesion, abrasion, diffusion, and oxidation [37]. In general, the tool life is determined when its wear value exceeds a limit that can be observed on a wear curve. This curve normally consists of three distinctive regions [5] according to the increase of tool wear versus cutting time: the initial wear or running-in period, steady wear stage and accelerated wear period as shown in Figure 2-1. However, most researchers in the field have referred to the steady wear period [6-8] which intuitively seems to be the right method to handle tool life problem. Therefore, the tool wear mechanisms at the instant moment of machining or at the first transition, between the initial and steady wear, and their evolution over time are still not clearly discussed yet in spite of numerous investigations conducted over the past decades. Otherwise, effect of the initial wear mechanism and initial conditions on the tool life has not clearly expressed in the literature.

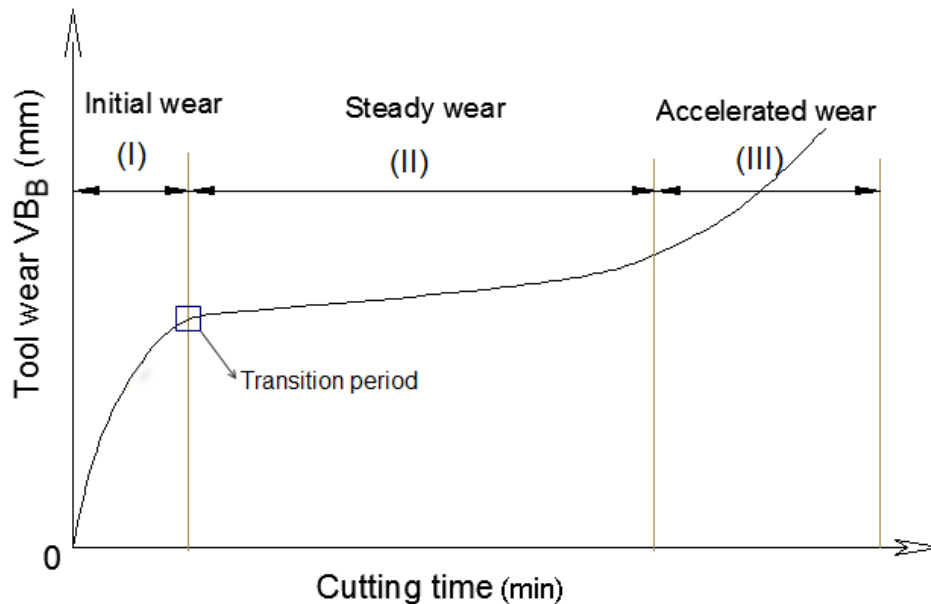


Figure 2-1: Three wear period of the tool wear vs. cutting time

The effect of the initial tool wear on the tool life could be compared to the influence of the running-in or break-in period on the wear mechanism of cylinder-engine systems. They are all closely related to progressive wear [9-11] and therefore control of the running-in process can thus extend the working life of engineering tribosystems [11, 13, 14]. As in the case of a piston ring and cylinder system the break-in is the most important period in the life of an engine because this wear period determines the performance of the system [12]. Running of the break-in condition is thus recommended for all new cars to extend the vehicle life. A Toyota (Series 2012) can be given here as a representative example: it is advised not to stop suddenly during the course of the first 300 km and not to be drive at extremely high speeds or constant speed for extended periods during the first 1600 km.

However, in the case of machining, the initial wear mechanism would be completely different to the case of surfaces being in continuous contact, like in the case of a car engine. During the cutting process, the two surfaces of the tool, rake face and clearance face, are constantly in contact with the newly generated surfaces, chip face and part face. Furthermore, during a machining operation, the chip flows on the rake face and the machined surface rubs the flank face, such that they never come back [38]. It essentially changes the running-in process. Accordingly, the initial tool wear behavior probably plays an important role in the tool wear evolution and tool life. Therefore, investigation on the initial tool wear behavior and its effect on the tool life for machining process are relevant.

2.3 Overview of the chaos theory

In 1963, Edward Lorenz reported the first chaotic attractor in a three-dimensional autonomous system when he studied the atmospheric convection by deterministic ordinary differential equations; Eq. (2-1) [39]. Later on, this model has been extensively studied in the field of chaos theory and dynamical systems [40].

$$\begin{aligned} X' &= \sigma(Y - X) \\ Y' &= rX - Y - XZ \\ Z' &= XY - bZ \end{aligned} \tag{2-1}$$

where σ , r , b are positive real parameters. The stability of a solution X , Y , Z is investigated by considering the behavior of small superposed perturbation governed by the linearized equation:

$$\begin{bmatrix} \dot{x}_0 \\ \dot{y}_0 \\ \dot{z}_0 \end{bmatrix} = \begin{bmatrix} -\sigma & \sigma & 0 \\ r-Z & -1 & -X \\ Y & X & -b \end{bmatrix} \begin{bmatrix} x_0 \\ y_0 \\ z_0 \end{bmatrix} \quad (2-2)$$

where the variation of the volume V_0 of a small region in phase space is determined by Eq. (2-3)

$$\dot{V}_0 = -(\sigma + 1 + b)V_0 \quad (2-3)$$

where the motion in phase space as the flow of a fluid is divergence by:

$$\lambda = \frac{\partial \dot{X}}{\partial X} + \frac{\partial \dot{Y}}{\partial Y} + \frac{\partial \dot{Z}}{\partial Z} = -(\sigma + b + 1) \quad (2-4)$$

At times τ_0 and τ_1 the volumes occupied by a specified set of particles satisfy the relation as given by Eq. (2-5) [39]

$$V_0(\tau_1) = e^{-\lambda(\tau_1 - \tau_0)} V_0(\tau_0) \quad (2-5)$$

Result from the exponent relationship Eq. (2-5) has shown that, the volumes in phase space shrink exponentially fast; if we start with an enormous solid of initial conditions, it eventually shrinks to a limiting set of zero volume. This behavior was quantified by a dimensional exponent λ . It is considered as the quantitative dimension of the chaotic behavior that represents an average rate of divergence or convergence of trajectories in the phase space.

Based on the set of parameters $\sigma = 10$, $b = 8/3$, $r = 28$, Lorenz proved that the system above is chaotic as depicted in Figure 2-2. He found that even a little difference in the initial value leads ultimately to significantly different behavior later on; this diagram represents the sensitive dependence on initial conditions of the system and came to be known as the “butterfly” [41, 42]. Further information on the butterfly effect can be found within Edward Lorenz’s work entitled “does the flap of a butterfly’s wings in Brazil set off a tornado in Texas?” The flapping wing represents a small change in the initial condition of the system, which causes a chain of events leading to large-scale phenomena might have been vastly different; this effect was explained as sensitive dependence on initial conditions.

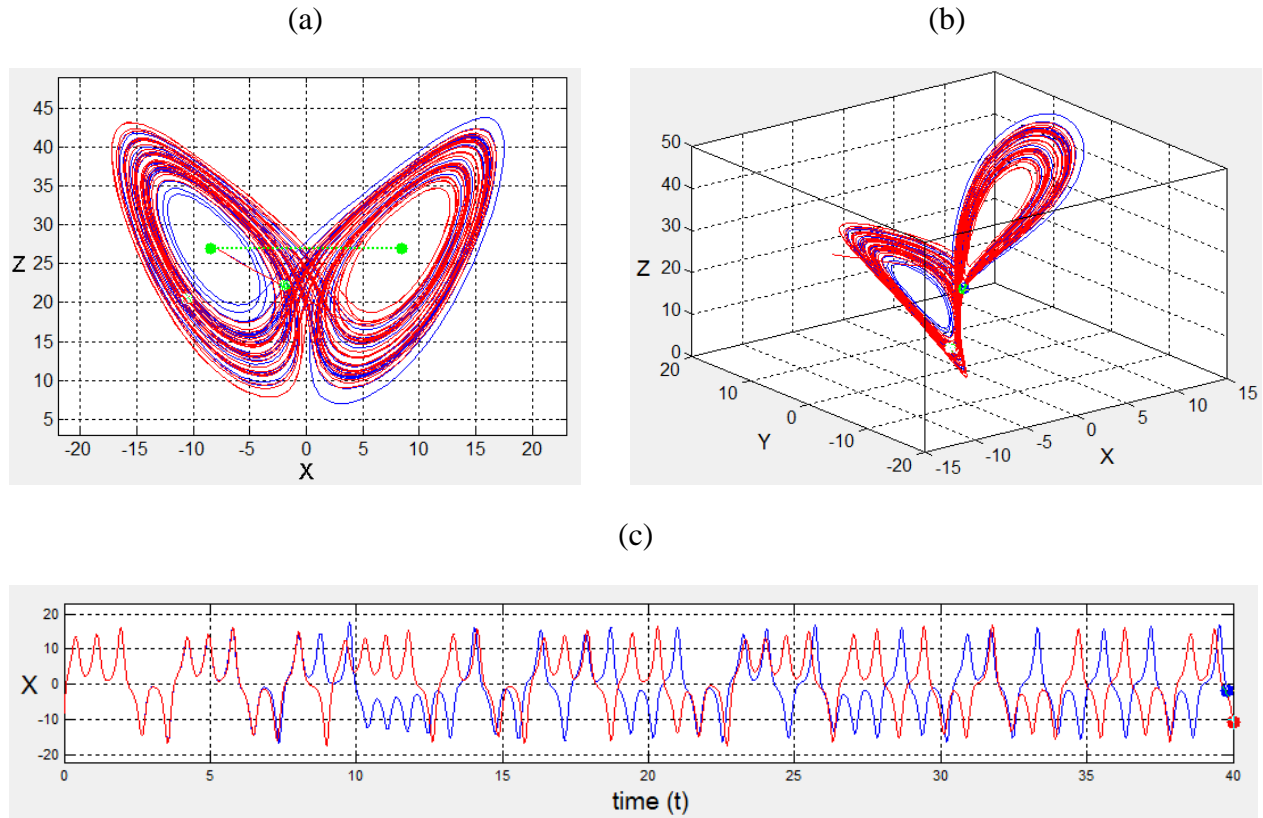


Figure 2-2: Lorenz attractor generated from Eq. (2-1); (a) 2D animated, (b) 3D animated, (c) evolution in the space time; (sourced from: <http://www.mathworks.com>)

Nowadays, chaos is considered as an aperiodic long-term behavior and exhibits sensitive dependence on initial conditions in a deterministic system [1]. The sensitive dependence on the initial condition has been widely quantified by the largest Lyapunov exponent, which is the average rate of divergence or convergence of two neighboring trajectories in the phase space as shown in Figure 2-3. The two orbits are considered as a function of time; they are generated under small different initial conditions δt_0 . The property of sensitivity to initial conditions of the divergence δt_k can be quantified by the exponential rate of divergence of two initially close orbits through the relation as given by Eq. (2-6) [43, 44].

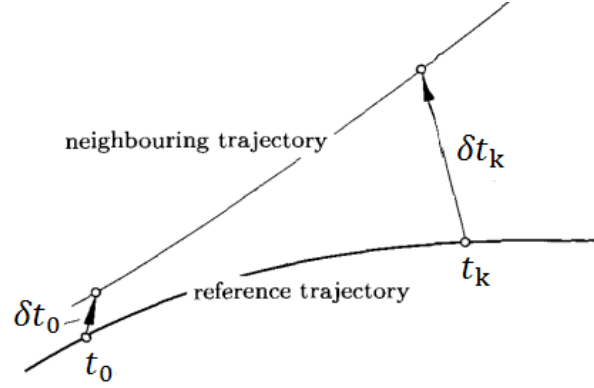


Figure 2-3: Two trajectories evolution in a phase space [44]

$$|\delta t_k| \approx |\delta t_0| e^{k\lambda} \quad (2-6)$$

where λ is the Lyapunov exponent that means the rate of separation of trajectories in the system. Function of the Lyapunov exponent can be expressed as in the case of an iterative one dimensional discrete system of a logistical equation, (2-7) [43, 44]

$$t_{n+1} = f(t_n) \quad (2-7)$$

where the values t_n belong to a finite interval. For $n \rightarrow \infty$ we consider how the point sequence $t = \{t_i\}$ differ from the point sequence $t' = \{t'_i\}$ that evolves from a slightly modified initial condition. Applying Eq. (2-6) to the case of the logistical model the Lyapunov exponent λ is defined based on the one dimensional discrete map, as given by Eq. (2-8).

$$\lambda = \frac{1}{k} \lim_{k \rightarrow \infty} \sum_{i=0}^{k-1} \ln |f'(t_i)| \quad (2-8)$$

For example, the Lyapunov exponent of Eq. (2-8) is calculated for the logistic map determined by Eq. (2-9).

$$x_{n+1} = \alpha x_n (1 - x_n) \quad (2-9)$$

where x_n is a function of the control parameter α . The long-term behavior of the x_n is generated in accordance with a bifurcation diagram, Figure 2-4(a) while Figure 2-4(b) shows the

corresponding evolution of the Lyapunov exponent λ with the dependence α . As seen here, the Lyapunov exponent was found to be negative when $\alpha < \alpha_\infty \approx 3.57$; the evolution behavior of λ is then approached to zero at the period-doubling bifurcations, $\alpha \approx 3.57$ see Figure 2-4(a). The positive values of the λ was found at $\alpha = 3.57$ and mostly increases later on corresponding to $\alpha > 3.57$. Therefore this system was chaotic and exhibited a sensitivity dependence on initial conditions.

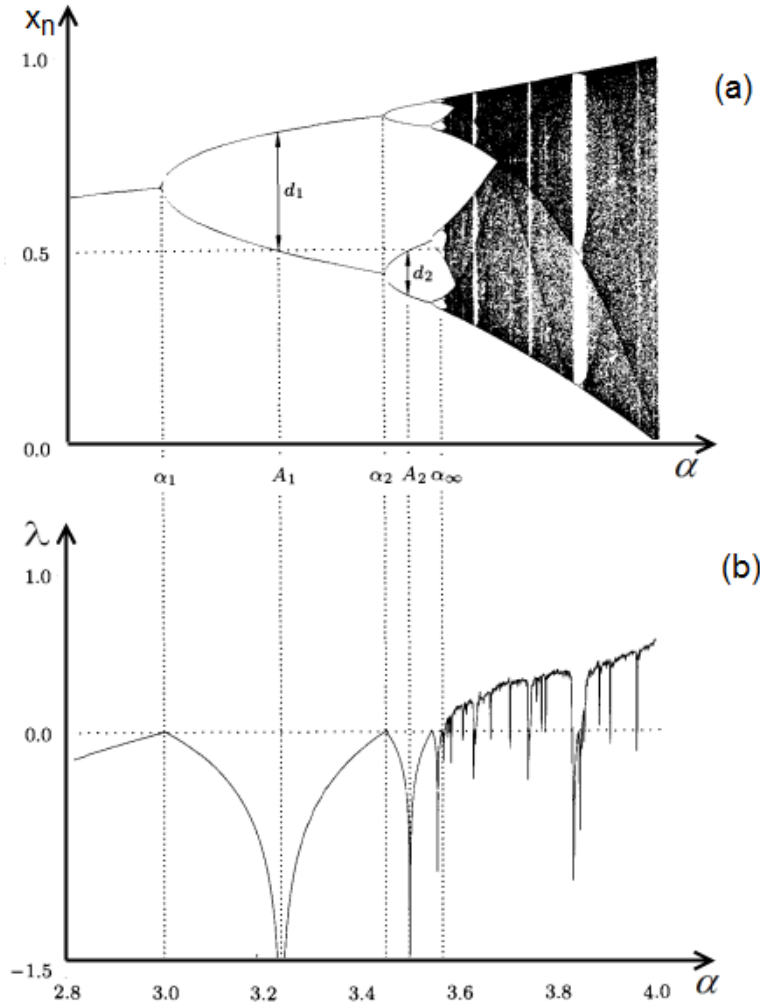


Figure 2-4: Bifurcation diagram and Lyapunov exponent [44]

Chaos theory is a field of study in mathematics. The application of chaos has primarily found dealing with the behavior of a deterministic, nonlinear dynamical systems based on the sensitive dependence on initial conditions [1]. Therefore it has been widely used to explain how something changes over time and predicting the behavioral change in a system based on the

initial conditions. The characteristics of chaos are increasingly attractive for a range of applications in engineering [2, 45-47]. Since, chaos theory refers to the dynamical systems, hence most researchers in the fields of machining [1, 46, 48] and mechanical friction [49, 50] have investigated the chaotic behavior in dynamical or complex systems. For example, chaotic dynamics of the cutting process [48, 51, 52], dynamics and chaos in manufacturing processes [46], chaotic and fractal dynamics [53], chaotic and stochastic dynamics of orthogonal metal cutting [54], controlling chaotic instability of cutting process [55] and chaotic vibrations in machining [56-58].

In fact, the chaotic motion can be found in relatively simple systems [59]. Buff and Cheritat [4] proved the existence of quadratic polynomials with a Julia set of positive area that can be used to quantify a signal of chaos in a simple dynamical system and the chaos is the rule. This new philosophy can dramatically change in machining theory research methods. In particular, the application of chaos was proved efficient in explaining how something change over time and predicting the behavioral change in a system [43]. The prediction based on the characteristics of chaos was recently developed and applied not only to the short term but also the long-term behavior of numerous technical systems [2], even to predict something deemed unpredictable [3]. Consequently, the sensitive dependence on the initial conditions of chaos appears as a potential method to investigate the dependence of the tool life on the initial cutting conditions.

In general, Lyapunov exponent λ measures the rate of exponential divergence between neighboring trajectories in the phase space to quantify the chaotic motion in a system [60]. It can be determined by ordinary differential equations [42]. Hence, the influence of initial conditions of a deterministic system can be described by a fractional differential equation [61, 62]. Unfortunately, most mathematical model investigating chaotic behavior has been developed for a non-linear or complicated system. Furthermore, solving these equations for the dynamical system to calculate the Lyapunov characteristic exponents is not simple even though numerous classical numerical methods including Runge–Kutta methods and the multistep methods have been developed for solving the initial condition problems of the ordinary differential equations [63, 64]. Trigeassou et al. [65] developed the Lyapunov exponent to study the stability of fractional differential equations that allows the definition of an elementary Lyapunov function. By utilizing a least square approximation of spatial-dependent factors, Bajcinca et al. [66] solved numerically various classes of differential equations with orthogonal polynomials. The algorithm for

approximating solutions to differential equations has also been supported by Ahmed [67] and Mittal et al. [68] when they studied the Bernstein polynomial. These B-spline methods are indeed linear multistep methods based on non-uniform meshes [69]. Mittal et al. [70] applied cubic B-splines for spatial variable and its derivatives which produce a system of first order ordinary differential equations. They have reported that the approximation solution using B-spline to these equations have a good agreement with the known solution. Accordingly, the B-spline functions of rational interpolation can be used to characterize the wear curve trajectories during machining process.

2.4 Fractal dimension

A fractal geometry is an object that displays self-similarity at various scales and it is quantified by a non-integer dimension, the fractal dimension [71]. Therefore, it has been widely used to characterize complex geometric forms or non-integer dimension object that could not be analyzed by the classical Euclidian geometry. Particularly, the fractal dimension is closely related to the Lyapunov exponent [72] in quantifying the chaotic motion in a system [1, 45]. The fractal dimension (D), by definition, is a parameter used for representing accurately shapes by means of a simple and compact set of equations as follows [44, 71]

$$D = \lim_{\varepsilon \rightarrow 0} \frac{\ln N(\varepsilon)}{\ln(1/\varepsilon)} \quad (2-10)$$

where $N(\varepsilon)$ is the number of self-similar pieces (number of new facsimiles); ε is a magnification factor (scaling ratio).

To express the definition of fractal dimension, let us consider some Fractal dimensions of Self-Similar; they are adapted from [71].

Cantor set

The Cantor set, proposed by a German mathematician Georg Cantor, in 1883, is a set of points on a single line segment. The first line is divided by three pieces and delete the middle one we get the first stage ($n=1$) as illustrated in Figure 2-5.

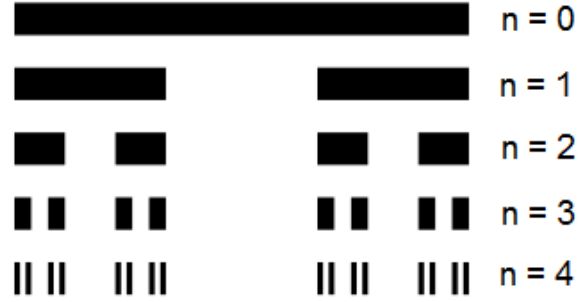


Figure 2-5: Cantor set fractal dimensions [71]

Continuing this construction repeatedly; one obtains the three equal sections of length $\varepsilon_1 = (1/3)^1$ and the number of pieces $N_1 = 2$. In the k -th step, the number of pieces is $N_k = 2^k$, the length measurement in this step is $\varepsilon_k = 1/3^k$ which are necessary to cover the set. Equation (2-10) applied to the case, gives the fractal dimension as follows:

$$D = \lim_{k \rightarrow \infty} \frac{\ln N_k}{\ln(1/\varepsilon_k)} = \lim_{k \rightarrow \infty} \frac{\ln 2^k}{\ln 3^k} = 0.6309 \quad (2-11)$$

Koch Curve and Koch snowflake

The Koch Curve is constructed as shown in Fig 3-6, we consider a straight line at the stage 0, the line is then divided into three equal segments, and then replaced the middle segment by the two sides of an equilateral triangle which own the same length as the segment being removed (stage 1). An identical principle can be continuously applied to the stage 2 and so on... By considering the Eq. (2-10) we finally obtain the fractal dimension, Eq. (2-12):

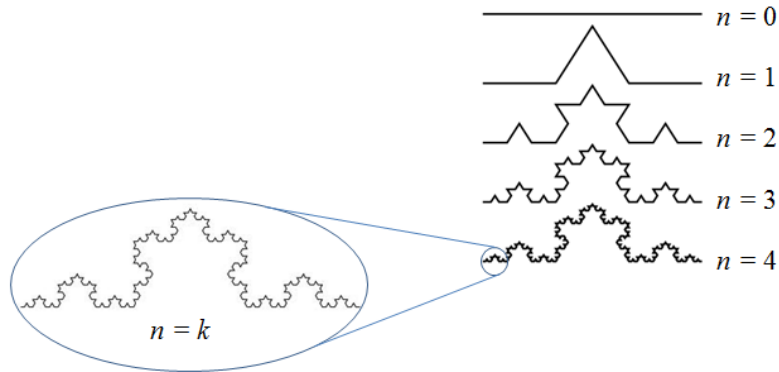


Figure 2-6: Koch curve generation of fractal dimension, expressed from [71]

$$D = \lim_{k \rightarrow \infty} \frac{\ln 4^k}{\ln 3^k} = 1.2619 \quad (2-12)$$

Sierpinski triangle

Let us start by a triangle in a plane (stage 0) as given in Figure 2-7. By shrinking the triangle to 0.5 of size and remove the middle one we obtain three copies of the first original triangle in half smaller (stage 1). $\varepsilon_1 = 1/2, N_1 = 3$. Repeat the construction with each of the smaller triangles (stage 2); $\varepsilon_2 = (1/2)^2, N_2 = 3^2$ and continue this construction at the k-th stages, $\varepsilon_k = (1/2)^k, N_k = 3^k$ we obtained the fractal dimension as given by Eq. (2-13)

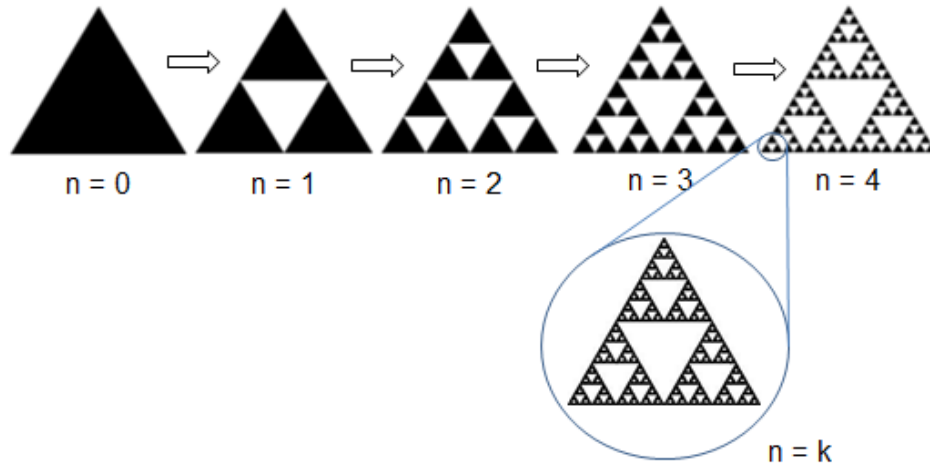


Figure 2-7: Sierpinski triangle generation of fractal dimension, expressed from [71]

$$D = \lim_{k \rightarrow \infty} \frac{\log 3^k}{\log 2^k} = 1.585 \quad (2-13)$$

Box-Dimension

We now consider three different objects of a line section, a square and a cube in the classical Euclidian geometry as shown in Figure 2-8. We divide the line, square and the cube by four smaller objects and each of them is similar to the original one. The length and the volume can be determined by Eq. (2-14)

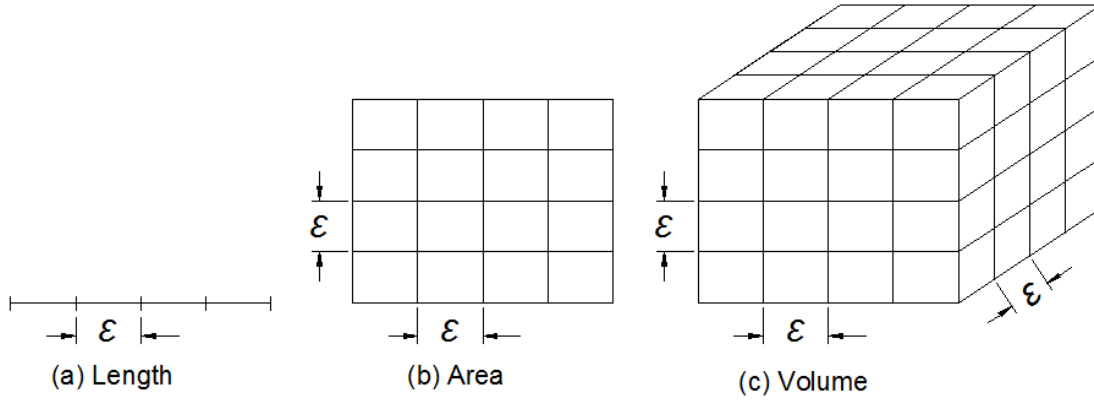


Figure 2-8: Fractal Box-dimensional [44]

$$L = N(\varepsilon) \cdot \varepsilon \quad (a)$$

$$A = N(\varepsilon) \cdot \varepsilon^2 \quad (b) \quad (2-14)$$

$$V = N(\varepsilon) \cdot \varepsilon^3 \quad (c)$$

If ε is small enough, the Box-dimension of the set equals to the exponent D in the power law is given by:

$$N(\varepsilon) \propto \frac{1}{\varepsilon^D} \quad (2-15)$$

where D is called the fractal capacity dimension or Box-dimension. In an n -dimensional space, $N(\varepsilon)$ denotes the minimum n -dimensional of edge length ε required to cover the set. By taking the logarithm on both of sides of Eq. (2-15), we also obtain the fractal box-dimension as defined above by Eq. (2-10). For example, the length of a coastline can be estimated in the map by using a pair of compasses based on box-counting method as shown in Figure 2-9 [71]. The length of a coastline was defined by Eq. (2-14) (a); where N is the number of sides needed for a round trip along the coast and ε is the compasses setting; the values was calculated as given in the Table 2-1 [73].

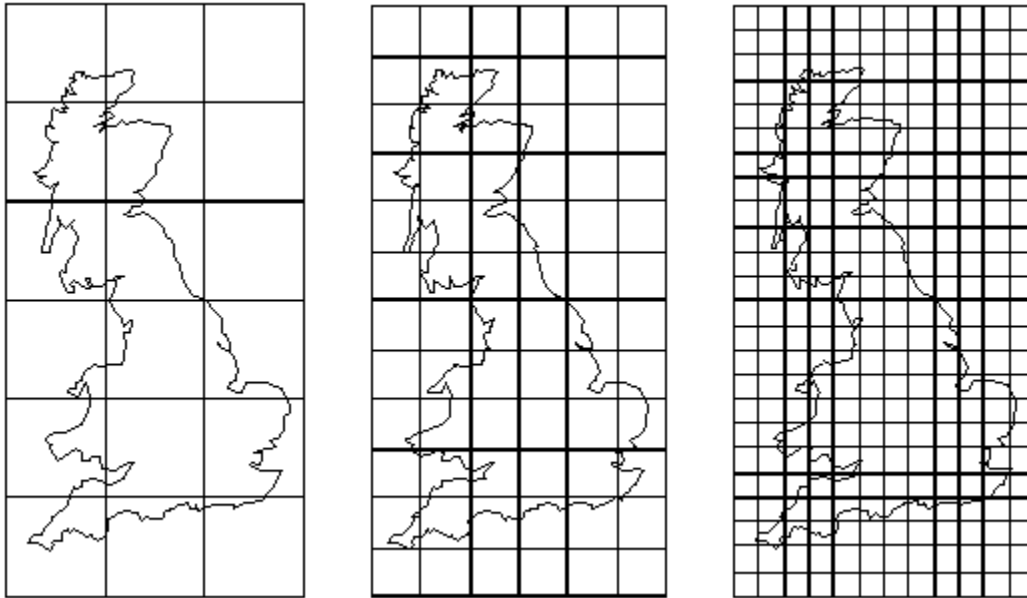


Figure 2-9: Three different size grids for Great Britain [71]

Table 2-1: The length of a coastline [73]

$N(\varepsilon)$	ε (km)	L (km)
6	500.00	3000
12	258.82	3106
24	130.53	3133
48	65.40	3139
96	32.72	3141
192	16.36	3141

As a new geometry, the Fractal theory has been used to describe the structural irregularities and complexities of the natural system [74], analysis and characterize of surface engineering [75, 76], tool wear and machined surface [77-80] and analyzed surface wear contact [76, 79, 81-83]. Fractal analysis of surface includes the calculus of fractal dimension profile or surface characterization with the help of many assisted image analysis methods such as: microscopy, optical profiling or SEM images... as shown in Figure 2-10 and Figure 2-11.

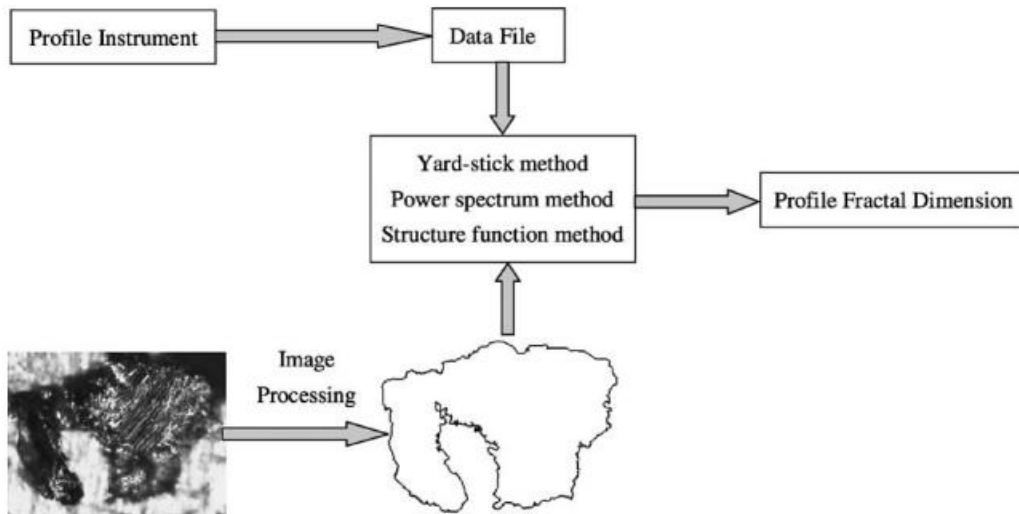


Figure 2-10: Fractal calculation of profiles [76]

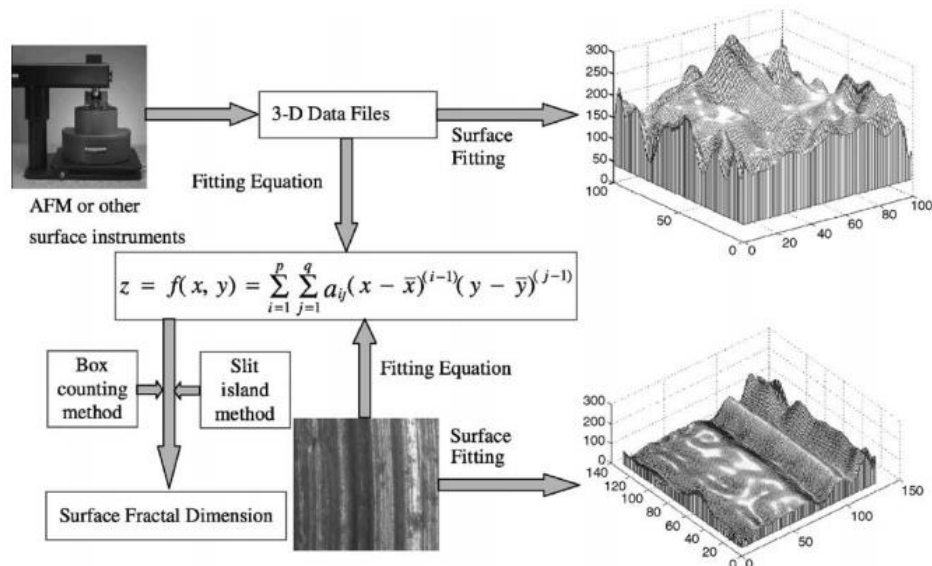


Figure 2-11: Fractal calculation of surfaces [76]

In order to calculate numerically the fractal dimension a Power spectrum has been developed for a scaling curve based on the function of Weierstrass–Mandelbort as given by Eq. (2-16) [84]

$$W(x) = \sum_{n=-\infty}^{\infty} \frac{(1 - e^{i\gamma^n x}) e^{i\phi_n}}{\gamma^{(2-D)n}}; \quad 1 < D < 2; \gamma > 1; \phi_n = \text{arbitrary phases}; \quad (2-16)$$

where D is the fractal dimension of the graph $W(x)$ depends on γ , which determines how much of the curve is visible for a given range of t , Φ_n is a random phase. A fractal profile $z(x)$ can be obtained as the real part by setting $\Phi_n = 0$ as follows

$$z(x) = RW(x) = \sum_{n=-\infty}^{\infty} \frac{(1 - \cos \gamma^n x)}{\gamma^{(2-D)n}} \quad (2-17)$$

where the power spectrum $S(\omega)$ of $z(x)$ is proportional to the square of its Fourier transform, given by Eq. (2-18) [84]

$$S(\omega) = \sum_{n=-\infty}^{\infty} \frac{\delta(\omega - \gamma^n)}{\gamma^{(4-2D)n}} \quad (2-18)$$

This model has been developed to characterized elastic contact and heat transfer by (Komvopoulos and his colleagues 1994), as given by Eq. (2-19) and then applied for a 3D isotropic fractal surface [85] as Eq. (2-20)

$$z(x) = L \left(\frac{G}{L} \right)^{D-1} \sum_{n=n_1}^{n_{\max}} \frac{\cos(2\pi \gamma^n x / L)}{\gamma^{(2-D)n}} \quad (2-19)$$

$$z(x, y) = L \left(\frac{G}{L} \right)^{D-2} \left(\frac{\ln \gamma}{M} \right)^{1/2} \sum_{m=1}^M \sum_{n=0}^{n_{\max}} \gamma^{(D-3)n} \left\{ \cos \Phi_{m,n} - \cos \left[\frac{2\pi \gamma^n (x^2 + y^2)}{L} \cos \left(\tan^{-1} \left(\frac{y}{x} \right) - \frac{\pi m}{M} \right) + \Phi_{m,n} \right] \right\} \quad (2-20)$$

where L is the measurement length, M is the number of superimposed ridges, $\Phi_{m,q}$ is a random phase uniformly distributed in the range [86] by a random number generator to prevent the coincidence of different frequencies at any point of the surface profile, q is a spatial frequency index, L_s is cut-off length; it can be defined by $n_{\max} = \text{int}[\log(L / L_s) / \log \gamma]$. Based on the wear contact of elastic-plastic, Eq. (2-20) is generated for the different parameters as shown in Figure 2-12 [81, 85]

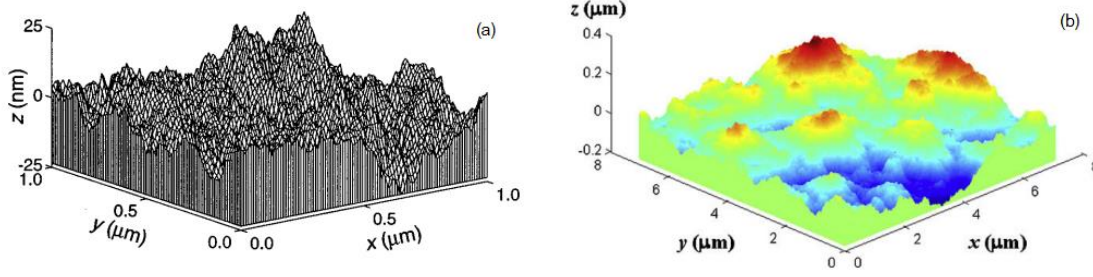


Figure 2-12: 3-D Fractal surface generated from Eq.3.20 [81]

In this model a 2D profile of a fractal surface is truncated by a plane is shown in Figure 2-13 with power-law relationship:

$$N(a') = \left(\frac{a'_L}{a'} \right)^{(D-1)/2} \quad (2-21)$$

where a' can be determined from the total truncated area S of the equivalent rough surface using a formula as given by Eq. (2-22) [83]

$$S = \int_{a'_S}^{a'_L} a' n(a') da' = \frac{D-1}{3-D} a'_L 1 - \left(\frac{a'_S}{a'_L} \right)^{(3-D)/2} \quad (2-22)$$

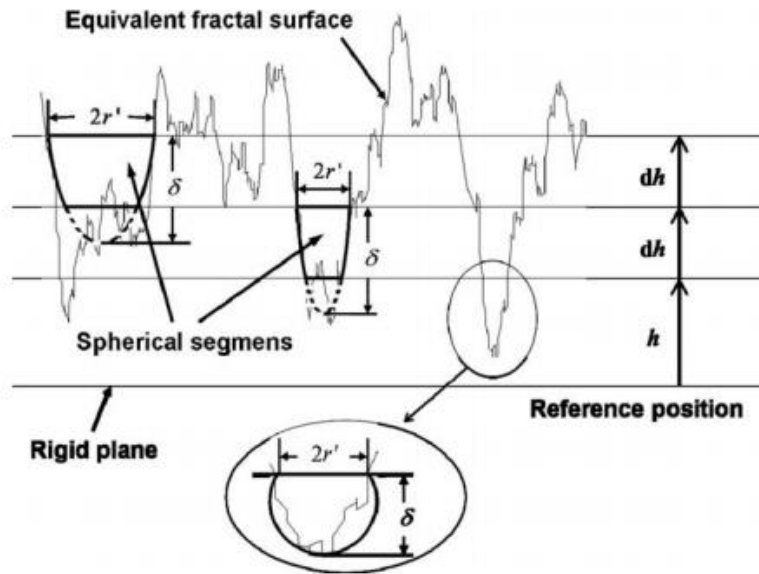


Figure 2-13: 2D profile of a truncated rough (fractal) surface [82]

Based on the total wear volume of surface contact elastic-plastic to characterize the abrasive wear rate as given by Eq. (2-23)

$$\frac{V}{S} = \int_{a'_s}^{a'_w} \frac{\Delta V(a')}{S} n(a') da' \quad (2-23)$$

where DV/S is the wear volume per unit sliding distance at the micro contact level; the model of Eq. (2-23) was applied to analyze the adhesive wear at the contact between rough solids [87].

CHAPTER 3 ARTICLE 1: INITIAL TOOL WEAR BEHAVIOUR DURING MACHINING OF TITANIUM METAL MATRIX COMPOSITE (TiMMCs)¹

This chapter is devoted, for the first time in the field of tool wear, to the study on initial tool wear during machining of TiMMCs. Herein, the initial tool wears behavior and their evolutions over time were investigated by specially taking in to consideration the wear mechanism at the first moments of machining. The obtained results have shown that the initial wear mechanisms of diffusion and adhesion are primarily found for all cutting conditions tested; even though all previous research efforts have reported that abrasion is the most important mechanism when machining metal matrix composites. In our special case, rapid initial wear occurs within a very short period of cutting time, as soon as the cutting action begins and extends to only few seconds at the most. The effect of chemical stresses at high cutting temperature during the course of accelerated cutting force leads to the diffusion wear. The atmospheric oxygen reacts spontaneously with the tool layer material and oxidizes titanium and aluminum of the workpieces materials. These elements participate in the cutting process and form a very hard thin layer at the first transition period. The latter, hereafter called “wear shield”, is considered as a protection wear layer at the beginning of the steady wear period. The discovered the new wear shield allows a better explanation of the wear rate and how the initial tool wear mechanism affect significantly the tool wear evolution over time and the entire tool life.

3.1 Introduction

Titanium metal matrix composites (TiMMCs) have been known as a new generation material which offers several advantages compared to titanium alloys and metal matrix composites. They are generally distinguished by the characteristics of the reinforcement, such as particles of titanium carbide (TiC) and titanium boride (TiB) [18-21]; whiskers, continuous or discontinuous fibers of silicon carbide (SiC) [16, 22, 23]. Among them, reinforcing with the hardest refractory metal carbides such the TiC particles providing superior properties at elevated

¹ D. Xuan-Truong, M. Balazinski, R. Mayer, *Initial Tool Wear Behaviour during Machining of Titanium Metal Matrix Composite (TiMMCs)*, Machining science and technology (2015), REF: LMST-2015-0083, *under review*.

temperature and exceptional wear resistance [18, 21, 24]. Due to their high strength, stiffness, and creep resistance at high temperatures; the TiMMCs are increasingly attractive for a range of applications in aerospace and automotive industries [15, 16]. However, the combination of both machining problems associated with metal matrix composites (MMCs) and titanium alloys into the (TiMMCs) that all together leading to the machining of this material become a real challenge in our field [15, 17].

The poor machining characteristics of titanium alloys are high reactivity, low thermal conductivity, relatively low modulus, and maintains their high strength and hardness at elevated temperatures [25, 26]. The low thermal conductivity of titanium leads to a significant increase in cutting temperature at the tool-workpiece interface during machining; therein, the cutting tool material tends to react chemically with titanium at high temperature and causes adhesion of the workpiece material to the cutting edge [7]. Consequently, the adhesive wear through plastic deformation and welding rapidly develops [27, 28]. In addition, the high tensile strength in combination with the low Young's modulus of titanium alloys caused high temperature and high mechanical stresses at the cutting edge which lead to a particularly fast tool wear [29].

Metal matrix composites are also considered as a difficult to cut material due to the abrasive properties of hard particle reinforcement [21, 30, 31]. The MMCs reinforced with ceramic particulates provide a number of advantages compared to their base metals such as higher specific strengths and moduli, higher wear resistance at elevated temperature and lower coefficients of thermal expansion [32]. As a result, machining of MMCs lead to poor tool life and inconsistent machined surface quality [33]. Hence, the abrasion is found to be the dominant wear mechanism in almost all investigated cutting conditions [17, 34, 35]. Moreover, the abrasive wear is accelerated and depends on the percentage of reinforcement in the MMCs due to the interference between the reinforcement particles [36].

In general, tool life is determined when its wear value exceeds a limit that can be observed on a wear curve. This curve normally consists of three distinctive regions according to the increase of tool wear versus cutting time: the initial wear or running-in period (I), steady wear stage (II) and accelerated wear period (III) [5, 37] as illustrated in Figure 3-1. Among these wear periods, the initial wear period, is not fully understood yet in spite of numerous investigations

conducted over the past decades. In fact, most researchers in the field have referred to the steady wear period [6, 63, 88] which intuitively seems to be the right method to handle tool life problem.

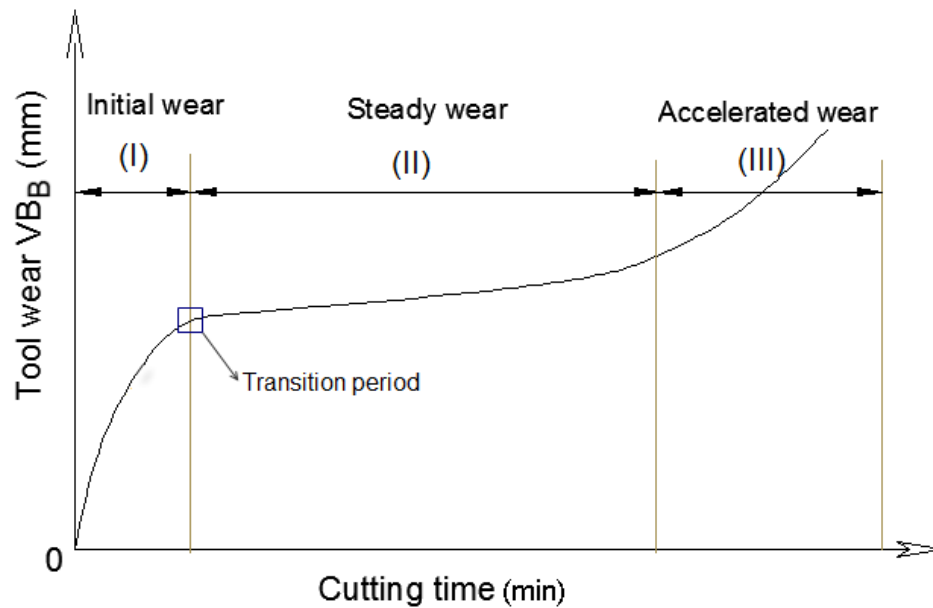


Figure 3-1: Tool wear curves evolution versus cutting time

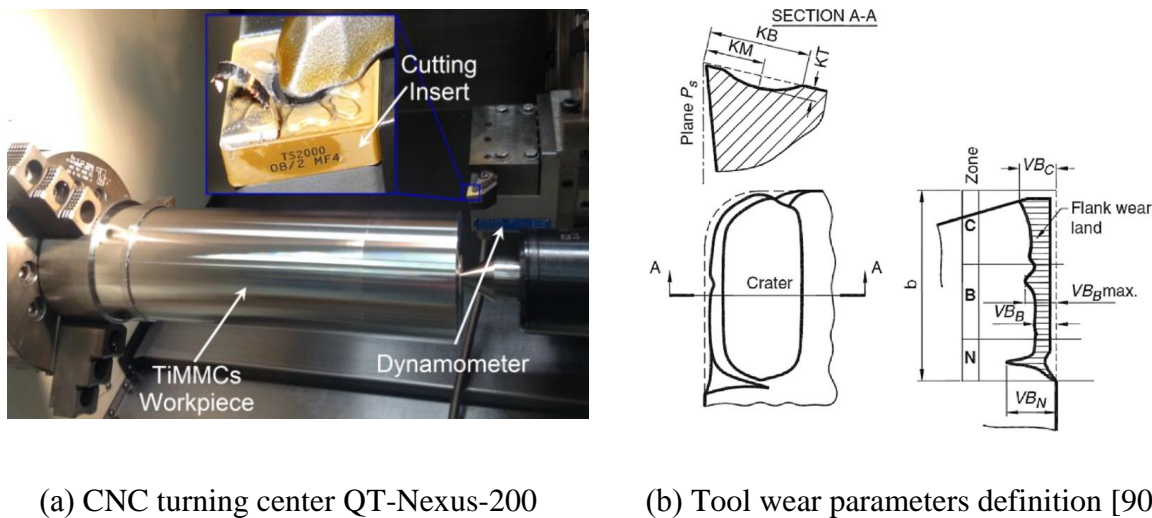
The effect of the initial tool wear on the tool life could be compared to the influence of the running-in or break-in period on the wear mechanism of cylinder-engine systems. They are all closely related to progressive wear [9-11] and therefore control of the running-in process can thus extend the working life of engineering tribosystems [11, 13, 14]. As in the case of a piston ring and cylinder system the break-in is a most important period in the life of an engine because this wear period determines performance capability of the system [12]. Running of the break-in condition is therefore recommended for all new cars to extend the vehicle life. A Toyota (Series 2012) can be given here as a representative example: A new car is advised not to be stopped suddenly during the course of the first 300 km and not to be driven at extremely high speeds or constant speed for extended periods during the first 1600 km.

However, in the case of machining, the initial wear mechanism would be completely different than in the case of surfaces being in continuous contact, as in the case of a car engine. This is because, during the cutting process, the two surfaces of the tool, rake face and clearance face, are constantly in contact with the newly generated surfaces, chip face and part face. Furthermore, during a machining operation, the chip flows on the rake face and the machined surface rubs the flank face, such that they never come back [38]. It essentially changes the

running-in process. Therefore, the tool wear mechanism at the moment cutting probably plays an important role in the tool wear evolution and tool life; studying the initial tool wear during machining process is especially interested. The initial wear behavior when machining TiMMCs is investigated for the first time in the study of tool wear and tool life.

3.2 Experimental procedure

The machining tests were performed on a CNC turning center Mazak QT-Nexus-200 as shown in Figure 3-2(a). The workpiece material was TiMMCs reinforced with TiC particles distributed in a matrix of titanium alloys Ti-6Al-4V. The mean Rockwell hardness of the TiMMCs was 40 HRC with an approximate tensile strength of 182 000 psi. The tool wear progression is observed on the wear curves where the flank wear values are measured after certain cutting time using an optical microscope and a high resolution digital camera connected. The tool wear is characterized by its formulation that takes into account the ISO standard of VB_B on the flank face and KT on the race face as shown in Figure 3-2(b) [89, 90]. The initial wear mechanism is analyzed using a Scanning Electron Microscope (SEM) and an Energy Dispersive X-ray (EDX).



(a) CNC turning center QT-Nexus-200

(b) Tool wear parameters definition [90]

Figure 3-2: Experimental set-up

As clearly started in the introduction, TiMMCs is a difficult to cut material and its machinability information is still limited in the open literature. The cutting tool material and cutting conditions in this work are considered using several factors. Cutting tools made of

polycrystalline diamond (PCD), cubic boron nitride (CBN) and PVD coated carbide inserts are widely recommended for machining titanium alloys Ti-6Al-4V. PCD and CBN have lower wear rate while the coated carbide one is cheaper [91]. With the aim of analyzing the tool wear in the initial wear region, the wear rate should not be too fast to achieve sufficiently accurate measurement. However, it should not be too slow to avoid the use of massive expensive material like TiMMCs. Furthermore, in our previous works [15, 17, 92, 93], the PVD coated inserts have already been used for machining of the TiMMCs. Considering all those facts, the PVD coated inserts of (Ti,Al)N+TiN manufactured by SECO were used in all experiments with the following specifications: rake angle $\gamma_0 = -6^\circ$, back rake angle $\gamma_p = -6^\circ$, nose radius $r_\epsilon = 1/32$ in, tool included angle $\epsilon_r = 80^\circ$, tool cutting angle $\kappa_r = 95^\circ$ and insert thickness $s = 3/16$ in. The cutting conditions are chosen by taking into account not only the recommendation of cutting tool manufacturers or the mentioned papers above but also by our preliminary machining tests for the special case of the first wear zone.

In order to determine exactly what is the initial wear, as well as when it occurs; the experiments were performed under different cutting speeds of 20, 40, 50 and 60 m/min whereas feed rate and depth of cut were kept constant at 0.15 mm/rev and 1.5 mm respectively. The progressive wear is observed on the flank wear curves measured using an optical microscope and a high resolution digital camera. The initial wear period was analyzed not only by taking into account the wear rate and the wear values but also with a focus on the wear mechanisms. The initial wear mechanism at the first moment and transition period is specially considered.

3.3 Results and Discussion

3.3.1 Initial wear determination

It is well-known that tool life is affected by a number of cutting parameters including machine tool, workpiece material, cutting tool and cutting parameters. In the cutting process, the tool life is also influenced significantly by the machining characteristics such as cutting force, vibration, cutting temperature, chip formation and tool wear behavior. Therefore, the definition of a universal tool life criterion for all these quantitative variables is far from simple. In fact, the cutting speed has been considered as the most important factor influencing the tool life. Hence our experiments were performed with different cutting speeds to determine the wear periods and tool life.

As a result, the tool wear evolutions depending on the cutting speed are characterized by each wear curve as shown Figure 3-3; they are recognized in four groups in accordance with the cutting speed; each curve group is observed three differential wear periods, for example, three wear periods under cutting speed $V_4 = 60$ m/min are indicated: initial wear period (I), steady (II) and rapid wear (III).

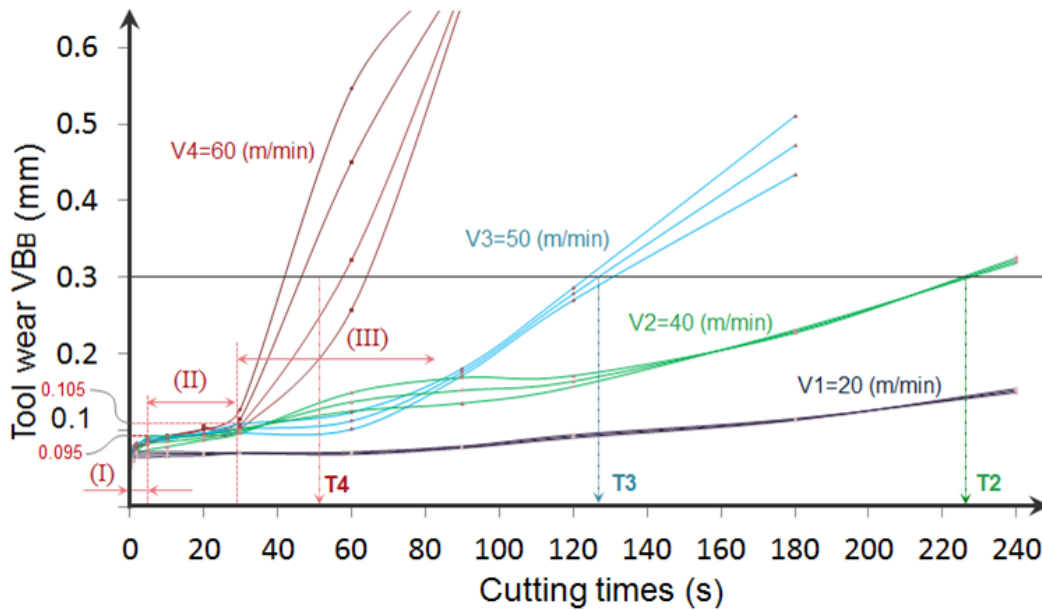


Figure 3-3: Tool wears during machining TiMMCs under different cutting speeds

As seen here, tool wear rate increases rapidly in the first and third wear period while the steady wear zones are kept constant. More importantly, we can find here the initial wear period even happens within a very short of cutting time but their wear values are taken much more than the second wear period. The percentage of tool wear values in comparison between the two periods is different depending on the cutting speeds; for example, under cutting speed $V_4 = 60$ m/min, the average initial wear value was 0.095 mm equal 90.5% compares to the steady wear period was 0.01 mm equal 9.5%, see Figure 3-3 while under speed of $V_3 = 50$ m/min, their percentage of initial and steady wear period were taken 66.4% and 33.6% respectively. It is therefore believed that the initial wear period plays a critical role the tool life during machining TiMMCs.

Figure 3-4(a) shows the average wear curves while the initial wear period is magnified in Figure 3-4(b). We have considered the variation of the initial wear curve based on the critical wear rate; the initial values (V_{bi}) do indeed increase rapidly with the cutting speed and approach

a limit at the transition between regions (I) and (II). They all occur as soon as the cutting action begins and extend to only two seconds at low speed of 20 m/min and ten seconds at the highest speed. If we considered that the cutting time corresponding to the initial wear at V_{bi} max is the tool life of the first wear period, we can observe both the initial wear and initial life increased with the cutting speed. This increment does not mean the tool life has improved at higher cutting speed but the initial life depends significantly on the cutting speed and also on the wear rate. Therefore, definitions of the critical value for the initial tool wear required further analyzing the wear mechanism at the initial wear period.

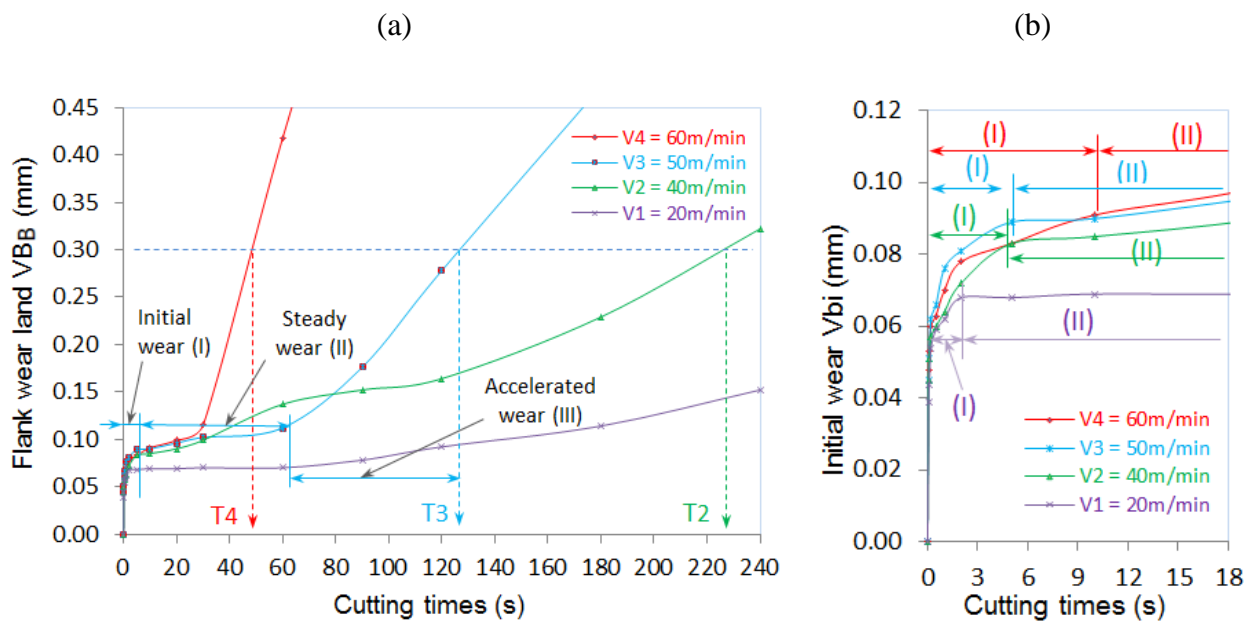


Figure 3-4: The initial wear period during machining of TiMMCs

3.3.2 Initial wear mechanism

As discussed in the introduction, the main wear mechanism during machining of TiMMCs has been found to be abrasion under almost all experimental cutting conditions [17, 34]. This mechanism depends on the nature and percentage of the hard particles reinforcement inside the composite [36]. However, the mentioned works have indeed investigated the tool wear in the steady region. So in order to elucidate the effect of the hard particles of TiC on the tool wear mechanism at the first wear zone, the initial wear mechanism when turning TiMMCs is investigated at various scales based on the SEM micrograph and EDX analysis.

First of all, the chemical analysis of the TiMMCs is given in Table 3-1. Therein, the percentage of carbon is 1.91 % that is mainly linked to the non-metallic phase titanium carbide, about 10% in weight according to the manufacturer) distributed in a matrix of Ti-6Al-4V, see Figure 3-5(a). In line with the chemical analysis, EDX analysis, Figure 3-5(b) shows the presence of hard TiC particles on the substrate where the amounts of Ti and C elements are, as expected, found to be rich. Besides, it is observed that the hard particles of TiC are non-uniform and their dimensions are less than 25 μm . These physical and chemical properties are then used to analyze the effect of the hard particles on the initial wear in this work.

Table 3-1: Chemical composition of the TiMMCs

Elements	Mo	Cr	Co	Mn	Ni
wt. %	< 0.005	0.007	0.011	0.010	0.020
Elements	Sn	Cu	Fe	Si	C
wt. %	< 0.03	0.029	0.062	0.065	1.910
Elements	V	Al	Ti	Others	
wt. %	3.955	5.560	85.050	Balance	

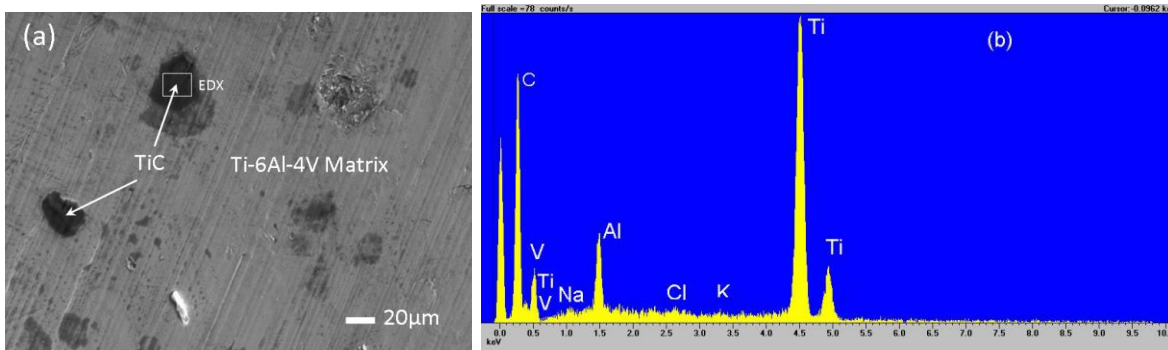


Figure 3-5: TiC particles in the machined surface of TiMMC and EDX analysis

In the first moment of machining, the cutting forces influence mainly through a small area between tool-workpiece interfaces. The tool wear is thus mostly found in the flank face and close to the cutting edge with different wear mechanisms as shown in Figure 3-6. We can see here the cutting edge deformed even at low cutting speed of 20 m/min after only 0.05 sec Figure 3-6(a) and tends to increase with the increase in cutting forces and temperature. The increase in cutting forces in general and thrust force in particular lead to high contact stress and high friction between poorly conforming surfaces at the tool–workpiece interface. Accordingly, several hard

particles in the damage zones are taken out (chipping) with high wear rate due to overload of mechanical tensile stresses, as illustrated in Figure 3-6(b). However, at higher cutting speed of 60 m/min we observed mostly adhesive wear in the location of clearance face damage and adhering to the cutting edge, Figure 3-6(c).

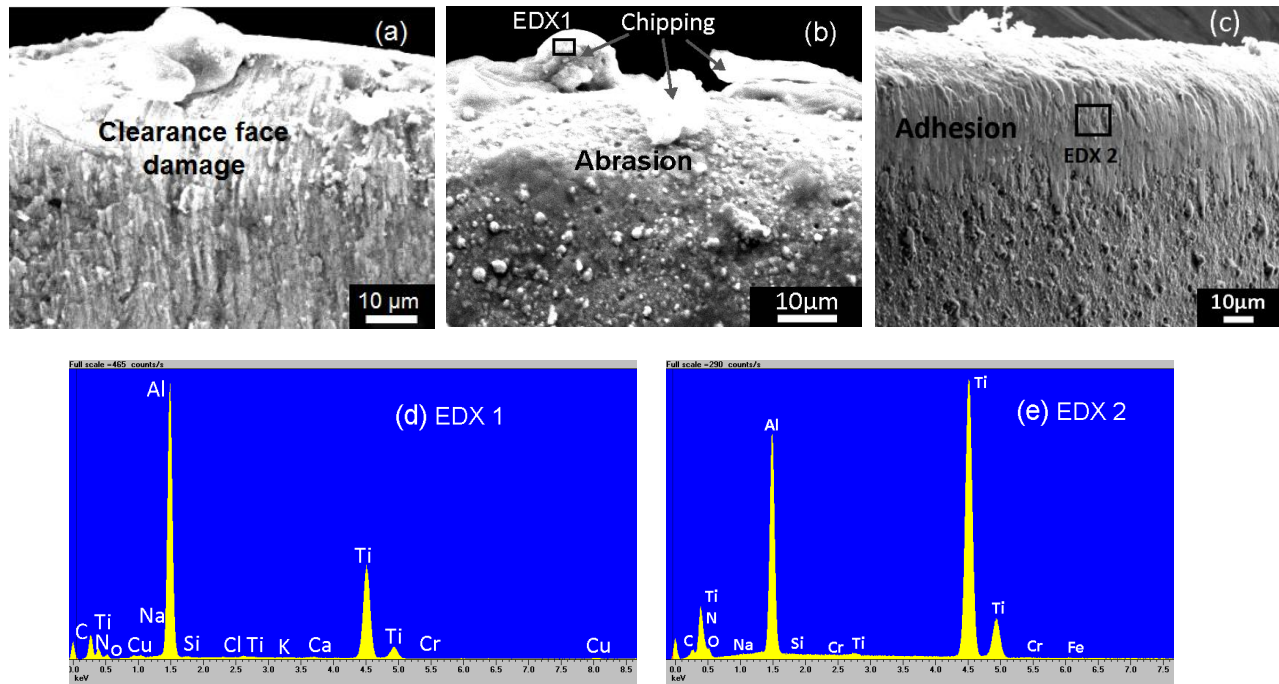


Figure 3-6: Initial tool wear mechanism at the first moment cutting (0.05 sec); (a) V=20 m/min; (b) V=40 m/min; (c) V=60 m/min, (d & e) EDX analysis

The rare appearance of the abrasion during the first wear period is attributed to accelerated wear caused by the increase of cutting force resulting in high residual stress and friction between un-conforming surfaces at the tool–workpiece interface under dry cutting condition. Indeed, this initial tool wear mechanism does not agree well with the abrasion in the second wear zone as reported when machining metal matrix composites [15, 33]. When machining the Ti-6Al-4V, M.J. Bermingham et al. [94] have shown that the cutting temperature gradient increase very fast, from 20⁰C to 500⁰C within the first seconds of cutting and resulted in the adhesion at the cutting edge. Figure 3-6(d) and (e) present the EDX analysis of wear mechanism at the location of EDX1 and EDX 2. As seen here, the coating layers of the inserts are primarily found on the cutting edge where the presence of Ti, Al and N elements were found to be plentiful in the wear surface under all cutting speeds. They are spread from the coating layer with aluminum and titanium in the

workpiece material. The tool layer elements then react spontaneously with atmospheric oxygen and oxidize the titanium and aluminum especially at high pressure and elevated temperature under all working conditions. On the other hand, the effect of the hard particle of titanium carbide reinforcement lead to the cutting edge being directly weakened by oxidation of the workpiece material and being easily taken away by the chip with high wear rate. It is thus believed that, the initial wear mechanism at this instant is a result of the combined effect of layers damage, friction - tribological wear and adhesion as well.

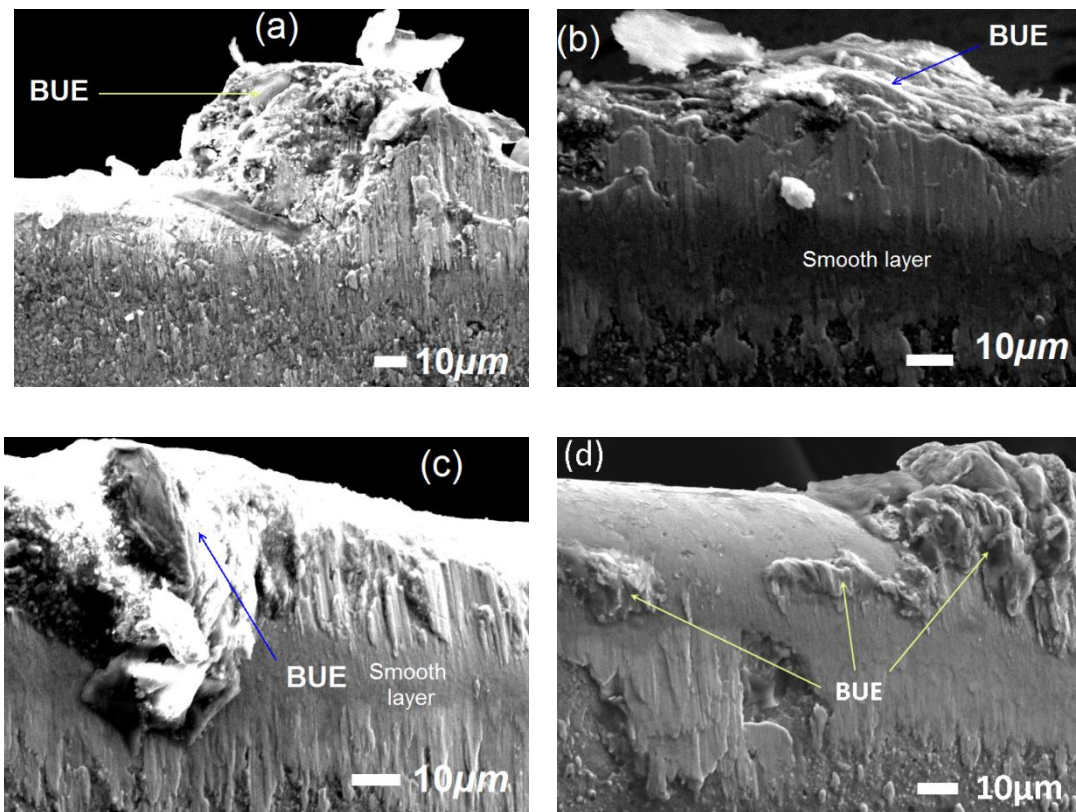


Figure 3-7: The BUE occurs within initial wear period when machining TiMMCs; (a) $V=20$ m/min-1.0sec; (b) $V=40$ m/min-1.5sec; (c) $V=50$ m/min-2.0sec; (d) $V=60$ m/min-5.0sec

The progression of wear mechanism is investigated until the wear values reach the steady wear region. The initial wear increases very fast while the initial life and their wear values depend sensitively on the cutting speed; the low thermal conductivity of titanium alloys is the main reason leading to an increase in cutting temperature at the tool-workpiece-chip interfaces. Hence the poor surface of workpiece material and coating tool layer get into contact and resulting in micro welding between them. As a result, a micro-welding and built-up-edge (BUE) are

formed under sufficient pressure at the cutting edge under all experimental cutting conditions as shown in Figure 3-7. The initial wear behaviors has taken place over very short periods of time so the friction and tribological wear can be considered at the contact of two new surfaces where the sliding velocities between the two fresh surfaces at a small cutting edge are close to zero [95, 96]. Hence the contact surface appears smooth and clean thus inducing quasi-static friction [97]. In the case study, the smooth layers are observed in the middle of the wear area at certain cutting time as illustrated in Figure 3-7(b) and (c); they are discussed in the next section.

Paying more attention on the chemical composition the elements of titanium, aluminum, vanadium and carbide are primary found in the adherent material. Even the presence of the reinforcement of hard particles (TiC) is found to be rich on the wear surface; the BUE has still generated by plastic deformation under high pressure and thermal softening at elevated temperature that can be cause stress inside the adhesion wear. This is a chemical wear mechanism that is affected by the cutting tool material reacting chemically with titanium [7]. On the contrary, the hard particles have been reported as a main reason that leads to abrasive wear under all cutting condition [17]. Unfortunately, the abrasion was not clearly observed in our special case of the initial wear period. Zhu et al. [98] confirmed that the relative motion of adhesion points on these two friction surfaces leads to adhesive wear when the grain or grain group is taken away by shear or tension. Hence, the forming of BUE is also affected by the adhesive force between atoms by the plastic deformation which occurred in the actual contact area of friction surfaces. Considering all the evidence results when machining TiMMC, we confirm that the adhesive wear is the most important mechanism of the initial wear period under all experimental cutting conditions tested.

3.3.3 Initial tool wear at the transition period

For the wear mechanism discussed above, a smooth diffused layer appears around the transition period; see Figure 3-7(b) and (c). The adhesion layer on the cutting tool and the BUE are soluble mutually at elevated temperature. This layer exists within the cutting tool as a whole where it is involved in the machining process. Hence, the physical properties of the tool material are changed. On the other hand, several wear patterns such as tool layer damage, friction and adhesive wear occur simultaneously at the tool-chip interface; they react chemically with each other at elevated temperature. The diffusion wear is then generated due to the movement of a

substance from the chip formation with high concentration to the cutting edge as shown in Figure 3-8.

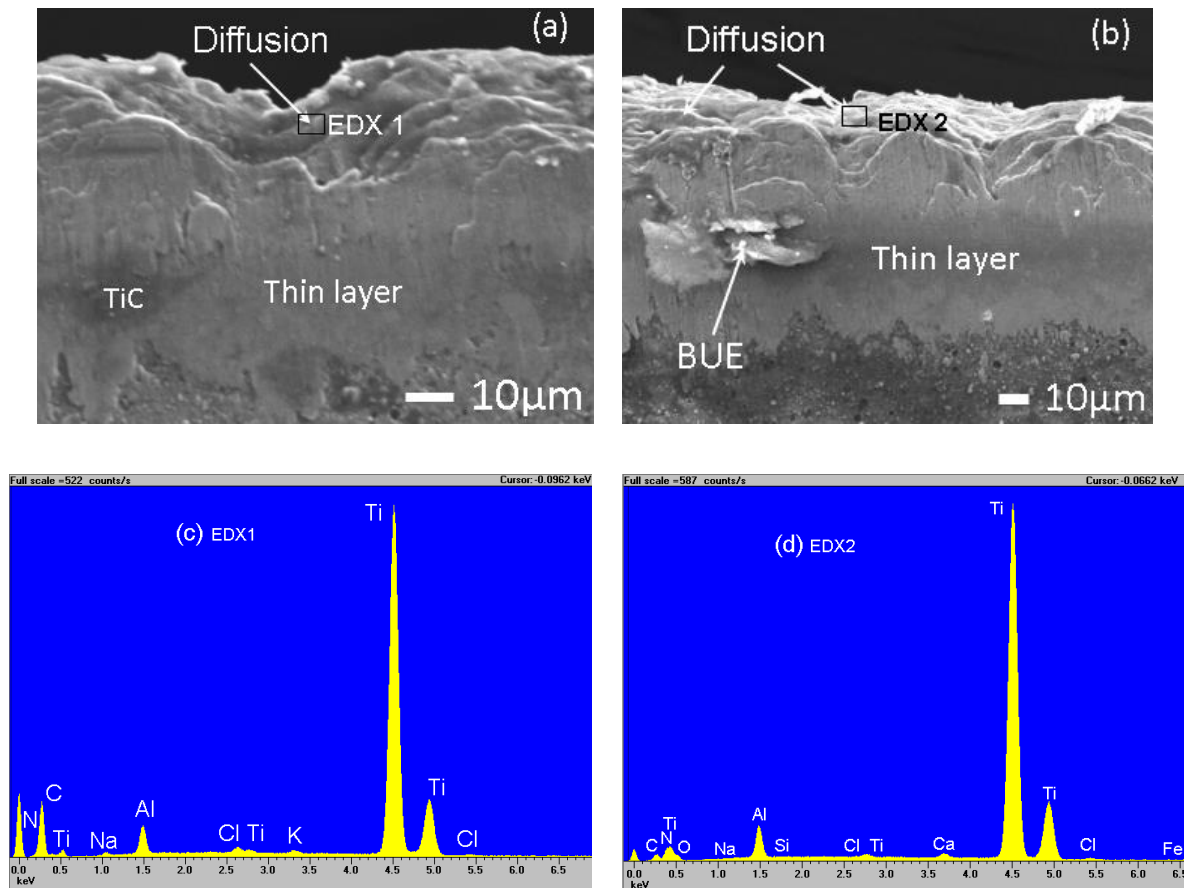


Figure 3-8: Tool wear mechanism close to the location of the transition point; (a) $V=20\text{m/min}$; (b) $V=60\text{m/min}$; (c and d) EDX analysis

The EDX analysis of the chemicals at the tool wears in the diffusion zone, Figure 3-8 (c) and (d), reveal a number of adhesions on the cutting edge including carbon elements that still exist under the form of titanium carbide and then dissolved within the tool layer. In particular, the hard TiC particles in the TiMMCs have not affected strongly enough to disable the adhesive wear. Hence we did not observe the abrasive wear any more until the flank wear land reaches the second wear region. In addition, the presence of nitrogen is evidence of the chemical wears, which the titanium and aluminum diffuses in the mass of the coating tool material of (Ti, Al)N and TiN. These adhesion materials tend to decrease at the transition period which the effect of chemical stresses at high cutting temperature has thus let to a hard thin layer. This layer is called

“brace wear” which the adhesive layer is formed as a whole at nanometer-scale as shown in Figure 3-9. This new wear form is a result of the combination of both wear mechanisms, the adhesive of titanium alloys and hard particles slide against machined surface of MMCs have also associated with the coating layer of (Ti, Al)N.

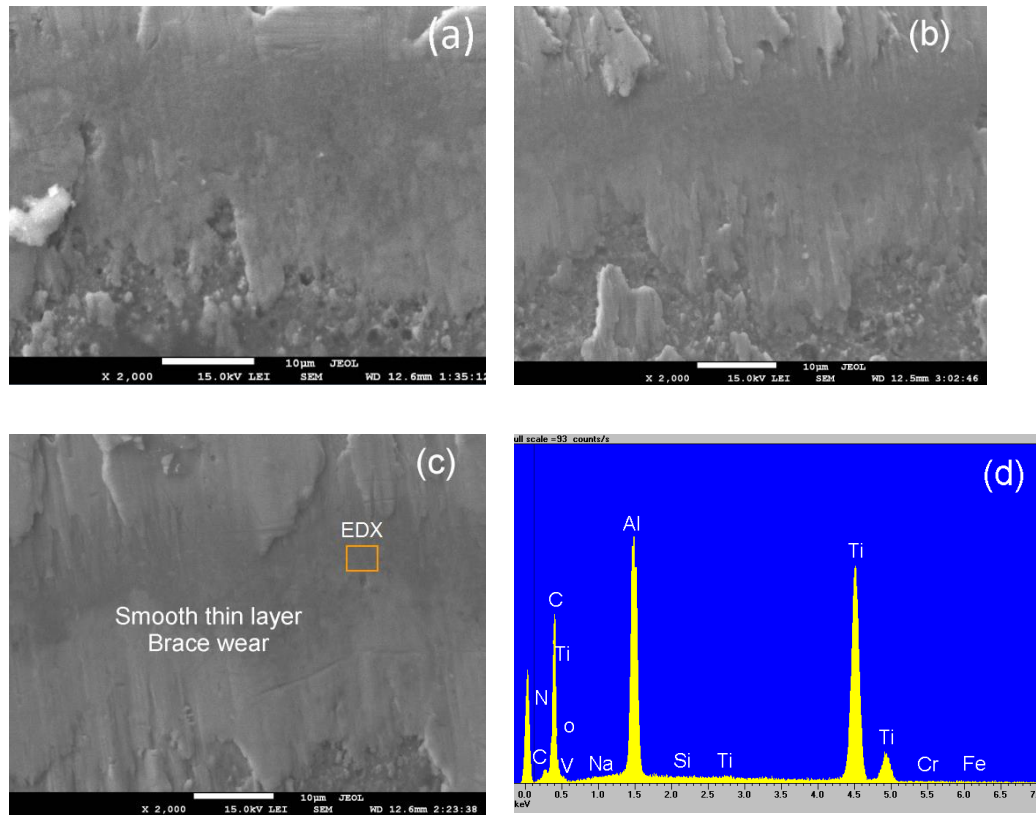


Figure 3-9: Brace wear at the location of transition wear period; (a) V=20m/min; (b) V=40m/min; (c) V=50m/min; (d) EDX analysis

The experiments were conducted repeatedly several times for each cutting condition. The brace wear was mostly found only from the end of the initial period, where the wear rate tends to decrease during machining process. The thicknesses of the brace wear are estimated to be in the range of 0.5 to 3 μm which is equal to the coating layer thickness of the inserts. By friction test and spectrograms, Calatoru et al. [89] also reported that the disappearance of the built up layer material on the cutting tool resulted in a polished surface as the surface was polished by the aluminum oxide particles formed by the oxidation of aluminum at high temperature. In the special case of initial tool wear when machining TiMMC, the transfer of atoms between the carbide tool and workpiece material depends on the level of chemical reactivity between the

elements [27]. These hard thin layers participate in the cutting on the workpiece material; they tend to decrease with the increase of flank wear land in the steady region. The formations of the brace wear at the first transition period could be considered as a 'wear shield' or protection layer since it lets us have a good explanation of the key question, why the wear rate suddenly decrease at the first point of the steady wear period and seem to maintain constant for a relatively long term as we have discussed in the previous section.

3.4 Conclusions

The initial wear behavior during machining of TiMMCs has been now investigated for the first time in the study of tool wear with the following original results:

The initial wear occurred from the first moment of cutting with extremely high wear rate. It was found to be less than only two seconds under cutting speed of 20 m/min and tends to increase to ten seconds maximum at higher cutting speed. The initial wear behavior during machining TiMMCs is the result of several wear mechanisms. At the first moment of machining, the effect of accelerated cutting force and temperature gradient lead to high stress and friction between the poorly conforming cutting tool and workpiece surfaces resulting in tool layer damage associated friction and tribological wear. The damage layer occurred during the first moment of machining with very high wear rate. On the other hand, the increasing of cutting force and temperature lead to micro welding and built-up-edges (BUE) form at the cutting edge. The effect of chemical stresses at high temperature was the main reason leading to the diffusion wear because the tool layer material reacts spontaneously with atmospheric oxygen and oxidizes the titanium and aluminum. Therefore, the adhesive wear is the most important mechanism during the initial wear period under all experimental conditions tested.

The adhesion layer damage of the cutting tool and BUE are soluble mutually at elevated temperatures. They still include the hard particles of TiC reinforcement in the workpiece material but these particles were not affected strongly enough to disable the adhesive wear within the first wear zone. Actually, the combination of these mechanisms, associated with the coating layer of (Ti,Al)N generated a new wear form as a whole involving in the machining process. The effect of TiC in the chemical wear that exists in the form of diffusion is then formed a new hard thin layer at the end of the initial wear period which is here called "brace wear" or "wear shield". By considering the experimental results, we believe that the wear shield is a protection wear layer for

the steady period. The appearance of the wear shield leads to the tool wear rate decreasing abruptly at the transition point between the first and second wear regions.

Acknowledgement

The authors would like to gratefully acknowledge the financial supported from Government of Vietnam - Ministry of Education and Training (scholarship scheme - Project 322). In addition, the Natural Sciences and Engineering Research Council of Canada (NSERC), and, Laboratory of GRDFP - Ecole Polytechnique Montreal are acknowledged for their contribution and partially supported.

CHAPTER 4 ARTICLE 2: CHAOTIC TOOL WEAR DURING MACHINING OF TITANIUM METAL MATRIX COMPOSITE (TiMMCs)²

The purpose of this chapter is to describe as clearly as possible the effect of initial cutting conditions on the tool life during machining TiMMCs based on the Chaos theory through our experimental results. The initial tool wear during machining of titanium metal matrix composite (TiMMCs) is the result of several wear mechanisms: tool layer damage, friction - tribological wear, adhesion, diffusion and wear shield. This phenomenon occurs at the first instant and extends to only ten seconds at most. In this case the adhesive wear is the most important mechanism while the brace wear is considered as a resistance wear layer at the beginning of the steady wear period. The effect of the initial tool wear and initial cutting conditions on tool wear progression and tool life is discussed. We proposed herein a new mathematical model based on the scatter wear and Lyapunov exponent to study quantitatively the “chaotic tool wear”. The Chaos theory, which has been proved efficient in explaining how something changes in time, was used to demonstrate empirically the dependence of the tool life on the initial cutting conditions and thus contribute to a better understanding of the influence of the initial cutting condition on the tool life. On the basis of our chaotic model, the scatter wear dimension and Lyapunov exponents were found to be positive in all case of the initial favorable cutting conditions including initial speed, feed rate and depth of cut. The initial cutting speed appears however as the most significant impact on tool life. In particular, the mathematical model was successfully applied to the case of machining TiMMCs. It was clearly shown that changing the initial cutting speed by 20 m/min for the first two seconds of machining instead of keeping it constant at 60 m/min during the whole cutting process leads to an increase in the tool life (up to 24%).

4.1 Introduction

Tool wear during machining is the result of complicated physical, chemical and thermo-mechanical phenomena. It has been widely evaluated through the wear curve which is commonly divided into three regions according to the increase of tool wear versus cutting time: initial wear,

² D. Xuan-Truong, M. Balazinski, R. Mayer, *Chaotic Tool Wear during Machining of Titanium Metal Matrix Composite (TiMMCs)*; ASME 2014 International Mechanical Engineering Congress and Exposition, American Society of Mechanical Engineers, 2014, pp. V02BT02A018-V002BT002A018.

steady and accelerated wear period [5, 37]. Among these wear regions, the first one was recently investigated by the author that initial wear occurs at the first instant and extends to only ten seconds when machining of TiMMCs. The wear mechanism at the first transition period is affected sensitively by the cutting conditions. Furthermore, the initial tool wear behavior and initial cutting conditions affect significantly the tool wear evolution and the entire tool life.

As a result, the effect of the initial wear and initial cutting conditions on the tool life is now of potential interest such the behavior is a good candidate. This is the most important for study the tool wear using chaos theory. Chaos is considered as an aperiodic long-term behavior that exhibits sensitive dependence on initial conditions [1]. It has been proved efficient in explaining how something changes in time [43]. A meteorologist, Edward Lorenz, first reported chaos theory in 1963 [39] when he was trying to predict the weather by computing equations. He found that even very little difference in the initial value leads ultimately to very different evolutionary paths after a certain period. This phenomenon was explained as sensitive dependence on initial conditions of a system, and has been known as the butterfly effect.

Chaotic phenomena have been found in many fields of engineering systems [47] and a number of models have been developed to discuss the chaotic behavior on the machining process. For example: chaotic dynamics of the cutting process [48, 51, 52], dynamics and chaos in manufacturing processes [46], chaotic and fractal dynamics [53], chaotic and stochastic dynamics of orthogonal metal cutting [54], controlling chaotic instability of cutting process [55] and chaotic vibrations in machining [56-58].

The application of chaos to analyze the tool wear during machining process has not been investigated yet. The effect of the initial tool wear on the tool life is similar to the influence of running-in or break-in period on the wear mechanism of engine-cylinder systems. They are all closely related to progressive wear [9-11]; hence control of the running-in process can thus extend the working life of engineering tribosystems as well as ensure stable operation [11]. By changing initial conditions, “good running-in” and “poor running-in” were investigated in the running-in behavior of tribological system; Freser et al. [13] reported that small different initial condition led to a significantly different in term of ultimate results for the wear track and wear area. Mezghania et al. [14] also confirmed that the texture change during running-in alters the performance and efficiency of a tribo-mechanical system.

Accordingly, the purpose of this research is to apply characteristics of chaos theory in investigating the effect of the initial condition, as well as initial wear behavior, on the tool life. We propose a mathematical model to quantitatively measure chaotic wear based on Lyapunov exponent and the scatter during machining. First, Lyapunov exponent and Fractal dimension will be described in order to identify the chaotic behavior in a system. Part of the work is then applying them to characterize how initial wear affect the tool life through scatter wears when cutting TiMMCs.

4.2 Modelling of Chaotic tool wear

4.2.1 Quantitative measures of Chaotic tool wear

There are several dimensions that can be used to describe a chaotic system and its attractors. The first mathematical model was discovered by Edward Lorenz when he studied the 3D-equation as given by Eq. (4-1) [39]; which has been extensively studied in the field of chaos theory and dynamical systems [40].

$$\begin{aligned} X' &= \sigma(Y - X) \\ Y' &= rX - Y - XZ \\ Z' &= XY - bZ \end{aligned} \tag{4-1}$$

where σ , r , b are positive real parameters. Based on the set of parameters $\sigma = 10$, $b = 8/3$, $r = 28$, Lorenz proved the system above is chaotic; this behavior was quantitative measure by a dimensional equation as given by Eq. (4-2). This chaotic attractor is depicted in Figure 4-1.

$$V_0(\tau_1) = e^{-\lambda(\tau_1 - \tau_0)} V_0(\tau_0) \tag{4-2}$$

where λ is considered as the quantitative dimension of the chaotic behavior. It is determined by Eq. (4-3) that represents an average rate of divergence or convergence of trajectories in the phase space.

$$\lambda = \frac{\partial X'}{\partial X} + \frac{\partial Y'}{\partial Y} + \frac{\partial Z'}{\partial Z} = -(\sigma + b + 1) \tag{4-3}$$

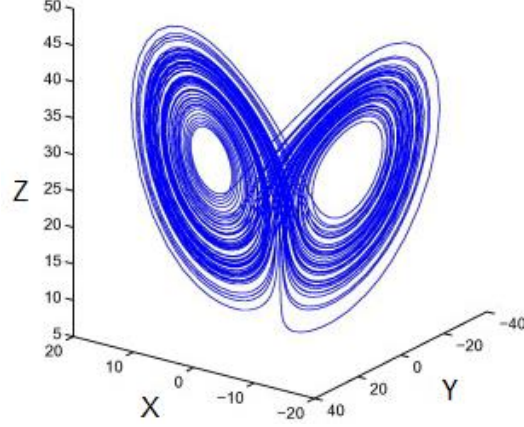


Figure 4-1: Dimensional projections of Lorenz attractor [42]

This so-called “butterfly effect” represents the sensitive dependence on initial conditions of the system. In other words, a small change of initial condition can result in a large effect later on.

The function of logistical, Eq. (4-4) can be given here as a representative example for the orbits measurement of the average rate of divergence or convergence of a typical trajectory; this is adapted from [1, 43, 44, 99].

$$x_{n+1} = f(x_n) \quad (4-4)$$

where the values x_n belongs to a finite interval, for $n \rightarrow \infty$ we consider how the point sequence $x_0, x_1, x_2, \dots, x_k, \dots$ differ from the point sequence $\{\bar{x}_n\} = \bar{x}_0, \bar{x}_1, \bar{x}_2, \dots, \bar{x}_k, \dots$ that evolves from a slightly modified initial condition $\bar{x}_0 = x_0 + \delta x_0$.

We have, in general,

$$\begin{aligned} \bar{x}_k &= x_k + \delta x_k \\ &= f(x_{k-1}) + \delta x_k \\ &= f(x_{k-1}) + f'(x_{k-1})\delta x_{k-1} + \dots \end{aligned} \quad (4-5)$$

After k iterations, by linearization of Eq. (4-5), we obtained the dimension as follows:

$$\delta x_k = f'(x_{k-1})\delta x_{k-1} \quad (4-6)$$

If we repeatedly apply the recursion rule, the Eq. (4-6) can be rewritten as:

$$\begin{aligned}\delta x_k &= f'(x_{k-1})f'(x_{k-2})\dots f'(x_0)\delta x_0 \\ &= \prod_{k=0}^{k-1} f'(x_k)\delta x_0.\end{aligned}\tag{4-7}$$

The distances of δx_k and δx_0 that calculate from Eq. (4-7) can be positive or negative depending on which value to be subtracted. In the case study, these distances are determined through scatter wear dimension. Therefore, we are interested their absolute values as the mean exponential divergence of neighbouring sequences of points. When $k \rightarrow \infty$ the Lyapunov exponent is defined as follows:

$$\lambda = \frac{1}{k} \lim_{k \rightarrow \infty} \sum_{i=0}^{k-1} \ln |f'(x_i)|\tag{4-8}$$

In addition, the Lyapunov exponent is closely related to the fractal dimension by Eq. (4-9) [72].

$$D = j + \frac{\sum_{i=1}^j \lambda_i}{|\lambda_{j+1}|}\tag{4-9}$$

Fractal geometry has been known as an object that displays self-similarity at various scales. The fractal dimension (D) is defined as a parameter used for representing accurately shapes by means of a simple equations as given by Eq. (4-10) [71].

$$D = \lim_{\varepsilon \rightarrow 0} \frac{\ln N(\varepsilon)}{\ln(1/\varepsilon)}\tag{4-10}$$

where $N(\varepsilon)$ is the number of self-similar pieces (number of new facsimiles); ε is the magnification factor or scaling ratio.

More importantly, the relationship between fractal dimension and tool wear during machining process has been reported. Kang et. al. [79] used the fractal dimension to characterize tool wear volume by Eq. (4-11)

$$D = \lim_{\varepsilon \rightarrow 0} \frac{\log \left[\int_{x \in \Gamma} g(x) d\mu(x) \right]^{\frac{1}{v}}}{\log \varepsilon} \quad (4-11)$$

where V is the tool wear volume loss during machining, it is calculated by Eq. (4-12), ε is scaling ratio of the total measuring length. Further information of the fractal dimension dealing with tool wear can be found within: analyzed wear area contact [100, 101] and adhesive wear in normal contact [81, 85, 87, 102].

$$V = \int_{x \in \Gamma} g(x) d\mu(x) \quad (4-12)$$

4.2.2 Chaotic tool wear modeling

In order to characterize the sensitivity to the initial cutting condition of the tool wear during machining, this section aims to develop a new model based on the Lyapunov exponent to quantitative measure a chaotic signal of tool wear. First of all, the divergence or convergence of the wear curves is defined by a scatter wear dimension of δ_{VB_i} . This dimension determines how differences in the tool wear evolution over time and tool life between a reference of wear curve and others. Part of the work then to calculate the Lyapunov exponent (λ) based on this scatter wear dimension during machining.

The λ has been widely determined through the average rate of divergence or convergence of two neighboring trajectories in the phase space. We therefore consider herein two trajectories of two wear curves progression over time during a machining process; (a reference and a neighbor) as shown in Figure 4-2.

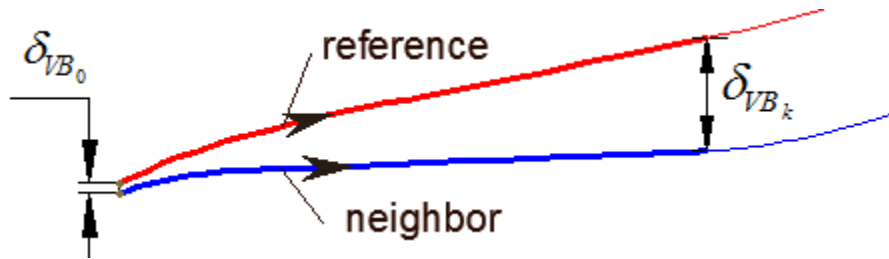


Figure 4-2: Two trajectories evolution in a phase space

Assume that both two trajectories start at very small different initial condition of δ_{VB_0} . If t_0 is considered as the initial cutting time of the reference wear curve, a nearby point of δ_{VB_0} is the initial condition for the neighbor curve. It is noted that the initial separation of δ_{VB_0} is extremely small and can be described by a function of cutting time and flank wear land; δ_{VB_k} is variation of scatter wear at t_k cutting time.

The property of sensitivity to initial conditions of the tool life can be quantified by the divergent exponential rate of the initially close trajectories. According to the rule of Eq. (4-2) and Eq. (4-8) the scatters wear dimension and Lyapunov exponent are defined by Eq. (4-13) and Eq. (4-14) respectively.

$$|\delta_{VB_k}| \approx |\delta_{VB_0}| e^{k\lambda} \quad (4-13)$$

$$\lambda = \lim_{k \rightarrow \infty} \left(\lim_{\delta_{VB_0} \rightarrow 0} \frac{1}{k} \ln \left| \frac{\delta_{VB_k}}{\delta_{VB_0}} \right| \right) \quad (4-14)$$

where the initial condition δ_{VB_0} depends on the cutting parameters including the cutting speed, feed rate and depth of cut; λ is the Lyapunov exponent. As a result, a model of the chaotic tool wear is proposed to investigate how significant dependence on initial cutting conditions of the tool life as shown in Figure 4-3.

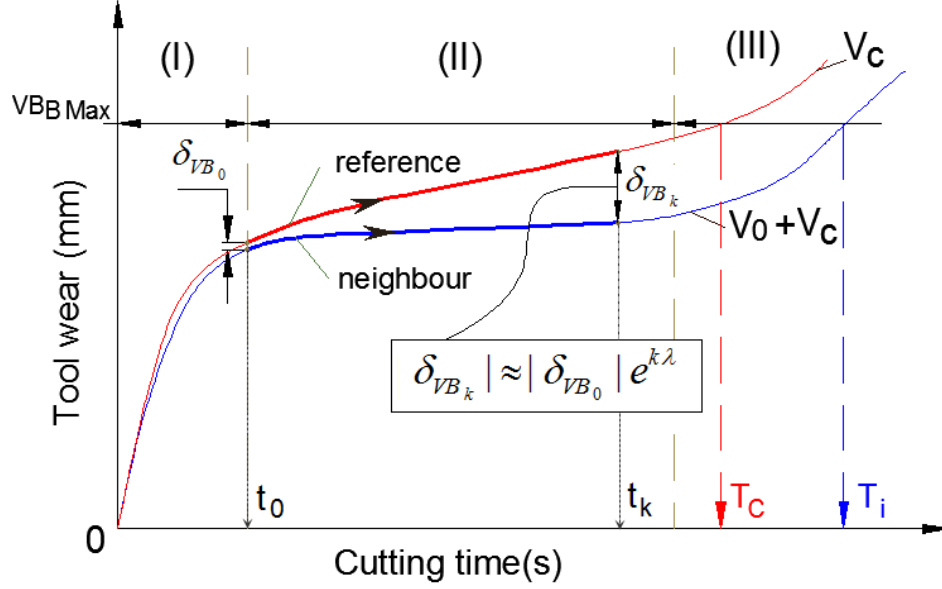


Figure 4-3: Chaotic tool wear modeling

The Lyapunov exponent in this case represents rate of the wear curve separation during cutting process; it depends on the initial cutting condition of δ_{VB_0} . On the other hand, the progression of λ provides a quantitative diagram of the chaotic system. Therefore, results of the Eq. (4-14) can be separated into three temporal patterns: $\lambda < 0$, $\lambda = 0$ and $\lambda > 0$.

When $\lambda > 0$ the system is unstable and the tool wear during machining is chaotic. The trajectories of such tool wear evolution in time and tool life are highly sensitive to changes of the initial conditions. On the contrary, $\lambda < 0$ belong to a periodic orbit of steady wear stage; while $\lambda = 0$ in accordance with neutral of fixed point when nothing change of two experimental wear curves.

4.3 Experimentation

The machining tests were performed on a CNC turning center Mazak QT-Nexus-200. The workpiece material was TiMMCs which has been reported as an extremely difficult-to-machine material [15, 17]. The mean Rockwell hardness of the TiMMCs was 40 HRC with the physical properties as given by Table 4-1. The cutting tools used in all experiments were PVD coated (Ti,Al)N+TiN manufactured by SECO with the following specifications: rake angle $\gamma_0 = -6^\circ$, back rake angle $\gamma_p = -6^\circ$, nose radius $r_\epsilon = 1/32$ in, tool included angle $\epsilon_r = 80^\circ$, tool cutting angle $\kappa_r = 95^\circ$ and the insert thickness $s = 3/16$ in.

Table 4-1: Physical properties of TiMMCs [15]

Density	4500 kg/m ³
Yield strength	1014 MPa
Tensile strength	1082 MPa
Elastic modulus	135 GPa
Shear modulus	51.7 MPa
Thermal conductivity	5.8 W/mK
Specific heat	610 J/kgK

The experiments were devised in two stages. The first one is to determine the tool life during machining of TiMMCs in general. The cutting conditions in this case are performed under different speeds in the range of 20 to 60 m/min whereas feed rate and depth of cut were kept constant at 0.15 mm/rev and 1.5 mm respectively. The tool wear progression is observed on the wear curves where the flank wear values are measured after certain cutting time by using an optical microscope and a high resolution digital camera connected. The tool wear mechanism is analysed by using a Scanning Electron Microscope (SEM) and an Energy Dispersive X-ray (EDX).

The initial wear mechanism during machining of TiMMCs has been investigated in our previous study; it is further investigated in the current work. In order to study the effect of the initial cutting condition, as well the initial wear mechanism on the wear evolution over time and tool life several strategies for the initial condition of machining TiMMC were applied. Therein, the initial cutting speed strategy is specially taken into consideration.

4.4 Results and discussion

4.4.1 Initial tool wear during machining process

Titanium metal matrix composites (TiMMCs) have been extensively used in various manufacturing in aerospace and automotive industries; due to their high strength, stiffness, and

creep resistance at elevated temperature. However, TiMMCs have been classified as one of the most difficult to machine materials.

When machining TiMMCs, abrasive wear has mostly been reported [17, 34], because tool wear depends on the nature and percentage of the hard particles reinforcement inside the composite [36]. However, within our special case of the initial wear period, the adhesive wear plays an important role under all experimental condition. At the instant cutting of 0.05 sec, the initial wear behavior is a result of the complicated mechanism between layer damage, friction and tribological wear as shown in Figure 4-4(a).

The rare appearance of the abrasive wear was explained by the increase of cutting force resulting in high contact stress and high friction between poorly conforming surfaces at the tool–workpiece interface under dry cutting condition.

In addition, the low thermal conductivity and high reactivity of titanium alloys is the main reason that leads to increased cutting temperature at the tool-workpiece-chip interface [7, 25]. Based on the EDX analyse, we observe a number of adhesion materials on the cutting edge. They included the coating layer of the insert where the presence of the Ti, Al and N elements is rich. These elements then react spontaneously with atmospheric oxygen and oxidized of the titanium and aluminum; they diffuse from the coating layer and the TiMMCs at high pressure and elevated temperature. As a result, the plastic deformation leads to a micro welding and built-up-edge (BUE) formed at the cutting edge under all cutting condition, Figure 4-4(b).

Figure 4-4(c) shows the wear mechanism close to the location points of the transition period. We found that a thin layer is formed at the middle of the adhesion area along the cutting edge whereas diffusion still remained at low speed.

Our previous studies have shown that this layer exists where the cutting tool is involved in the machining process which is the result of the diffusion between the adhesive of the titanium alloys and hard particles sliding against the machined surface of MMCs combining with the coating layer of (Ti,Al)N at high pressure and elevated temperature. The so-called “brace wear” of this thin layer is then formed as a new wear form at the transition wear period. The brace wear has been shown by the authors to be a resistance wear layer for the steady wear period. The formation such a new protective layer at the beginning of the steady wear region has contributed to a better understanding of the tool wear progression over time when machining TiMMCs. This

interesting result will thus serve in the next section to study the influences of the initial wear and its condition on the tool life.

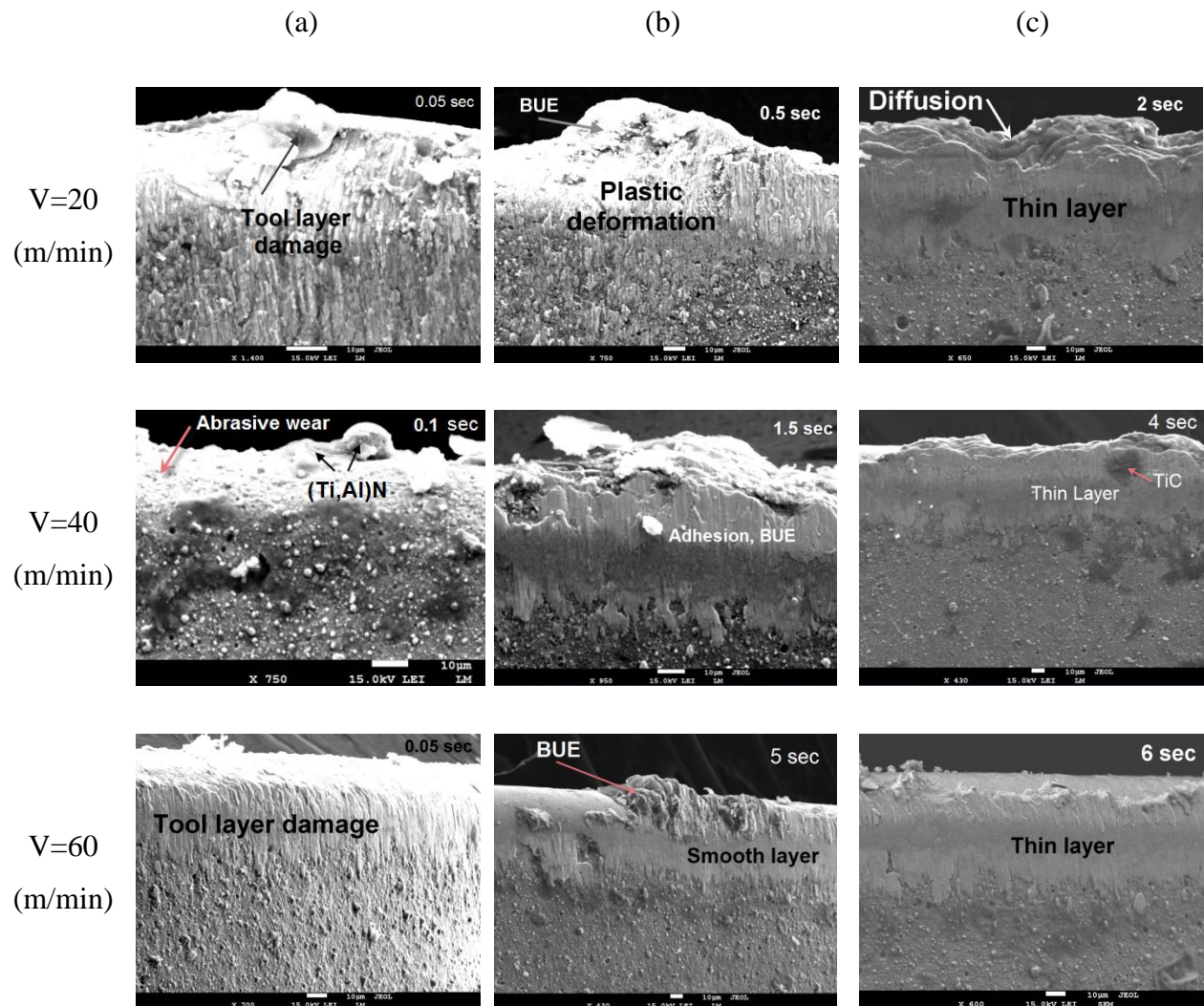


Figure 4-4: Initial tool wear mechanism on the clearance face during machining of TiMMCs

Figure 4-4(c) shows the wear mechanism close to the location points of the transition period. We found that a thin layer is formed at the middle of the adhesion area along the cutting edge whereas diffusion still remained at low speed. This layer exists where the cutting tool is involved in the machining process which is the result of the diffusion between the adhesive of the titanium alloys and hard particles sliding against the machined surface of MMCs combining with the coating layer of (Ti,Al)N at high pressure and elevated temperature. The so-called “brace wear” of this thin layer was formed as a new wear form at the transition wear period. The brace

wear has been shown by the authors to be a resistance wear layer for the steady wear period. The formation such a new protective layer at the beginning of the steady wear region has contributed to a better understanding of the tool wear progression over time when machining TiMMCs. These interesting results will thus be served in the next section to study the influences of the initial wear and its condition on the tool life.

4.4.2 Chaotic tool wear during machining of TiMMCs

As discussed above, the initial wear behavior and initial cutting condition have affected significantly the tool wear progression. There are a number of initial cutting parameters that can contribute to the chaotic model. Therefore, they are all can be used to quantify any sensitivity of the tool life to the initial conditions. Based on the chaotic modeling developed above, the experiments are carried out with three variables for the different initial cutting condition. The dimension that describes the average rate of divergence or convergence of the scatter wear curve is defined to calculate the Lyapunov exponent.

According to the initial wear behavior and specially its wear mechanism at the transition period previously discussed, the initial condition strategies would be applied for less than two seconds of machining. It is believed that this initial period is enough to obtain the positive value of a scatter wear exponent. In addition, the wear rate at low speed is better maintained constant during the steady wear period after only two seconds of the cutting time. Specially, when the brace wear had occurred as protection layer.

As a result, we apply here three strategies of initial condition during the first two seconds of machining, as given in Table 4-2. Among the three strategies, the first one is to change the initial cutting speed. During the first two second machining, the speed of $V_0=20$ m/min was used; then increase and kept constant at $V_c=60$ m/min while the feed rate and depth of cut are constant at 0.15 mm/rev and 1.5 mm respectively. Similar to the first one, the second and third strategies concern the changing of the initial feed rate and depth of cut. Each machining test is designed equal volume of metal removed.

Table 4-2: Experiment for the different initial condition strategies

No.	V _c (m/min)	f (mm/rev)	a _p (mm)	Time (sec)
1	20	1.5	1.5	(0 - 2)s
	60	1.5	1.5	after 2s
2	60	0.05	1.5	(0 - 2)s
	60	0.15	1.5	after 2s
3	60	0.15	0 - 1.5	(0 - 2)s
	60	0.15	1.5	after 2s

The machining tests were conducted several times for each different initial cutting condition and the final results averaged. Accordingly, the tool life of T_c , T_1 , T_2 , T_3 are generated corresponding with the regular machining, the first, second and third among experiment strategies as shown in Figure 4-5. As seen here, the tool life increased by 12.5%, 17.2% and 24.2% for condition strategy of No. 3, 2 and 1 respectively.

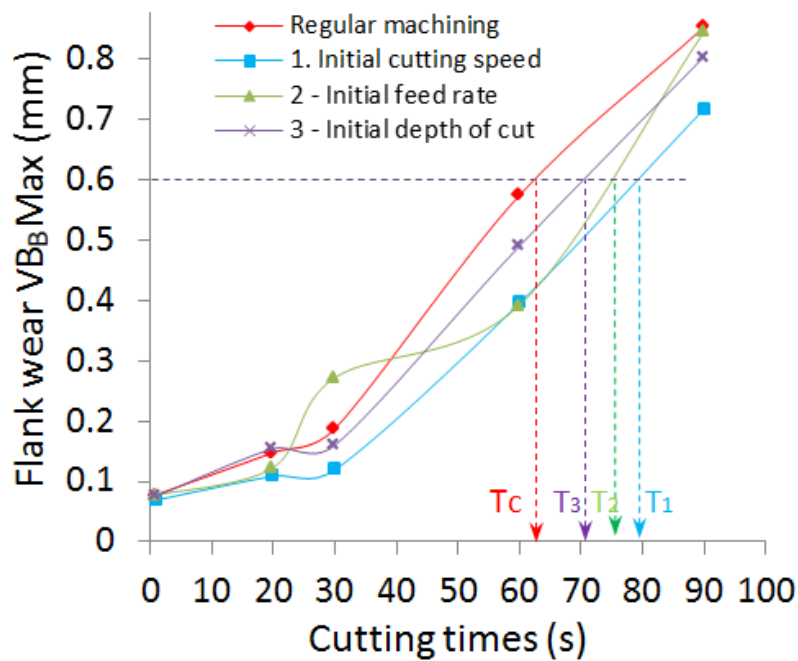


Figure 4-5: Cutting tool life for different initial conditions

As a result, for the strategy No.1 of the initial cutting speed we obtained the best of tool life, 24.2% improved. The initial cutting speed is one of the most important factors affect the wear evolution over time. Hence, the effect of the initial cutting speed on the tool life is paid much attention in our chaotic wear model.

Applying the scatter wear and Lyapunov exponent to the chaotic modeling, we have achieved the maximum of the scatter wear dimension as given in Table 4-3. In addition, the initial dimensions that belong to the different cutting conditions between the reference and neighbor are determined by δ_{VB_0} . The scatter wear dimensions are determined as shown in Figure 4-6. Therein, the tool wear is significant improved under all experimental conditions.

Table 4-3: Scatter wear dimension during machining of TiMMCs

Scatter wear exponents			
t_i (sec)	No. 1 ($v_0 + v_c$)	No. 2 ($f_0 + f_c$)	No. 3 ($a_{p_0} + a_p$)
δ_{VB_0}	0.0090	0.0004	0.0025
20	0.0391	0.0247	-0.0066
30	0.0683	-0.0846	0.0274
60	0.1791	0.1825	0.0841
90	0.1359	0.0082	0.0494

In this case, the sensitivity to initial cutting speed of the tool life is well explained by the protection layers of the wear shield; where the atoms of the substrate materials and the adhesive layer are formed as a whole at nanometer-scale and are involve in the machining process.

However, the sensitivity to the initial conditions of chaos is aperiodic for the long-term behaviors in a deterministic system [103]. Therefore, it is impossible to predict accurately for the long term behavior of the tool life; because of the exponentially developing distance between wear curves later on which leads to the failure of the cutting tool in the third wear region.

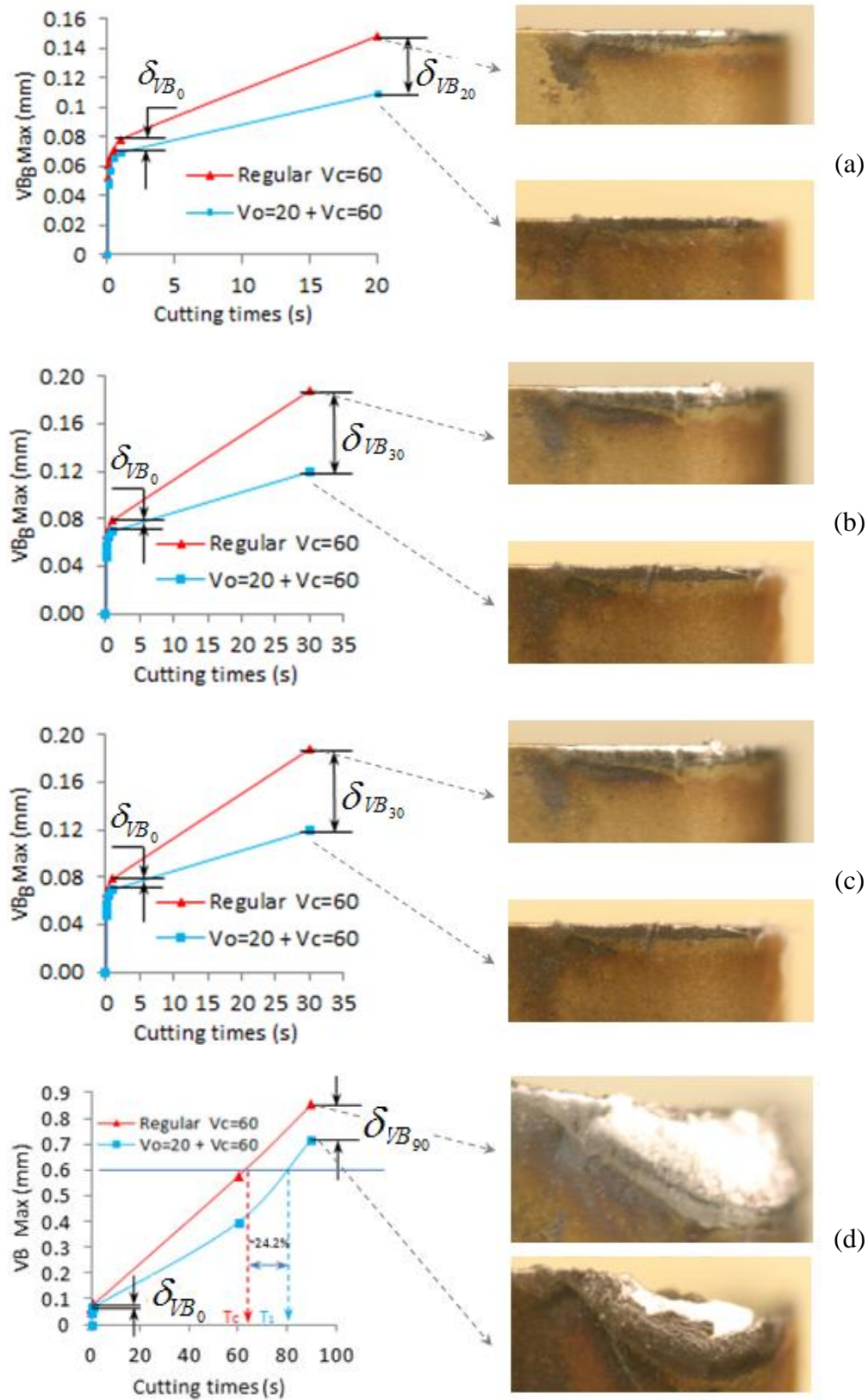


Figure 4-6: Scatter wear dimension; (a) after 20s, (b) - 30s, (c) - 60s and (d) after 90s

4.5 Conclusions

The so-called “chaotic tool wear” model which is proposed for the first time in this work has revealed that the initial tool wear and initial cutting conditions affect significantly the tool wear evolution and the entire tool life. The initial tool wear occurs at the first instant and extends to only ten seconds at most when machining TiMMC; while the adhesion mechanism plays a critical role under almost all experimental cutting conditions in the initial wear period.

The sensitivity to initial cutting condition of the wear evolution and tool life is quantitative measured through the scatter wear dimension and the Lyapunov exponent. By changing the initial cutting condition for the first two seconds of machining, as a good initial cutting condition for the cutting speed, feed rate and depth of cut, the tool life has improved in all cases of our tested strategies. However, the initial cutting speed is one of the most significant factors towards the tool life.

As a result, the effect of the initial wear period on the tool life has been explained by the sensitivity of the tool life to the initial cutting conditions. The formation of a “brace wear” at the transition period has been considered as a protection layer within the chaotic wear model. The initial wear behaved more importantly in the case of difficult-to-cut materials such the TiMMCs due to their fast tool wear and relatively short tool life.

Applying the chaotic model to machining TiMMCs with a very small difference in the initial conditions for the first seconds of machining, $\delta_{VB_0} = 0.009, 0.0004$ and 0.0025 mm; ultimately may lead to a tool life improvement of 24.2%, 17.2% and 12.5% respectively. Based on the scatter wear dimension, values of the lyapunov exponent can be found positive in all case of our tested initial cutting conditions such as initial speed, feed rate and depth of cut. It is therefore believed that the tool wear during the machining process exhibits sensitivity on initial cutting conditions.

Acknowledgement

The authors would like to gratefully acknowledge the financial supported from The Vietnam government through the Project 322 “Training scientific and technical cadres in institutions overseas with the state budget”.

CHAPTER 5 ARTICLE 3: A NEW CONCEPT FOR TOOL WEAR DURING MACHINING PROCESS BASED ON CHARACTERISTICS OF CHAOS THEORY ³

A novel method to investigate tool wear during machining process is presented within this chapter 5. Part of the work will be presented at the VMPT 2015 conference (June 2 – 5 2015 UBC Vancouver, BC; Canada) ⁴. As discussed in the previous chapters, the initial wear behavior or break-in wear period plays an important role towards the engineering wear system; nevertheless no references were found in literature dealing with the effect of initial tool wear behavior to the tool life during a machining process. Chaos theory, a well-known mathematic one has been proven efficient in analyzing how something changes in time and predicting the behavioral change, is applied for the first time to analyze the tool wear during a machining process. We endeavor to develop herein a novel mathematical model to study the dependence of the tool life on the initial cutting conditions. Multistep method and Cubic B-splines collocation methods are used to solve an ordinary differential equation for quantifying a chaotic tool wear during machining process.

Both experimental and numerical results show that even such a relatively simple model of the tool wear system could exhibit the sensitive dependence on initial conditions of the tool life. A new concept of tool wear during machining process, entitled: “chaotic tool wear” is thus discussed through the relationship between the tool wear, Lyapunov exponent and fractal dimension. The chaotic tool wear provides a full explanation of the wear rate behavior at the first initial wear period and equally brings more insight on how the tool life depends significantly on the initial cutting conditions. More importantly, application of the chaotic tool wear model to change initial cutting conditions when machining TiMMCs improved the tool life by up to 24.5%. The success in development of that new concept in our research should leave open

³ D. Xuan-Truong, M. Balazinski, R. Mayer, *A New Concept for Tool Wear during Machining Process Based on Characteristics of Chaos Theory*, International Journal of Machine Tools and Manufacture; May (2015); Ref. No.: IJMACTOOL-D-15-00438, *under review*.

⁴ D. Xuan-Truong, M. Balazinski, R. Mayer, *A Novel Method to Investigate Tool Wear and Tool Life during Machining Process Based on Characteristics of Chaos Theory*, accepted for presentation at the 4th International Conference on Virtual Machining Process Technology (VMPT 2015) UBC, Vancouver, BC; June 2-5, 2015.

another alternative for the study of tool wear during machining process with the purpose of controlling the precision of machining and reducing manufacturing cost.

5.1 Introduction

In 1963, Edward Lorenz reported the first chaotic attractor in a three-dimensional autonomous system when he studied the atmospheric convection by deterministic ordinary differential equations [39]. He found that even a little difference in the initial value leads ultimately to significantly different behavior later on; this phenomenon was explained as sensitive dependence on initial conditions of the system and has been known as the butterfly effect [41, 42]. Nowadays, chaos is considered as an aperiodic long-term behavior and exhibits sensitive dependence on initial conditions in a deterministic system [1]; it is increasingly attractive for a range of applications in engineering [2, 45-47]. Indeed, chaos theory refers to the dynamical systems; hence most researchers in the fields of machining [1, 46, 48] and mechanical friction [49, 50] have investigated the chaotic behavior in dynamical or complex systems. However, the chaotic motion can be found in relatively simple systems [59]. For example, Buff and Cheritat [4] proved the existence of quadratic polynomials with a Julia set of positive area that can be used to quantify a signal of chaos in a system. In particular, the application of chaos was proved efficient in explaining how something change over time and predicting the behavioral change in a system [43]. The prediction based on the characteristics of chaos was recently developed and applied not only to the short term but also the long-term behavior of numerous technical systems [2], even to predict something deemed unpredictable [3].

More recently Duong et al. [93] used the sensitive dependence on the initial conditions to explain the dependence of the tool life on the initial cutting conditions. In particular, using small initial cutting conditions including initial speed, initial feed rate and initial depth of cut within the first wear period improved the tool life when machining the TiMMCs. In this case, the chaotic motion in the tool wear system was found relatively with the positive values of the largest Lyapunov exponent (λ). However, λ was calculated empirically through scatter wear; the model has therefore difficulties in determining a good initial conditions as well as investigating how exactly is the tool life affected by initial cutting conditions. On the other hand, most mathematical model investigating chaotic behavior have been used for non-linear or complicated

system; chaos theory has not been applied to cutting tool wear so far. It is thus worth developing a new mathematical model to investigate chaotic tool wear during a machining process.

In general, λ measures the rate of exponential divergence between neighbouring trajectories in the phase space to quantify the chaotic motion in a system [60]. It can be determined by ordinary differential equations [42]. Hence, the influence of initial conditions of a deterministic system can be described by a fractional differential equation [61, 62]. Unfortunately, solving these equations for the dynamical system to calculate the Lyapunov characteristic exponents is very complicated even though numerous classical numerical methods including Runge–Kutta methods and the multistep methods have been developed for solving the initial condition problems of the ordinary differential equations [63, 64]. Trigeassou et al. [65] developed the Lyapunov exponent to study the stability of fractional differential equations that allows the definition of an elementary Lyapunov function. By utilizing a least square approximation of spatial-dependent factors, Bajcinca et al. [66] solved numerically various classes of differential equations with orthogonal polynomials. The algorithm for approximating solutions to differential equations has also been supported by Ahmed [67] and Mittal et al. [68] when they studied the Bernstein polynomial. These B-spline methods are indeed linear multistep methods based on non-uniform meshes [69]. Mittal et al. [70] applied cubic B-splines for spatial variable and its derivatives which produce a system of first order ordinary differential equations. They have reported that the approximation solution using B-spline to these equations have a good agreement with the known exact solution. Accordingly, the B-spline functions of rational interpolation can be used to characterize properly the wear curve trajectories during machining process.

In order to investigate how sensitively is the tool life affected by the initial cutting conditions the chaotic tool wear [93] should be quantified numerically. In this case, the wear curves that are being used to calculate the Lyapunov exponents need to be characterized by a continuous function. Accordingly, in this study a new mathematical model is developed to quantify properly the chaotic tool wear during a machining process. First, the divergence of the chaotic wear curves under different initial cutting conditions is modelled by ordinary differential equations and expressed by a cubic B-spline function of rational interpolation. In addition, the variations in tool wear rate under the different initial cutting parameters are assessed by a fractal dimension. As a result, the Lyapunov exponents with respect to the scatter wear are then determined at any time of the cutting process; the nature of chaotic tool wear is finally analysed

and quantifies the sensitive dependency on the initial cutting conditions of the tool life. To the best of our knowledge, this is the first study on rational interpolation dealing with chaos and tool wear during the machining process.

5.2 Chaotic tool wear modelling

The sensitive dependence on initial conditions means by chaos has suggested the use of chaos theory to explain effect of initial cutting conditions on the tool life in our previous work [93]. Therein, a chaotic model of wear during the machining process has allowed quantifying the evolution of wear under different initial conditions as shown in Figure 5-1.

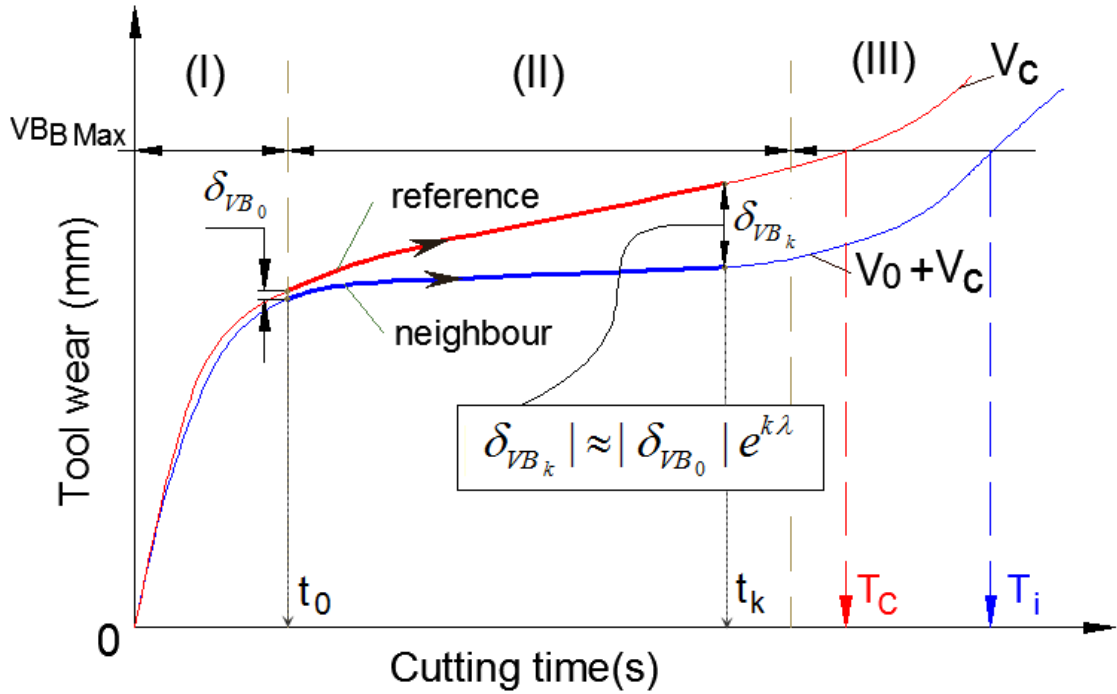


Figure 5-1: Chaotic tool wear modeling [93]

Scatter wear at cutting time t_k is calculated intuitively as sensitivity on initial cutting conditions, they are expressed by Eq. (5-1)

$$|\delta_{VB_k}| \approx |\delta_{VB_0}| e^{k\lambda} \quad (5-1)$$

where δ_{VB_k} is the scatter wear dimension at cutting time t_k and represents the divergence of the wear curves under difference initial cutting conditions δ_{VB_0} , λ is the Lyapunov exponent. The largest positive value of λ quantifies a chaotic motion in a system [72] by controlling the rate of

exponential divergence between the two trajectories in the phase space. As a result, the evolution over time of the wear curves which started very close together, then diverge rapidly from each other and become completely different at the maximum tool wear (VB_{Bmax}). Thus, we obtain the different tool life T_c and T_i , see Figure 5-1.

Assuming $\delta_{VB_k} \rightarrow \infty$ and $\delta_{VB_0} \rightarrow 0$, λ is determined by Eq. (5-2) [93]

$$\lambda = \lim_{k \rightarrow \infty} \left(\lim_{\delta_{VB_0} \rightarrow 0} \frac{1}{k} \ln \left| \frac{\delta_{VB_k}}{\delta_{VB_0}} \right| \right) \quad (5-2)$$

By this model, the chaotic tool wear was discussed with positive values of the Lyapunov exponent and the tool life increases for favorable initial starting conditions. However, the calculation of the initial parameters to have good initial cutting conditions is far from simple. The initial cutting parameters were designed regarding to the cutting time t_0 ; it thus may reduce gradually the productivity when machining under different cutting conditions at the same limitation of time within the chaotic wear model [93]. This is because the wear volume removal depends significantly on the cutting parameters [104]. In addition, the Lyapunov exponent was calculated empirically on an experimental wear curve; so we cannot determine properly their values at any interval cutting time. Therefore, to deal with the mentioned problems above it is important to develop a new mathematical model to solve the chaotic wear models both empirical and numerically. First, a wear curve during machining process is modeled by a mathematical equation that being characterized by continuous functions. We are then able to calculate exactly the scatter dimension and Lyapunov exponent at any period of cutting time during a machining process.

5.2.1 Chaotic wear curve definition

In order to investigate a chaotic behavior in the tool wear system, the sensitive dependence of the tool life on the initial conditions should be expressed, such as: how tool wear rate varies with the different initial cutting conditions? In the case study, we focus on how much tool life changes under slight changes of initial cutting conditions. In order to describe the processes of chaotic wear behavior, our current work is motivated by the fact that actual wear curve divergence changes with initial cutting parameters. Due to a wear curve evolution depends on

cutting conditions [90, 104] and the tool life is influenced by initial cutting parameters [93]; we thus consider herein an ordinary differential equation, Eq. (5-3) to characterize and investigate empirically a scatter wear variation under different initial cutting conditions.

$$\begin{cases} \frac{\partial y}{\partial t} = \xi(t, y(t)) \\ y = f(t_0, y_0) = \partial_{VB_0} \end{cases} \quad t \in [t_0, Tc] \quad (5-3)$$

where function $y(t)$ are dimensional vectors in phase space of tool wear and cutting time, $y = f(t_0, y_0) = \partial_{VB_0}$ are initial conditions. In the case study, the chaotic wear behavior is considered within interval $t \in [t_i, Tc]$, $i = 0, 1, 2, k, \dots$, and Tc is the tool life during a machining process.

Solving the Eq. (5-3) for the different initial conditions mean that we need to find all functions $y = y_i(t)$ such that at each point of the interval $t \in [t_i, t_{i+1}]$; so the solution of the differential equation (5-3) can express by given by Eq. (5-4).

$$y = y_i(t) = \begin{bmatrix} y_1(t) \\ y_2(t) \\ \vdots \\ y_n(t) \end{bmatrix}, \quad \xi(t, y(t)) = \begin{bmatrix} \xi_1(t, y(t)) \\ \xi_2(t, y(t)) \\ \vdots \\ \xi_n(t, y(t)) \end{bmatrix} \quad (5-4)$$

The function $\xi(t, y(t))$ does not depend explicitly on the independent variable t , as in the case of an iterative one dimensional discrete system, Eq. (5-5) [43, 44]

$$t_{n+1} = f(t_n), \quad t \in [t_0, Tc] \quad (5-5)$$

where the values t_n belong to a finite interval. For $n \rightarrow \infty$ we consider how the point sequence $t = \{t_i\}$ differ from the point sequence $t' = \{t'_i\}$ that evolves from a slightly modified initial condition $t'_0 = t_0 + \delta t_0$. After k iterations, using Taylor's theorem [105] to give an approximation of a k times differentiable function around a given point by (k^{th}) order, we obtain

$$t'_k = t_k + \delta t_k = f(t_{k-1} + \delta t_{k-1}) = f(t_{k-1}) + f'(t_{k-1})\delta t_{k-1} + \dots \quad (5-6)$$

By linearization of Eq. (5-6) and repeatedly applying the recursion rule, the scatter dimension from Eq. (5-1) is now determined by the following function, Eq. (5-7)

$$\delta t_k = f'(t_{k-1})\delta t_{k-1} = f'(t_{k-1})f'(t_{k-2})\dots f'(t_0)\delta t_0 = \prod_{k=0}^{k-1} f'(t_k)\delta t_0 \quad (5-7)$$

From Eqs. (5-1) and (5-7) the mean exponential divergence of the scatter wear is determined by Eq. (5-8).

$$e^{k\lambda} = \prod_{i=0}^{k-1} f'(t_i) \quad (5-8)$$

By applying the algorithm to Eq. (5-8), the Lyapunov exponent λ is defined base on the one dimensional discrete map, as given by Eq. (5-9).

$$\lambda = \frac{1}{k} \lim_{k \rightarrow \infty} \sum_{i=0}^{k-1} \ln |f'(t_i)| \quad (5-9)$$

When changing even a small amount of initial cutting conditions, we encourage ensuring all experimental strategies to be performed under the same volume removed material. It means that machining under different initial cutting conditions, the initial cutting time t_0 of each experimental stage would certainly be different. Therefore, the initial conditions are taken into account both scatter wear ∂_{VB_0} and cutting time t_0 . On the other word, the initial conditions ∂_{VB_0} depend on both initial cutting time δt_0 and scatter wear dimensions δ_{VB_0} as shown in Figure 5-2.

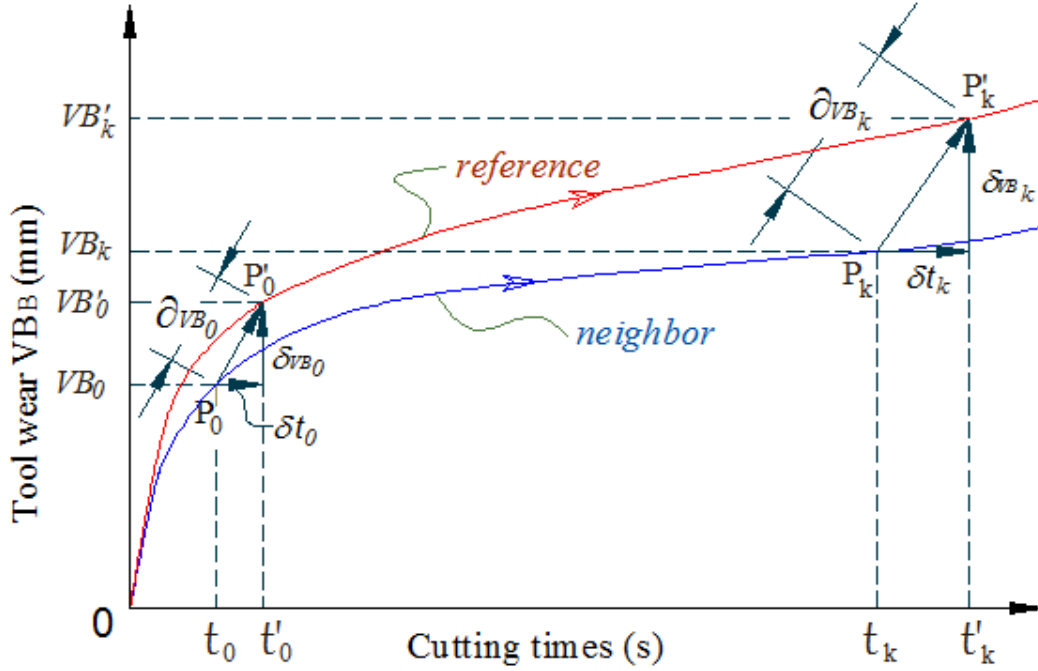


Figure 5-2: Scatter wear dimension and chaotic wear curve definition

In general, the separation between two points is measured by the distance between the two points; however, in the case study, for example the δ_{VB_i} and δt_i at cutting time t_i are considered as variations of tool wear and cutting time respectively under different initial conditions. We therefore consider here a wear – time plane to quantify the initial cutting conditions, see Figure 5-2. In this special the case ∂_{VB_i} is variation in both cutting time and tool wear that can be determined by Eq. (5-10).

$$\partial_{VB_i} = \sqrt{\delta t_i^2 + \delta_{VB_i}^2} \quad (\text{wear-time interval}) \quad (5-10)$$

In order to calculate the actual value of ∂_{VB_i} , the cutting time $t_i(s)$ is transferred to the length of

cutting (l_i), $l_i = N \cdot f \cdot \frac{t_i}{60} (mm)$; where $f (mm/rev)$ is the feed rate, $N (rev/min)$ is spindle

speed, $N = \frac{1000 \cdot V_c}{\pi \cdot D} (rev/min)$; D is diameter and $V_c (m/min)$ is the cutting speed. The δt_i is

thus determined by the variation of the cutting length (δl_i), $\delta t_i = \frac{60 \cdot \delta l_i}{N \cdot f} (mm)$. Accordingly, the

variation of scatter wears during machining process from Eq. (5-10) is then determined by Eq. (5-11)

$$\partial_{VB_i} = \sqrt{\left(\frac{60 \cdot \delta l_i}{N \cdot f}\right)^2 + \delta_{VB_i}^2} \quad (mm) \quad (5-11)$$

In order to determine properly the Lyapunov exponent in accordance with the initial cutting condition the chaotic wear equation (5-3) must be solved numerically. The reference and neighbor wear curves, as illustrated in the Figure 5-2 are required characterizing by a continuous function. We suppose that the function $f(t, y(t))$ satisfies a Lipschitz condition on the interval (t_0, T_c) . If the differential Eq. (5-3) is integrated within (t_0, t_i) , we obtain a chaotic wear curve as given by Eq. (5-12).

$$y(t_i) = y(t_0) + \int_{t_0}^{t_i} \xi(t, y(t)) dt \quad (5-12)$$

To carry out the integration of function ξ in Eq. (5-12) numerous classical numerical methods including Runge–Kutta methods [64], multistep methods [63, 64], Cubic B-splines collocation method [69, 70, 106, 107] and approximate method to solve numerically various classes of differential equations by using orthogonal polynomials [64, 66] have been developed for solving the initial value problems of ordinary differential equations. In this study, the chaotic wear data are obtained experimentally; therefore we approximate the $\xi(t, y(t))$ by a polynomial that interpolates at n point, $t_i, t_{i-1}, \dots, t_{i-n+1}$. If there is a mesh-size η , $\eta = (t_{i+1} - t_i)/n$ that depends on both ξ and the interval such that $\xi(t_i) - \xi(t_{i+1}) \leq \eta(t_i - t_{i+1})$ then there exists a solution $y(t) \in [t_0, T_c]$.

Based on the multistep method we can rewrite Eq. (5-12) as Eq. (5-13)

$$y(t_i) = y_{0i} + \eta \cdot \sum_{i=0}^n P_i \cdot \xi(t_i, u_i) \quad (5-13)$$

If $y(t_i)$ is the exact solution to Eq. (5-3), its diagram is a curve in the (y, t) – plane passing through the point $P_i(t_i, y_i)$, or $y(t_0) = y_0$. Therefore, a discrete numerical solution to Eq. (5-13)

can be defined to be a set of points $P = \{P_i\} = [P_0, P_1, \dots, P_{n-1}, P_n]$; where each point $P_i(t_i, y_i)$ is an approximation to the corresponding point of $(t_i, y(t_i))$ on the solution wear curve and u_j is a replacement function. Indeed, the solution of a partial differential equation can be described through a cubic B-spline [70, 106, 108].

We denote herein the class of functions $y = y(t)$ that are continuous on the domain $D \subset R^n; t_i \in [t_0, Tc]$; the solutions to Eq. (5-13) are then rewritten as a rational interpolation formula as follows:

$$y(t_i) = y_{0i} + \eta \cdot \sum_{i=0}^m P_i \cdot \psi_{i,n}(t) \quad (5-14)$$

where $\{P_i\}$ are the set of control points and $t = t_0, t_1, t_2, \dots, t_{m+n}$ are knot sequence vectors (as an increasing sequence of real numbers). The function $\varphi(t_i) = \sum_{i=0}^m P_i \cdot \psi_{i,n}(t)$ is thus considered as a non-uniform rational basis spline (NURBS).

4. In Eq. (5-14) $\psi_{i,n}(t)$ are B-spline function base of order n ; ($0 \leq n \leq m$). These basic functions are given by Eq. (5-15) The first question deals with the initial tool wear behavior, such as what exactly the initial tool wear phenomenon during machining TiMMCs is? What is the mechanism of wear at the first moment of cutting as well as when does it occur, how long does it take and why its wear rate increases so fast within the first wear period and then decreases abruptly to the steady period?

when $n = 0$ and when $n > 0$ respectively.

$$\psi_{i,n}(t) = \begin{cases} 1 & \text{if } t_i \leq t < t_{i+1}; \\ 0 & \text{otherwise} \end{cases}; \quad (n = 0) \quad (5-15)$$

$$\left[\frac{t - t_i}{t_{i+n} - t_i} \psi_{i,n-1}(t) + \frac{t_{i+n+1} - t}{t_{i+n+1} - t_{i+1}} \psi_{i+1,n-1}(t); \quad (n > 0) \right]$$

Considering the second order $n = 2$, the B-spline basic functions are determined as follows:

$$\psi_{i,2}(t) = \left(\frac{t-t_i}{t_{i+2}-t_i} \right) \psi_{i,1}(t) + \left(\frac{t_{i+3}-t}{t_{i+3}-t_{i+1}} \right) \psi_{i+1,1}(t) \quad (5-16)$$

Repeated for the orders of $n = 0$ and 1 , we obtain the second order functions as given by Eq. (5-17)

$$\psi_{i,2}(t) = \begin{cases} \frac{(t-t_i)^2}{(t_{i+1}-t_i)(t_{i+2}-t_i)} & \text{if } t_i \leq t < t_{i+1} \\ \frac{1}{(t_{i+2}-t_{i+1})} \left[\frac{(t-t_i)(t_{i+2}-t)}{t_{i+2}-t_i} + \frac{(t-t_{i+1})(t_{i+3}-t)}{t_{i+3}-t_{i+1}} \right] & \text{if } t_{i+1} \leq t < t_{i+2} \\ \frac{(t_{i+3}-t)^2}{(t_{i+3}-t_{i+1})(t_{i+3}-t_{i+2})} & \text{if } t_{i+2} \leq t < t_{i+3} \\ 0 & \text{otherwise} \end{cases} \quad (5-17)$$

Similarly, for the third order $n = 3$, the cubic functions of B-spline are determined by Eq. (5-18), where $\psi_{i,2}(t)$ and $\psi_{i+1,2}(t)$ are determined by Eq. (5-17)

$$\psi_{i,3}(t) = \left(\frac{t-t_i}{t_{i+3}-t_i} \right) \psi_{i,2}(t) + \left(\frac{t_{i+4}-t}{t_{i+4}-t_{i+1}} \right) \psi_{i+1,2}(t) \quad (5-18)$$

According to [106, 109], we take into account the mesh-size η so the cubic functions of B-spline are defined as given by Eq. (5-19)

$$\psi_{i,3}(t) = \frac{1}{6 \cdot \eta^3} \begin{cases} (t-t_i)^3, & t_i \leq t < t_{i+1} \\ \eta^3 + 3\eta^2(t-t_{i+1}) + 3\eta(t-t_{i+1})^2 - 3(t-t_{i+1})^3, & t_{i+1} \leq t < t_{i+2} \\ \eta^3 - 3\eta^2(t-t_{i+3}) - 3\eta(t-t_{i+3})^2 + 3(t-t_{i+3})^3, & t_{i+2} \leq t < t_{i+3} \\ (t_{i+4}-t)^3, & t_{i+3} \leq t < t_{i+4} \\ 0, & \text{otherwise} \end{cases} \quad (5-19)$$

From Eqs. (5-12), (5-14) and (5-19) the chaotic wear curve is now characterized by cubic polynomial functions in the matrix form as given by Eq. (5-20)

$$y(t) = y_0 + \frac{1}{6 \cdot \eta^2} \begin{bmatrix} a_1 t^3 + b_1 t^2 + c_1 t + d_1 \\ a_2 t^3 + b_2 t^2 + c_2 t + d_2 \\ a_3 t^3 + b_3 t^2 + c_3 t + d_3 \\ a_4 t^3 + b_4 t^2 + c_4 t + d_4 \end{bmatrix} \cdot \begin{bmatrix} P_i \\ P_{i+1} \\ P_{i+2} \\ P_{i+3} \end{bmatrix} \quad \begin{matrix} t_i \leq t < t_{i+1} \\ t_{i+1} \leq t < t_{i+2} \\ t_{i+2} \leq t < t_{i+3} \\ t_{i+3} \leq t < t_{i+4} \end{matrix} \quad (5-20)$$

where the set of control points $P = \{P_i\}$ and spline polynomials a_i, b_i, c_i, d_i are determined empirically. As a result, the scatter wear dimension from Eq. (5-7) and Lyapunov exponent from Eq. (5-9) with respect to the reference trajectory in the chaotic wear system are determined exactly in the continuous function as given by Eq. (5-21) and (5-22) respectively.

$$\partial_{VB_k} = |\partial_{VB_0}| \frac{\eta}{k} \prod_{i=0}^{k-1} P_i \cdot (\psi_{i,3}(t_i))' \quad (5-21)$$

$$\lambda = \frac{\eta}{k} \lim_{k \rightarrow \infty} \sum_{i=0}^{k-1} \ln \left| \sum_{i=0}^m P_i \cdot (\psi_{i,3}(t_i))' \right| \quad (5-22)$$

where the mesh size η is determined based on the cutting time consideration $\eta = (t_{i+1} - t_i)/n$, $(\psi_{i,3}(t_i))'$ is the derivative of the cubic B-spline function. It is calculated by Eq. (5-19) and each controlled point $P_i(t_i, y_i)$ is determined on the wear curve function, see Eq. (5-20).

5.2.2 Sensitive dependence on initial conditions

In order to demonstrate the presence of a chaotic signal in the tool wear system it is required to find evidence of a sensitive dependence on initial conditions of the tool life. The chaotic relation between tool wear and initial cutting conditions will be assessed. The initial wear mechanism is also investigated. The chaotic wear curve evolution over time was modeled using Eq. (5-3) solved and characterized by continuous functions, see Eq. (5-14) and (5-20). Hence, the scatter wear dimension for different initial cutting conditions and Lyapunov exponent are calculated properly through these functions, Eq. (5-21) and Eq. (5-22). The initial conditions from Eq. (5-3) depend on a number of factors during the machining operation such as: cutting parameters, machine tool, cutting tool, workpiece material and machining techniques. In this case, the initial cutting parameters including cutting speed, feed rate and depth of cut play a very important role with respect to the tool wear [93]. The divergence in tool wear when machining

under various initial cutting conditions is the initial conditions, ∂_{VB_0} ; which are expressed by Eq. (5-23) As seen in Figure 5-2, the ∂_{VB_i} at cutting time t_i can thus be determined from the initial tool wear values at different cutting time, Eq. (5-11).

$$f(t_0, y_0) = \partial_{VB_0} = \begin{bmatrix} \partial_{VB_0} \\ \partial'_{VB_0} \\ \vdots \\ \partial^{(n-1)}_{VB_0} \end{bmatrix} \quad (5-23)$$

In this case, the two trajectories in the Figure 5-2 are considered as two wear evolution curves in time under small different initial conditions. The reference curve (red color) is generated by a regular cutting condition while the neighbor blue one is obtained by changing the initial cutting conditions ∂_{VB_0} . At a certain cutting time $t \in [t_i, t_{i+1}]$; $0 < t_i < Tc$; the variation of the scatter wear dimension from Eq. (5-21) is calculated by following equation:

$$\partial_{VB_i} = \Delta \left[\eta^2 - (t - t_i)^2 \right] - \eta \quad (5-24)$$

where Δ is a constant depends on the initial cutting conditions, ∂_{VB_0} , η is an experimental mesh size of the wear curve equation. This function has a recursion relation that regarding to the logistical map; whose iteration values (trajectory) have been widely used to generate chaos in a system [44]. So these wear curves functions can exhibit deterministic chaos in a tool wear system. For $\eta = 0.475$ and $t_i = 0.1$, we generate at a very small different value $\partial_{VB_0} = 0.001$ for the neighbour wear curve as shown in Figure 5-3

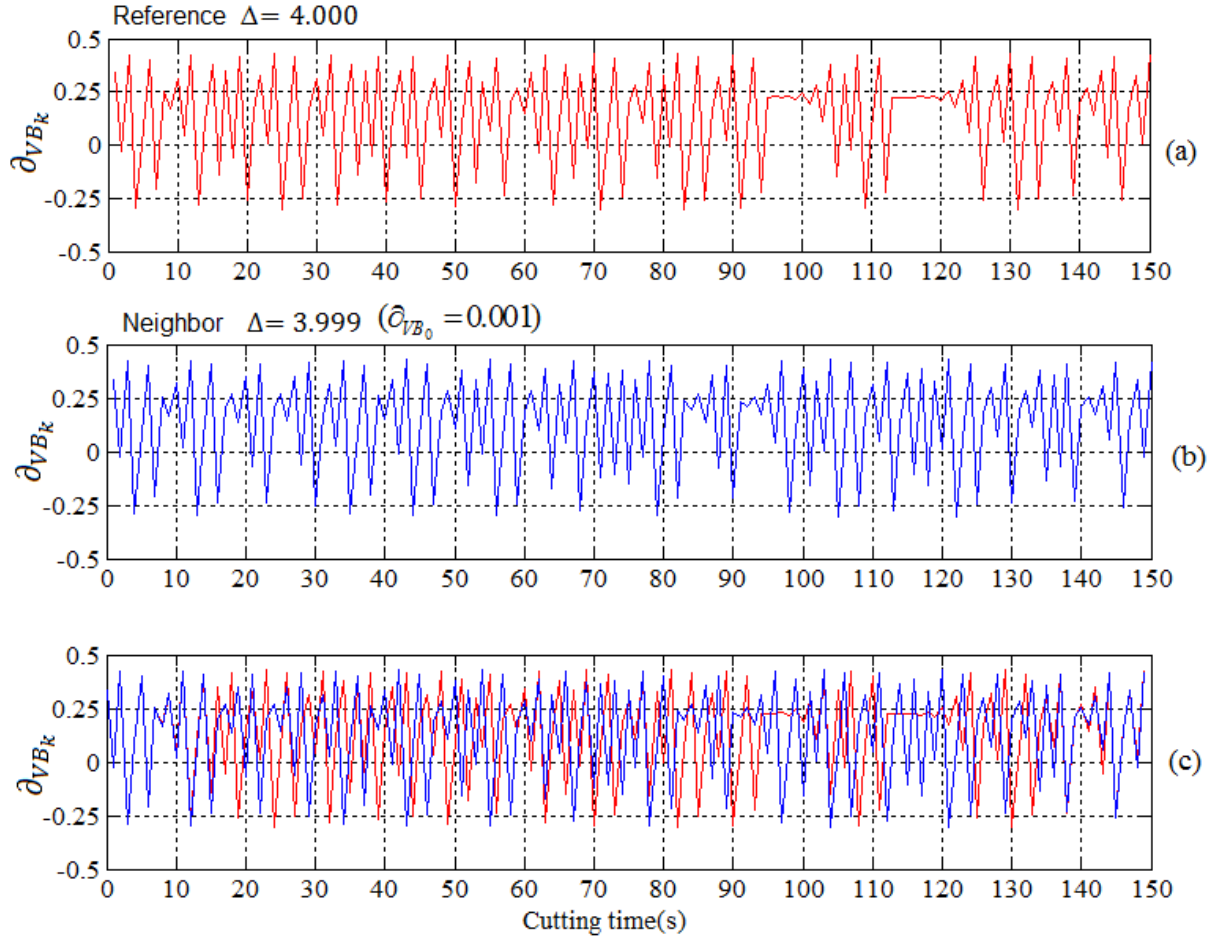


Figure 5-3: Sensitive dependency on initial conditions of two wear curve trajectories

(a) reference, $\Delta = 4.000$; (b) neighbor $\Delta = 3.999$; (c) the two curves in comparison

We can observe roughly here the reference trajectory Figure 5-3(a) and the neighbor trajectory Figure 5-3(b) developed similarly up to 70 seconds. Imagine when machining a hard to cut material that relatively short tool life; we would have difficulty observing the different in tool wear and tool life. However, if we plot both of them together, see Figure 5-3(c) we can see clearly their gradual dispersion from 14th seconds onwards with increasing divergence until they are completely different later on. As a result, the tool wear system during a machining process exhibits a sensitive dependence on the initial cutting conditions. It is being implemented in validating the outcome for a machining process in the next section.

5.2.3 Fractal dimension analysis

A fractal geometry is an object that displays self-similarity at various scales and it is quantified by a non-integer dimension, the fractal dimension [71]. Therefore, it has been widely used to characterize complex geometric forms or non-integer dimension object that could not be analyzed by the classical Euclidian geometry. Particularly, the fractal dimension is closely related to the Lyapunov exponent [72] in quantifying the chaotic motion in a system [1, 45].

Since the chaotic tool wear curves during a machining process is being characterized by the continuous functions in accordance with the mathematical model proposed earlier we therefore apply herein the fractal dimension to analyze the variations in tool wear rate under the different initial cutting conditions as shown in Figure 5-4(a). The fractal dimensions on each wear curve are calculated based on the Box-counting method as given by Eq. (5-25)

$$D = \lim_{\varepsilon \rightarrow 0} \frac{\ln N(\varepsilon)}{\ln(1/\varepsilon)} \quad (5-25)$$

where $N(\varepsilon)$ are the number of boxes needed to cover the wear curves or the area; they are also considered as the number of self-similar pieces; ε is the magnification or scaling ratio factor. The boxes for counting are produced as squares at various grid scales as shown in Figure 5-4(b). All boxes of the grid that contain any part of the curve are counted directly on each wear curve function.

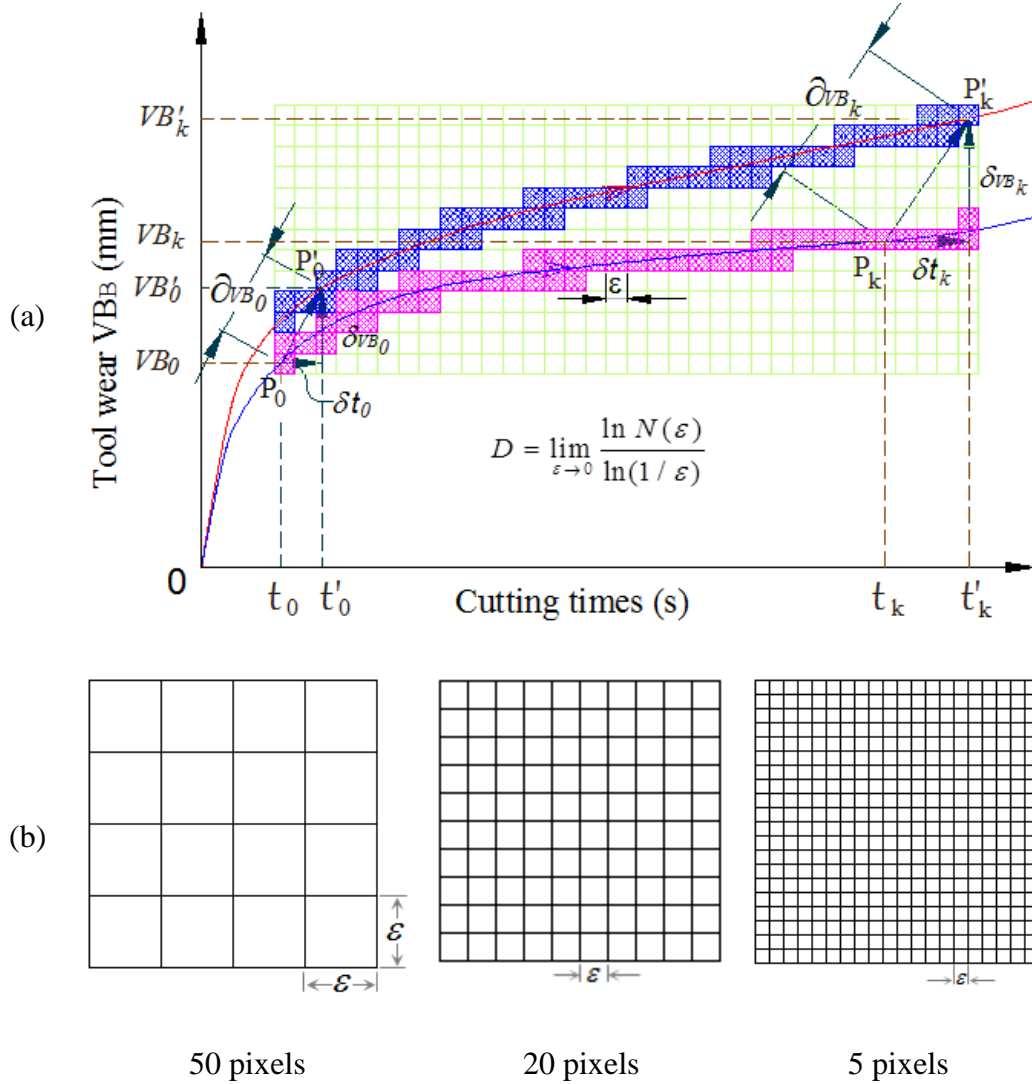
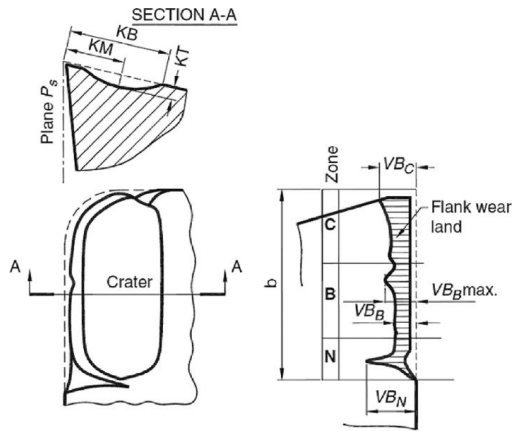


Figure 5-4: Fractal dimension analysis of a chaotic wear curve

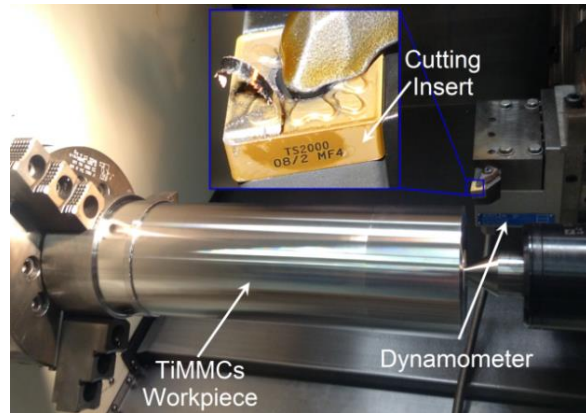
Accordingly, a chaotic tool wear during machining process is characterized by both Lyapunov exponent and fractal dimension, as illustrated in Figure 5-5. Therein, the wear curve evolutions in time are modeled by an ordinary differential equation. They are characterized by cubic B-spline rational interpolation function. Therefore, the determination of scatter wear dimension and Lyapunov exponent has no limitation within the chaotic tool wear model. The divergence in wear rate is quantitative measured by fractal dimension that is calculated based on the Box-counting method. Effective of the proposed model is being validated and applied to the machining of TiMMCs material (see the next section).

second experimental stage; the first strategy (No.1) is to change initial cutting speed while the second strategy (No.2) is a change in the initial feed rate. The third strategy (No.3) applies a ramping approach; therein, the depth of cut increases gradually from zero to a defined depth and is then kept constant.

The machining tests were performed on a CNC turning center Mazak QT-Nexus-200 as shown in Figure 5-6(b). The workpiece material used in this study was TiMMC that has been reported as an extremely hard to cut material. It has a mean Rockwell hardness of 40 HRC, tensile strength of 1082 MPa, yield strength of 4500 kg/m³ and thermal conductivity of 5.8 W/mK. The cutting tools used in all experiments were PVD coated (Ti,Al)N+TiN manufactured by SECO with the following specifications: rake angle $\gamma_0 = -6^\circ$, back rake angle $\gamma_p = -6^\circ$, nose radius $r_e = 1/32$ in, tool included angle $\epsilon_r = 80^\circ$, tool cutting angle $\kappa_r = 95^\circ$ and the insert thickness $s = 3/16$ in.



(a) Tool wear parameters definition [90]



(b) CNC turning center QT-Nexus-200

Figure 5-6: Experimental set-up

Indeed, cutting tools made of polycrystalline diamond (PCD) and cubic boron nitride (CBN) are widely recommended for machining titanium alloys Ti-6Al-4V and Metal Matrix Composite materials. PCD and CBN exhibit lower wear rate while the coated one is faster wear rate and cheaper [91]. With the aim of analyzing effect of the initial cutting conditions on the tool life that regarding to the tool wear mechanism from the first moment of the cutting process; hence, the wear rate should not be too rapid to achieve more accurate measurement. On the

contrary, it should not be too slow to avoid using large amounts of a very expensive material that is TiMMCs. Therefore the PVD coated cutting tool is used in this work. The cutting conditions are chosen by taking into account the recommendation of cutting tool manufacturers, our previous works [17, 92, 93] and also our preliminary machining tests for the special case of the first wear zone. Accordingly, the cutting speeds were: $V_c = 20 - 60$ m/min, the feed rate and depth of cut were in the range $f = 0.1 - 0.2$ mm/rev and $a_p = 1.0 - 2.0$ mm respectively.

5.4 Results and discussion

5.4.1 Tool wear evolution during machining of TiMMCs

For the first experimental stage the cutting parameters were $V_c = \{V1 - V4\} = 20 - 60$ m/min while the feed rate and depth of cut were kept constant at $f = 0.15$ mm/rev and $a_p = 1.5$ mm respectively. The tool wear evolutions are divided in four groups in accordance with the different cutting speed; each curve group is observed in three wear periods: initial wear period (I), steady wear period (II) and rapid wear period (III) as shown in Figure 5-7. The tool life obtained under cutting speed of $V4 = 60$ m/min was very short; therefore, one more of the wear curve experiment was performed to validate the result. As can be seen, tool wear rate increases rapidly in the first and third wear period while in the steady wear zones it is relatively constant.

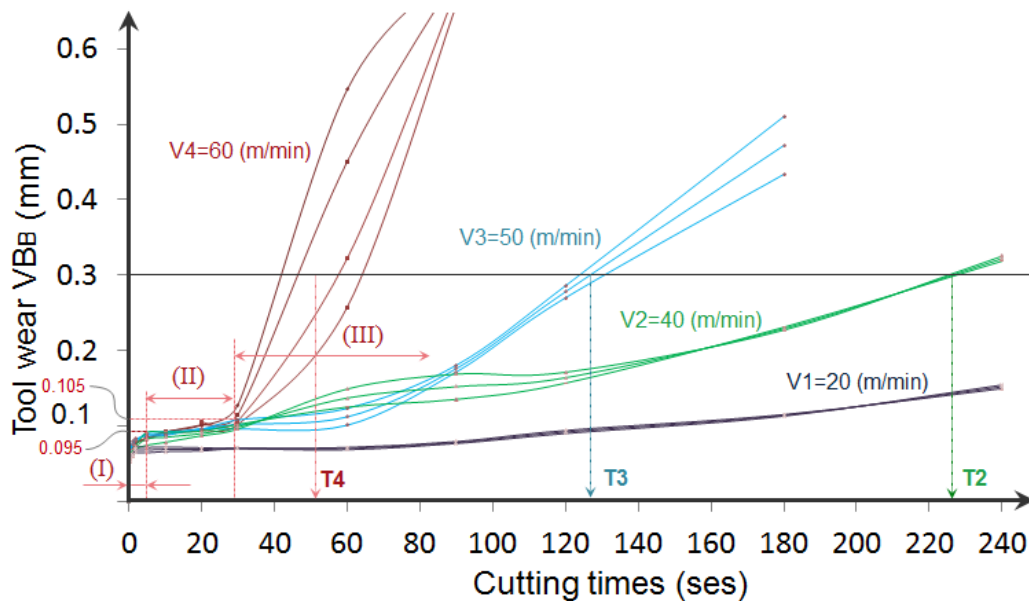


Figure 5-7: Tool wear during machining TiMMCs under different cutting speeds [110]

More importantly, the initial wear period happens within a very short cutting time but their wear volume lost within this period is much larger than that of the second wear period. The percentage of tool wear values between the two periods is different depending on the cutting speeds; for example, under cutting speed $V4 = 60$ m/min, the average initial wear value was 0.095 mm or 90.5% compared to the steady wear period which was 0.01 mm or 9.5%, see Figure 5-7 while under speed $V3 = 50$ m/min, the percentage of initial and steady wear period were 66.4% and 33.6% respectively. It is therefore thought that the initial wear period may play a critical role in the tool life when machining TiMMCs.

Taking into account the average wear values under speeds $V1$, $V2$, $V3$ and $V4$, we obtained roughly the tool life $T1$, $T2$, $T3$ and $T4$ respectively; the tool life $T1$ under speed of $V1=20$ m/min is so long (over 560 seconds) hence it is not presented in the diagram. For the highest speed $V4 = 60$ m/min tool the wear rate increases very rapidly in period (III) leading to a very short tool life while the tool wear at low speed $V1 = 20$ m/min shows negligible increase during the steady wear period starting as soon as only two seconds of machining. Furthermore, the wear rate decreases abruptly at the transition point between wear periods (I) and (II) and accelerates between periods (II) and (III).

In order to use the wear curves for the purpose of investigating chaotic tool wear, as well as enable the prediction of tool wear values and tool life the average of wear curves for a particular set of cutting conditions are characterized using the cubic functions of Eq. (5-20). It is a solution approximately based on the multistep methods for non-uniform meshes [69] that we have developed in the previous section. As a result, the wear curve evolutions in time are expressed by a continuous function as shown in Figure 5-8(a). Each curve is the combination of several functions joined with tangency constraints at each investigated cutting time (t_i), they are expressed by difference colors, see Figure 5-8. Accordingly, the tool life under $V1$, $V2$, $V3$ and $V4$ are determined properly on each wear curve function at $y_{(t)} = VB_B max = 0.3$ mm, the values of $T1$, $T2$, $T3$ and $T4$ are 560.4, 225.5, 126.4 and 50.7 seconds respectively.

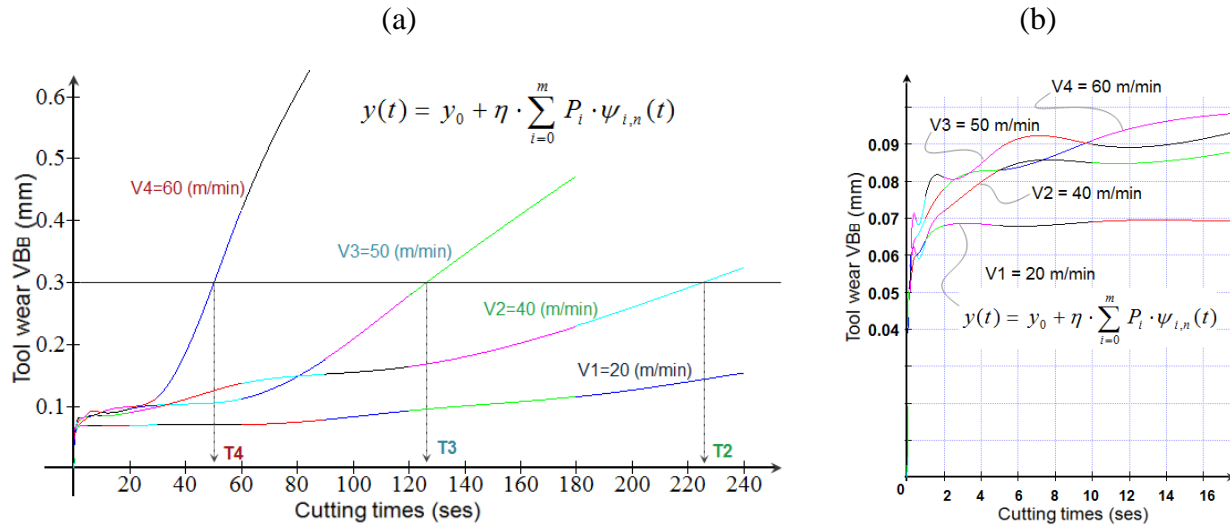


Figure 5-8: Cubic B-spline functions describe tool wear curves

In order to investigate the effect of the initial wear mechanism and initial cutting conditions on tool life, the initial wear period is magnified from the set of control experimental points and knot vectors at $VB_0 = y_0 = 0$ as illustrated in Figure 5-8(b). They are determined on each wear curve with respect to the critical wear rate and their values (V_{bi}) according to standard ISO 3685. As shown, the initial wear increases very rapidly and reaches a limit at the first transition between period I and II, less than 0.095 mm. The accelerated wear occurs as soon as the cutting action begins and extends to only two seconds at the low speed of 20 m/min and ten seconds under higher speed conditions.

Surprisingly, the tool wear at the first transition period under cutting speeds V_1 , V_2 and V_3 showed a similar wear mechanism as shown in Figure 5-9(a), (b) and (c). The initial wear behavior during machining TiMMCs, was recently investigated by the authors, showed that adhesion and diffusion are primarily found within the initial wear period under all experimental conditions tested. The initial wear mechanism is the result of complicated mechanisms including adhesion, diffusion, and oxidation while abrasion occurred rarely. This mechanism is opposite to the steady wear period where abrasion is the most important mechanism [17, 34, 35]. Furthermore, the low thermal conductivity and high reactivity of titanium alloys lead to increase cutting temperature at the tool-workpiece-chip interface [7, 25] resulting in micro welding and built-up-edges (BUE) being formed at the cutting edge [111].

By EDX analysis of the wear mechanism, Figure 5-9(d) the chemical wear at the first transition, between initial and steady wear period, included the coating layer of the insert with the presence of the Ti, Al and N elements are found to be rich. The effect of chemical stresses at high cutting temperatures was the main reason leading to the diffusion wear; therefore, they reacted spontaneously with atmospheric oxygen and oxidizes the titanium and aluminum and then diffuses from the coating layer and the TiMMCs at high pressure and elevated temperature. The combination of these mechanisms, associated with the coating layer (Ti,Al)N of the cutting tool and TiC reinforcement of the workpiece material generated a new hard thin layer as a whole involving in the machining process. This new wear layer which authors have coined “brace wear” is mostly found on the flank face; see Figure 5-5(a) at the first transition wear period.

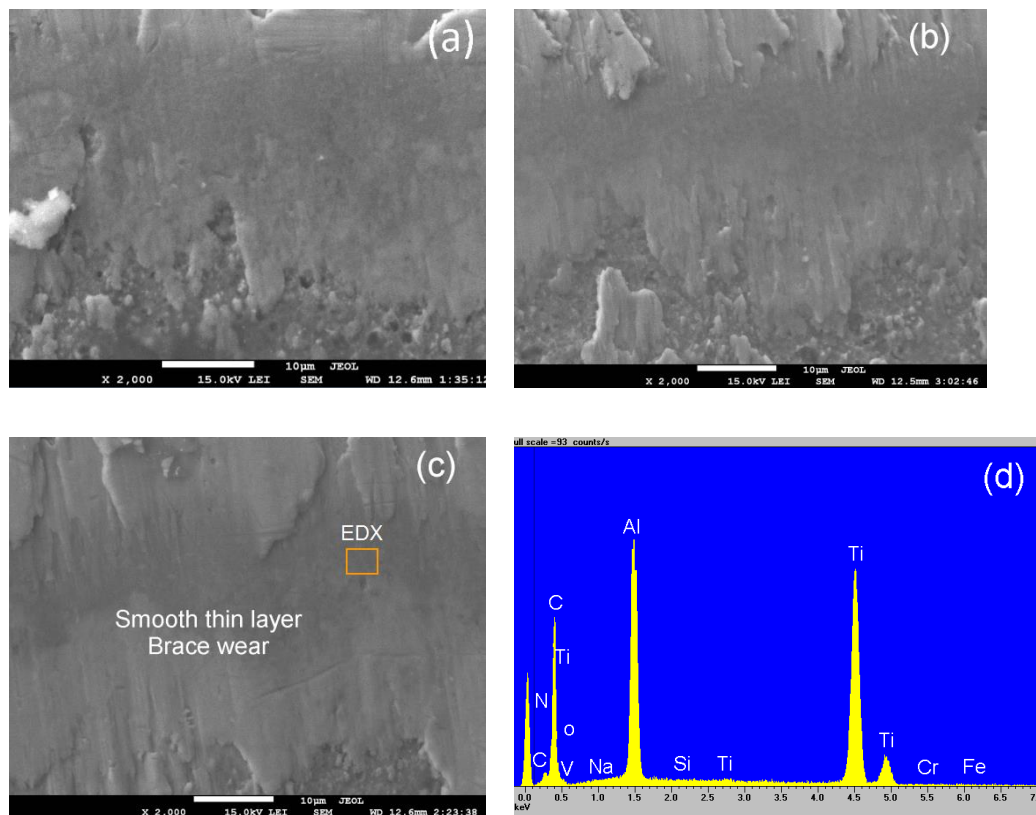


Figure 5-9: Initial tool wear during machining TiMMCs;(a) V=20m/min after 2s; (b) V=40m/min after 5s; (c) V=50m/min after 6s; (d) EDX analysis [110]

Accordingly, the “brace wear” is considered as a wear shield or protection layer for the steady wear region. The formulation of the wear shield provides a better explanation of wear rate during the first wear period with regards to the accelerated cutting force and temperature. In the

first instants of cutting, the cutting forces increase very rapidly over a short period of time so the friction and tribological wear can be considered at the contact of two new surfaces where the sliding velocities between the two fresh surfaces at a small cutting edge are close to zero [95, 96]. The contact surface appears smooth and clean thus inducing quasi-static friction [97]; hence the cutting forces influence mainly through a small area at the tool-workpiece interface and lead to high contact stress and high friction between poorly conforming surfaces. The rapid initial increase of the cutting forces occurred within one second and is followed by a reduced and constant rate of increase during the steady wear period. The rapid increase in cutting force resulted in an immediate increase of cutting temperature in the first initial wear zone, 20°C to 500°C when machining Ti-6Al-4V [94].

5.4.2 Effect of initial condition on the tool life

The wear shield was found at the first transition period for low cutting speed, low feed rate and small depth of cut within only 2 seconds [93]. On the other hand, no significant improvement of tool life was observed in our preliminary tests for the data considered when the initial period (t_0) lasted more than 2 seconds. So, we consider herein three experiment strategies to change initial cutting parameters at the transition period $t_0 \leq 2(s)$ in accordance with the Eq. (5-3) and Eq. (5-23) for each experiment. The first strategy is to change the initial cutting speed during the first two seconds of machining; an initial speed of 20 m/min is followed by an increased speed which is then kept constant at 60 m/min while both the feed rate and depth of cut are kept constant at 0.15 mm/rev and 1.5 mm respectively.

Table 5-1: Different initial cutting parameters for experiments

No.	Vc (m/min)	f(mm/rev)	ap (mm)	Time (s)
1	20	1.5	1.5	(0 - 2)s
	60			after 2s
2	60	0.05	1.5	(0 - 2)s
		0.15		after 2s
3	60	0.15	0 - 1.5	(0 - 2)s
			1.5	after 2s

The second and third strategies see a change in feed rate and depth of cut as shown in Table 5-1; all machining test are designed for equal volumes of metal removed. The machining experiments were performed and measured at several cutting time in accordance with the $t \in [t_i, Tc]$, $i = 0, 1, 2, k, \dots$, in the mathematical model proposed. According to Eq. (5-14), the control points require measurement on the flank face of the cutting inserts. Cutting inserts are changed or rotated to offer a new cutting edge for each interval tested; a total of 4 times 100 inserts offering 400 new cutting edges were used for the whole experimental study. In order to reduce the large amount of computation without compromising the accuracy of the model we considered the average of flank wear land at only 12 intervals (t_i) to calculate the polynomials and mesh size for the chaotic wear curves. As a result, the chaotic wear curve polynomials are averaged as given by Table 5-2; they are generated as shown in Figure 5-10

Table 5-2: B-spline polynomials of chaotic wear curve when machining TiMMCs

	$\{a_i\} * \{P_i\}$	$\{b_i\} * \{P_{i+1}\}$	$\{c_i\} * \{P_{i+2}\}$	$\{d_i\} * \{P_{i+3}\}$	η
No.1	-0.00631672	0	9.70418E-05	1.807E-22	0.004167
	0.006583573	-0.001935042	0.000193794	-1.613E-06	0.004167
	-0.00081815	0.00040556	-3.9398E-05	2.0702E-05	0.008333
	0.000928399	-0.00132501	0.000640433	0.00011999	0.025
	-0.00017235	0.000446263	-0.00028444	0.0006772	0.041667
	8.57442E-05	-0.000540408	0.001187683	0.00193365	0.083333
	0.000050625	-0.000537233	0.00203625	0.02317144	0.25
	-6.6281E-05	0.001611281	-0.00986173	0.09022833	0.416667
	7.66733E-05	-0.003808792	0.063092083	0.01911633	0.833333
	-1.4984E-05	0.001690654	-0.04689667	0.752375	0.833333
	-8.4922E-06	0.003843225	-0.08089013	3.3595875	2.5
	-2.5718E-05	0.006943913	-0.26693175	7.0804125	2.5

Table 5-2: B-spline polynomials of chaotic wear curve when machining TiMMCs

No.2	-0.00970132	0	0.000121753	-3.614E-22	0.004167
	0.011756604	-0.003218689	0.000282688	-2.682E-06	0.004167
	-0.00503262	0.002742955	-0.00043102	4.133E-05	0.008333
	0.003184733	-0.004400366	0.001938212	-1.586E-05	0.025
	-0.00085843	0.002334128	-0.00189476	0.00116907	0.041667
	0.000338623	-0.001980574	0.003738029	0.00090392	0.083333
	-3.2699E-05	0.000656666	-0.00332141	0.03277775	0.25
	-6.3752E-05	0.001417911	-0.00719534	0.08766463	0.416667
	0.000141377	-0.006219938	0.090134458	-0.0457275	0.833333
	-0.00010449	0.008531992	-0.20490408	1.92119625	0.833333
	0.000209174	-0.026673724	1.25971275	-13.747729	2.5
	-0.00012197	0.032932909	-2.3166855	57.780225	2.5
No.3	-0.00796949	0	0.000107424	0	0.004167
	0.009014104	-0.002547542	0.000234801	-2.123E-06	0.004167
	-0.00247076	0.001367996	-0.00021661	3.0035E-05	0.008333
	0.001274273	-0.001794698	0.000871823	8.223E-05	0.025
	-0.00034652	0.000843982	-0.0004929	0.00071419	0.041667
	0.000285242	-0.001638008	0.003042338	0.00118543	0.083333
	-7.7967E-05	0.001128776	-0.00436069	0.03183004	0.25
	-5.6463E-06	-2.84613E-05	0.003706698	0.06205052	0.416667
	5.889791667	-0.002558338	0.039271708	0.16671917	0.833333
	-2.7874E-05	0.002647992	-0.064855	0.86089583	0.833333
	1.93242E-05	-0.000485524	0.145829625	0.45283125	2.5
	-3.3254E-05	0.008978513	-0.42201375	11.8096875	2.5

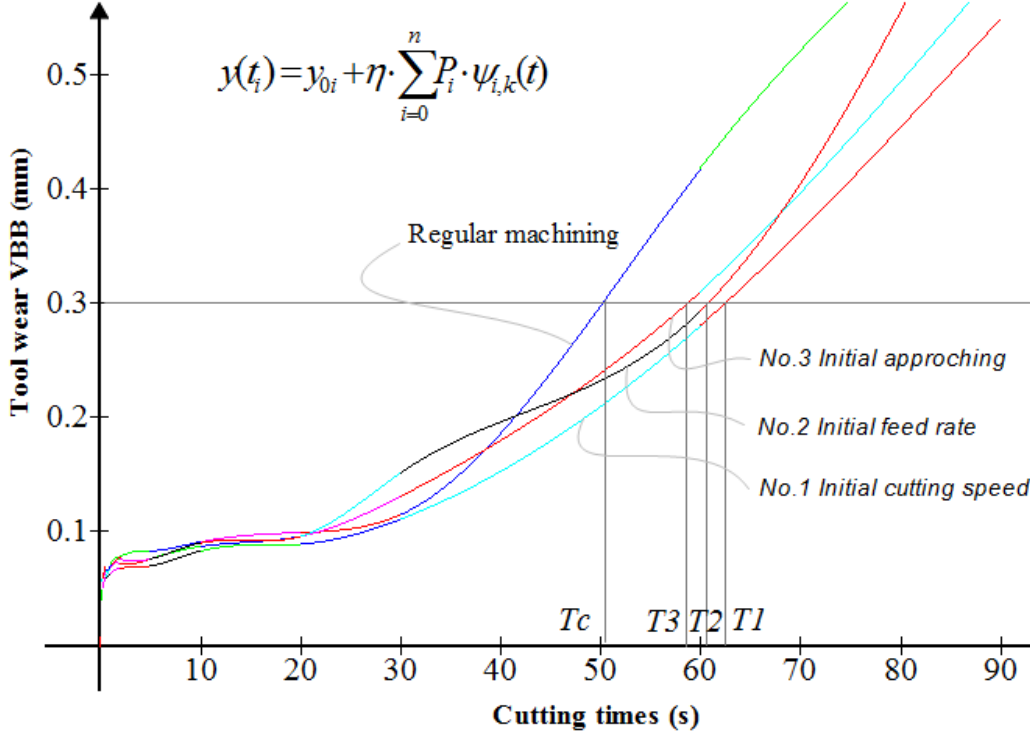


Figure 5-10: Chaotic wear curves in three initial condition strategies

Accordingly, the tool life values of T_c, T_1, T_2, T_3 are now calculated exactly based on the wear curves functions at the limited wear values $VB_{Bmax} = 0.3 \text{ (mm)}$ corresponding to the regular machining, the first, second and third experiment strategies respectively. The results show that tool life increased for both three advantages initial cutting conditions with improvement of 24.5%, 21.1% and 16.9% respectively.

5.4.3 Chaotic tool wear phenomenon during machining process

To investigate the tool life dependence on the initial cutting conditions as well as to detect any chaotic behavior of the tool wear during the machining process, the Eqs. (5-21), (5-11) and (5-24) are calculated by changing a small initial cutting condition $\partial_{VB_0} = 0.01, 0.002$ and 0.006 corresponding to the three strategies discussed above when machining TiMMCs. These initial condition values are calculated based on equations (5-23) and (5-11). We calculated the scatter dimensions with respect to the logistic map generating as shown in Figure 5-11(a), (b) and (c) respectively. It shows that the wear curves in all three strategies tested above diverge gradually after 7.5, 9.0 and 14.5 seconds respectively and evolve completely differently later on for all experiments. These results confirm that the initial cutting conditions influence significantly the

tool life. In this case, the initial cutting speed, as used in the first strategy, appears as the most important factor influencing the tool life during machining TiMMCs.

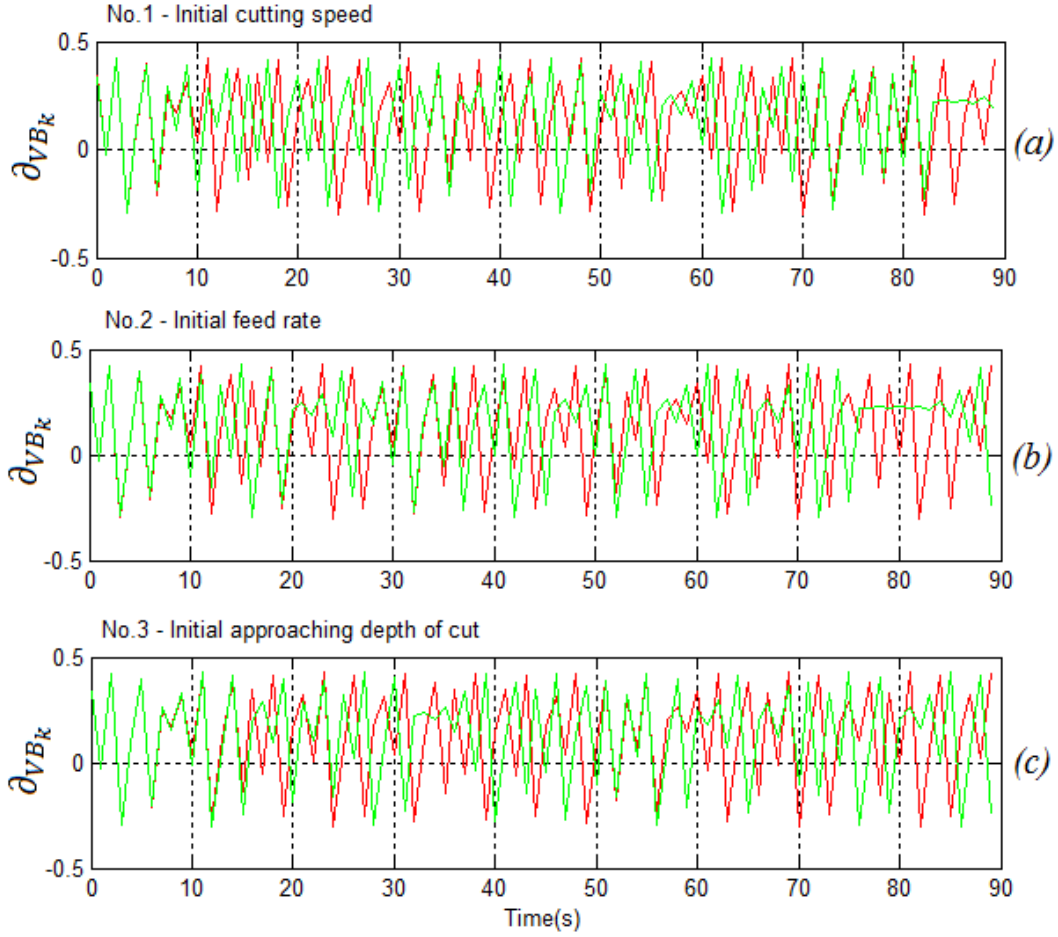


Figure 5-11: Scatter wear dimensions under different initial cutting conditions;

(a) No.1 - $\partial_{VB_0} = 0.01$, (b) No.2 - $\partial_{VB_0} = 0.002$, (c) No.3 - $\partial_{VB_0} = 0.006$

In order to quantify the exponential divergence of the chaotic wear trajectories and estimate the amount of chaos in a wear system, values for λ and D , of the proposed model, are calculated numerically from each wear curve equation. With these continuous functions we thus have no limitation on calculating the scatter wear and λ at any cutting time interval. In general, an n -dimensional system has n Lyapunov exponents, and there exist at least one positive λ in a chaotic system [50]. The D is calculated on the chaotic wear curve using the Box-counting method, Eq. (5-25). They are calculated directly from Eq. (5-14) that generated by using Function Grapher 2011.

Considering the tool wear evolution for the three experimental strategies based on different initial cutting conditions the λ and D are obtained and given in Table 5-3. From the obtained results in Table 5-3 we observe that positive values are found for all strategies tested, including initial cutting speed, initial feed rate and initial depth of cut. The fractal dimensions increased with the increase of Lyapunov exponent; their relationship with cutting time during the machining process is expressed as shown in Figure 5-12. It clearly shows that positive values of λ are found for D in the range of 0.7 to 1.1; λ increases with the decrease of D . In particular, λ increases quickly up to 1.1 while D reduces rapidly to 0.4 within 40 to 60 seconds cutting time. Indeed, this interval is an important period of tool wear where the tool life was increased by up to 24.5% as discussed in the previous section. On that basis it is believed that chaotic motion occurring in the tool wear system during the machining process plays a critical role on tool life.

Table 5-3: Lyapunov exponents (λ_i) and fractal dimension (D_i)

(t_i)	(λ_i)				(D_i)			
	No. 1	No. 2	No. 3	Average	No. 1	No. 2	No. 3	Average
∂_{VB_0}	0.001	0.002	0.006	0.006	0.477	0.477	0.477	0.477
10	-0.019	-0.060	-0.034	-0.038	0.699	0.778	0.778	0.752
20	0.001	0.036	-0.056	-0.006	1.041	1.041	1.041	1.041
30	-0.078	0.242	0.082	0.082	1.114	1.146	1.146	1.135
40	0.002	0.133	0.003	0.046	1.146	1.146	1.255	1.183
50	0.181	0.291	0.190	0.221	1.176	1.079	1.146	1.134
60	0.218	0.344	0.240	0.267	1.176	1.230	1.176	1.194
70	0.230	0.339	0.253	0.274	1.255	1.279	1.230	1.255
80	0.228	0.274	0.246	0.249	1.279	1.380	1.301	1.320
90	0.219	0.243	0.227	0.230	1.204	1.380	1.301	1.295

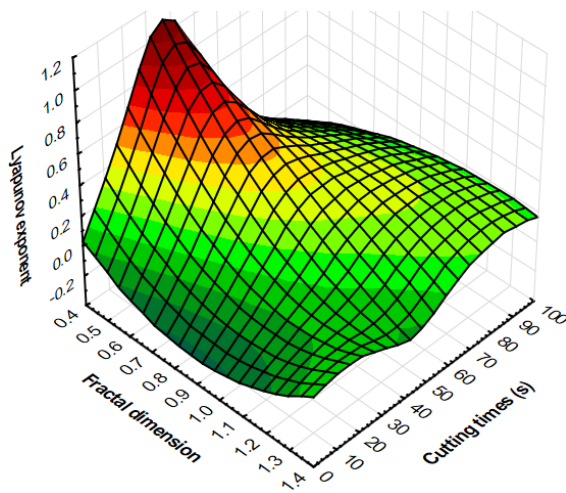


Figure 5-12: Relationship between λ and D and cutting time

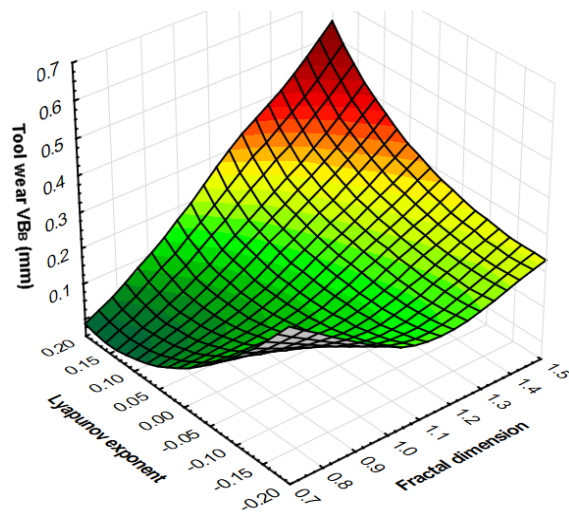


Figure 5-13: Relationship between λ and D and tool wear; (No.1 - Initial speed)

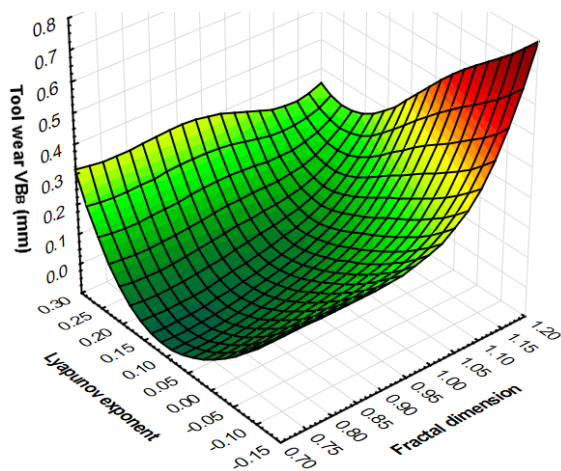


Figure 5-14: Relationship between λ and D and tool wear; (No.2 – Initial feed rate)

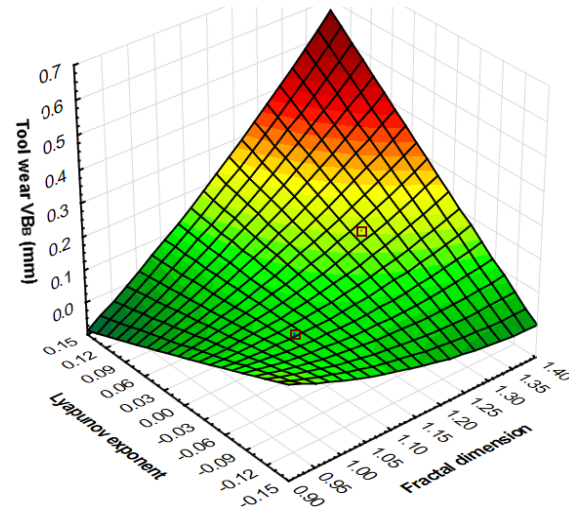


Figure 5-15: Relationship between λ and D and tool wear; (No.3 – Initial depth of cut)

In order to demonstrate how significantly the initial cutting conditions influence the tool wear evolution over time and the tool life, the relationship between λ , D and tool wear are investigated as shown in Figure 5-13, Figure 5-14 and Figure 5-15. The results reveal that both λ and D are closely related to the tool wear evolution over time. When D increase over 1.2 the tool wear increases rapidly and lead to tool failure in case of a negative λ for all strategies tested.

When λ is greater than 0.05, D increases rapidly with the increase of tool wear, see Figure 5-12 and Figure 5-14. On the other hand, the tool wear increases with the decrease of both D and λ . In contrary to strategies No.1 and No.3, with strategy No.2, of changing the initial feed rate, the fractal dimension is not much affected by the tool wear evolution, see Figure 5-14. The tool wear rate is reduced both for an increase or decrease of the λ value to 0.1; tool failure is noted only in the case of D greater than 1.15 and λ less than 1.0. As a result, the rapid increase in tool wear that quantitative measure by the fractal dimension is explained mean by the wear curves divergence under different initial cutting conditions; their relationship associated with λ is interpreted mean by a chaotic behavior that exhibited in the tool wear system. We would therefore report here that the chaotic motion can be found within the tool wear progression during machining process regarding to the positive values of Lyapunov exponent and fractal dimension of the wear curves less than 1.2. The chaotic motion occurred within the tool wear system we so-called ‘Chaotic tool wear’.

5.5 Conclusions

In this paper, the multistep method is developed to solve an ordinary differential equation for the chaotic tool wear system based on cubic B-spline rational interpolation function. The so-called “chaotic tool wear” is defined for the first time in this study based on both the Lyapunov exponent and fractal dimension. The numerical results reveal that even such a relatively simple model could exhibits chaotic nature of the tool wear during machining process. In addition, the wear curves evolution as a function of the cutting time, as characterized by cubic continuous functions in the phase space, allowed us to calculate the scatter wear dimension and quantify a chaotic motion at any interval of cutting time.

To demonstrate the accuracy and usefulness of the chaotic tool wear model, three experimental strategies for changing initial cutting conditions including initial cutting speed, initial feed rate, and initial approach for depth of cut were conducted. The initial cutting conditions were changed by very small amounts of $\partial_{VB_0} = 0.01, 0.002$ and 0.006 for the first, second and third strategies within two seconds when machining TiMMCs. Results were unexpected as tool life improved by 24.5%, 21.1% and 16.9% respectively. The improvement of tool life is explained by the influence of the initial cutting conditions on the tool life which is quantified relatively to the positive values of the largest λ and D in the range of 0.7 to 1.2.

Another important point to be noted is that a full explanation of the wear rate behavior at the first initial wear period is obtained through the chaotic tool wear for the first time in the study of tool wear, chaos theory and fractal geometry. That model equally brings more insight how the tool life depends significantly on the initial cutting conditions.

Acknowledgement

The authors would like to gratefully acknowledge the financial supported from the Natural Sciences and Engineering Research Council of Canada (NSERC) and Canadian Network for Research and Innovation in Machining Technology (CANRIMT). In addition, this study was supported by the Vietnam government through the Project 322.

CHAPTER 6 GENERAL DISCUSSION AND CONCLUSIONS

This chapter summarizes the significant results achieved from the research presented in the previous chapters. The dissertation's contribution to the advancement of knowledge and the development of technologies, as well as its limits and constraints are discussed. This thesis also leaves open some recommendations that should be addressed for future research.

6.1 Summary of Research Accomplishments

It is worth recalling that the Chaos theory, a field of study in mathematics that has been proven efficient in analyzing how something changes in time and predicting the behavioral change, has now been successfully applied to investigate the tool wear during a machining process. The original significant results have obtained from this PhD. Thesis are given as follows:

6.1.1. Conclusions on initial tool wear behavior during machining TiMMCs

During machining of TiMMCs the initial wear occurred from the first moment of cutting at extremely high wear rate. This wear evolution was found within only two seconds under a cutting speed of 20 m/min and tends to increase to ten seconds maximum at higher cutting speeds. In particular, even the initial wear period happens within a very short cutting time but their wear volume lost within this period is much higher than that of the second wear period.

At the first moment of machining TiMMCs the tool wear mechanisms are the results of tool layer damage associated with the friction between the two new contact interphase and tribological wear. This is because the effect of accelerated cutting force and temperature gradient leads to high stress and friction between the poorly conforming surfaces of cutting tool and workpiece material and hence causes a dramatically damaged layer. That explains the high wear rate at the very first moment of tool wear.

The increase of cutting force and temperature right after leads to micro welding and built-up-edges (BUE) form at the cutting edge. Chemical stresses at high temperature were attributed as the main reason of the diffusion wear because the tool layer material reacts spontaneously with atmospheric oxygen and thus oxidation of the titanium and aluminum takes place. Therefore, the adhesive wear is mostly found during the initial wear period under all experimental conditions

tested in this work. The observed behavior seems to be contradictory with the mechanism of abrasion wear in the steady wear period that has been reported in the literature.

The adhesion layer of the cutting tool and BUE are damaged and soluble mutually at elevated temperatures. However, that resulting material still includes the hard particles of TiC reinforcement in the workpiece material but the effect of these particles were not strong enough to disable the adhesive wear within the first wear zone. The combination of these mechanisms in association with the coating layer of (Ti,Al)N generated a new wear form as a whole participating in the machining process. The effect of TiC in the chemical wear that exists in the form of diffusion then formed a new hard thin layer at the end of the initial wear period. This new wear form is here called “brace wear”. By considering all the experimental results, we believed that the brace wear is a wear shield layer for the steady period. Due to the appearance of the brace wear, the rates of tool wear decreases abruptly at the transition point between the first and second wear periods.

6.1.2. Conclusions on chaotic tool wear during a machining process

Our experimental results have revealed that the initial tool wear mechanism and initial cutting conditions affect significantly the tool wear evolution and the entire tool life. In this case the relationship between initial cutting parameters and the tool life is found to be closely related to the initial wear mechanism. Only a minor modification of initial cutting condition is able to change the initial wear mechanism and results in a significant difference in the tool life.

This sensitive dependence behavior of the tool life on the initial conditions has suggested the application of chaos theory. As mentioned in the previous section, no research study is found analyzing a chaotic motion in the tool wear system and almost all applications of chaos have referred to a nonlinear dynamical system. Hence to investigate how sensitively the tool life is affected by the initial cutting conditions we proposed a new mathematical model entitled “chaotic tool wear” to investigate both empirically and numerically a chaotic tool wear phenomenon during a machining process. By changing the initial cutting condition for the first two seconds of machining, as a favorable cutting condition for the cutting speed, feed rate and depth of cut, the variation of scatter wear can be found positive in all experiments tested in the course of our work. In this situation the tool life has significantly been improved.

Since the chaotic tool wear model clearly shown that the tool life has been found to be exclusively influenced by the initial conditions; we therefore proposed a new mathematical model to quantify the sensitive dependence on initial conditions of the tool life during machining process. First, the wear curves evolution over time under different initial conditions that served to calculate the Lyapunov exponents are modeled by an ordinary differential equation, the so-called chaotic tool wear equation. It is then characterized by a continuous function on the basis of multistep and Cubic B-splines collocation methods. In addition, the variations in tool wear rate of these wear curve equations under the different initial cutting parameters are quantitatively measured by a fractal dimension.

As a result, a new mathematical model of chaotic tool wear was developed for the first time in the studies of tool wear. Based on the numerical results, the critical impact of the initial cutting conditions on the tool life is demonstrated through a sensitive dependence on the initial conditions of the chaotic wear. A new concept of tool wear, “chaotic tool wear” is discussed early in this thesis. The chaotic tool wear model provides with a full interpretation of the initial tool wear behavior and brings more insight on how the tool life depends significantly on the initial cutting conditions. More importantly, the chaotic tool wear model is successfully applied to adjust very small amounts of initial conditions (∂_{VB_0}) within only two seconds of changing initial cutting parameters when machining TiMMCs; tool life was improved by up to 24.5%.

6.2 Originality of the work and contribution to knowledge

The initial wear behavior or break-in wear period plays an important role in engineering wear system; nevertheless no references were found in literature dealing with the initial tool wear behavior and its effect to the tool life during a machining process, in general, or in the machining of the TiMMCs, in particular. Additionally, the application of chaos theory to investigate the dependence of tool life on the initial conditions has never been conducted so far. Therefore, it is expected that this research provides some new aspects and contributes to knowledge in our field:

- The initial tool wear during machining of TiMMCs occurs at the first instant and extends to only ten seconds under all experiments. The initial tool wear at the first moment of cutting is a result of complicated mechanisms; including coating layer damage, friction - tribological wear, diffusion and adhesion. Among them, the adhesion is however the most important mechanism occurring within the first or initial wear period; this wear

mechanism differed from the wear mechanism of abrasion in the steady wear period; **(Objective 1, Hypothesis 1);**

- Due to the effect of chemical stresses within the first moment of machining lead to the accelerated cutting force and a temperature gradient increase very fast; the adhesion materials therefore resulted in diffusion wear and spontaneously reacted with atmospheric oxygen. Later on, when the tool wear progression reaches to the first transition period, the combination of several wear mechanisms in association with the coating layer of (Ti,Al)N generated a new wear form as a whole participating in the machining process
- The oxidation reactions then generated a new hard thin layer as a whole involved in the machining process at the first transition wear period. This layer was coined “brace wear” and considered as a “wear shield” or protection layer for the steady wear period. The discovery of this new wear form provides a better explanation why the wear rate increases very fast during initial wear and then decreases abruptly at the transition point to the steady wear period; as well as allows interpreting how significantly the initial tool wear and initial cutting conditions affect the tool wear evolution and the entire tool life on the other. **(Objective 1, 2; Hypothesis 1);**
- The chaos theory is applied for the first time to analyze the tool wear during machining and particular for the machining of TiMMCs; we proposed a novel model to investigate the dependence of the tool life on the initial cutting conditions. In this thesis, a new mathematical model so called “chaotic tool wear” is proposed to quantify a chaotic tool wear during a machining process based on the Lyapunov exponent and fractal dimension. As expected, our model permits to quantify a chaotic behavior in the tool wear system based on scatter wear dimension and Lyapunov exponent to exhibit the sensitivity dependence on initial conditions of the tool life; **(Objective 3, 4; Hypothesis 2);**
- In order to analyze the chaotic tool wear at various cutting time the wear curves evolution over time that are being used to calculate Lyapunov exponents was proposed to characterize by a continuous function. This work was also aimed at solving precisely the chaotic tool wear model in general application for the study of tool wear. In this framework, the multistep and Cubic B-splines collocation methods are developed to

solve an ordinary differential equation of the chaotic tool wear. So that the chaotic model therefore are able to calculated the chaotic signal at any cutting time. Furthermore, the variations in tool wear rate under the different initial cutting parameters are quantitatively determined by a fractal dimension. As a result, a new concept of tool wears during machining process, entitled: “chaotic tool wear” is discussed through the relationship between the tool wear, Lyapunov exponent and fractal dimension. **(Objective 3, Hypothesis 2);**

- Another important point to be noted is that a full explanation of the wear rate behavior at the first initial wear period is obtained through the chaotic tool wear for the first time in the study of tool wear, chaos theory and fractal geometry. That model equally brings more insight on how the tool life depends significantly on the initial cutting conditions. More importantly, application of the chaotic tool wear model to change initial cutting conditions when machining TiMMCs improved the tool life by up to 24.5%. **(Objective 3, 4, Hypothesis 2, 3).**

REFERENCES

- [1] S.H. Strogatz, Nonlinear Dynamics and Chaos; with Applications to Physics, Biology, Chemistry, and Engineering Perseus books; Massachusetts 1994, pp. 498.
- [2] D.M. Curry, Practical Application of Chaos Theory to Systems Engineering, Procedia Computer Science, 8 (2012) 39-44.
- [3] A. Golestani, R. Gras, Can We Predict the Unpredictable?, Scientific reports, 4 (2014).
- [4] X. Buff, A. Chéritat, Quadratic Julia Sets with Positive Area, arXiv preprint math/0605514, (2006).
- [5] P.A. Viktor, Cutting Tool Wear, Tool Life and Cutting Tool Physical Resource, Tribology and Interface Engineering Series, Elsevier, 2006, pp. 220-275.
- [6] A. Ber, S. Kaldor, The First Seconds of Cutting, Wear Behaviour, CIRP Annals - Manufacturing Technology, 31 (1982) 13-17.
- [7] A.R. Zareena, S.C. Veldhuis, Tool Wear Mechanisms and Tool Life Enhancement in Ultra-Precision Machining of Titanium, Journal of Materials Processing Technology, 212 (2012) 560-570.
- [8] J. Xiong, Z. Guo, M. Yang, W. Wan, G. Dong, Tool Life and Wear of Wc–Tic–Co Ultrafine Cemented Carbide During Dry Cutting of Aisi H13 Steel, Ceramics International, 39 (2013) 337-346.
- [9] W.C. Yuefeng Yuan, Liansheng Gao, Tool Materials Rapid Selection Based on Initial Wear, Chinese Journal of Aeronautics, 23 (2010) 386-392.
- [10] G.C. Barber, K.C. Ludema, The Break-in Stage of Cylinder-Ring Wear: A Correlation between Fired Engines and a Laboratory Simulator, Wear, 118 (1987) 57-75.

- [11] P.J. Blau, On the Nature of Running-In, *Tribology International*, 38 (2005) 1007-1012.
- [12] E.C. International, Engine Break-in Instructions and Oil Management; Engine Components International, in: ECI (Ed.), 9503 Middlex San Antonio, TX 78217-5994, 2011.
- [13] S.P. Feser Tim, Mohr Felix, Dienwiebel Martin, The Running-in Mechanisms of Binary Brass Studied by in-Situ Topography Measurements, *Wear*, 303 (2013) 465-472.
- [14] S. Mezghani, I. Demirci, M. Yousfi, M.E. Mansori, Running-in Wear Modeling of Honed Surface for Combustion Engine Cylinderliners, *Wear*, 302 (2013) 1360-1369.
- [15] R. Bejjani, M. Balazinski, B. Shi, H. Attia, H. Kishawy, Machinability and Chip Formation of Titanium Metal Matrix Composites, *IJAMS- International Journal Advanced Manufacturing systems*, 13 (2011).
- [16] T.W. Kim, Microstructural Aspects of Titanium Metal Matrix Composites in Consolidation Processing, *Materials Letters*, 59 (2004) 143-147.
- [17] R. Bejjani, Shi, B., Attia, H., Balazinski, M., Laser Assisted Turning of Titanium Metal Matrix Composite, *CIRP Annals - Manufacturing Technology*, 60 (2011) 61-64.
- [18] S. Abkowitz, S. Abkowitz, H. Fisher, P. Schwartz, Cermeti® Discontinuously Reinforced Ti-Matrix Composites: Manufacturing, Properties, and Applications, *JOM*, 56 (2004) 37-41.
- [19] I. Montealegre Melendez, E. Neubauer, P. Angerer, H. Danninger, J.M. Torralba, Influence of Nano-Reinforcements on the Mechanical Properties and Microstructure of Titanium Matrix Composites, *Composites Science and Technology*, 71 (2011) 1154-1162.
- [20] C. Poletti, M. Balog, T. Schubert, V. Liedtke, C. Edtmaier, Production of Titanium Matrix Composites Reinforced with Sic Particles, *Composites Science and Technology*, 68 (2008) 2171-2177.

- [21] Ö.N. Doğan, J.A. Hawk, J.H. Tylczak, R.D. Wilson, R.D. Govier, Wear of Titanium Carbide Reinforced Metal Matrix Composites, *Wear*, 225–229, Part 2 (1999) 758-769.
- [22] H.-X. PENG, Manufacturing Titanium Metal Matrix Composites by Consolidating Matrix Coated Fibres, *J. Mater. Sci. Technol.*, 21 (2005) 647-651.
- [23] C.M. Ward-Close, L. Chandrasekaran, J.G. Robertson, S.P. Godfrey, D.P. Murgatroyde, Advances in the Fabrication of Titanium Metal Matrix Composite, *Materials Science and Engineering: A*, 263 (1999) 314-318.
- [24] J.-S. Kim, K.-M. Lee, D.-H. Cho, Y.-Z. Lee, Fretting Wear Characteristics of Titanium Matrix Composites Reinforced by Titanium Boride and Titanium Carbide Particulates, *Wear*, 301 (2013) 562-568.
- [25] F.C. Campbell, Titanium, *Manufacturing Technology for Aerospace Structural Materials*, Elsevier Science, Oxford, 2006, pp. 119-174.
- [26] E.O. Ezugwu, Z.M. Wang, Titanium Alloys and Their Machinability—a Review, *Journal of Materials Processing Technology*, 68 (1997) 262-274.
- [27] R.B. da Silva, Á.R. Machado, E.O. Ezugwu, J. Bonney, W.F. Sales, Tool Life and Wear Mechanisms in High Speed Machining of Ti–6Al–4V Alloy with PCD Tools under Various Coolant Pressures, *Journal of Materials Processing Technology*, 213 (2013) 1459-1464.
- [28] M. Nouari, H. Makich, Experimental Investigation on the Effect of the Material Microstructure on Tool Wear When Machining Hard Titanium Alloys: Ti–6Al–4V and Ti-555, *International Journal of Refractory Metals and Hard Materials*, 41 (2013) 259-269.
- [29] F. Zanger, V. Schulze, Investigations on Mechanisms of Tool Wear in Machining of Ti-6Al-4V Using Fem Simulation, *Procedia CIRP*, 8 (2013) 158-163.

- [30] T. Rajmohan, K. Palanikumar, Application of the Central Composite Design in Optimization of Machining Parameters in Drilling Hybrid Metal Matrix Composites, *Measurement*, 46 (2013) 1470-1481.
- [31] T. Rajmohan, K. Palanikumar, S. Prakash, Grey-Fuzzy Algorithm to Optimise Machining Parameters in Drilling of Hybrid Metal Matrix Composites, *Composites Part B: Engineering*, 50 (2013) 297-308.
- [32] F.C. Campbell, *Metal Matrix Composites, Manufacturing Technology for Aerospace Structural Materials*, Elsevier Science, Oxford, 2006, pp. 419-457.
- [33] V. Songmene, M. Balazinski, Machinability of Graphitic Metal Matrix Composites as a Function of Reinforcing Particles, *CIRP Annals - Manufacturing Technology*, 48 (1999) 77-80.
- [34] H.A. Kishawy, Kannan, S., Balazinski, M., Analytical Modeling of Tool Wear Progression During Turning Particulate Reinforced Metal Matrix Composites, *CIRP Annals - Manufacturing Technology*, 54 (2005) 55-58.
- [35] A.K. Sahoo, S. Pradhan, A.K. Rout, Development and Machinability Assessment in Turning Al/Sicp-Metal Matrix Composite with Multilayer Coated Carbide Insert Using Taguchi and Statistical Techniques, *Archives of Civil and Mechanical Engineering*, 13 (2013) 27-35.
- [36] X. Li, W.K.H. Seah, Tool Wear Acceleration in Relation to Workpiece Reinforcement Percentage in Cutting of Metal Matrix Composites, *Wear*, 247 (2001) 161-171.
- [37] W. Grzesik, Tool Wear and Damage, *Advanced Machining Processes of Metallic Materials*, Elsevier, Amsterdam, 2008, pp. 163-VII.
- [38] C. Claudin, J. Rech, W. Grzesik, S. Zalisz, Characterization of the Frictional Properties of Various Coatings at the Tool/Chip/Workpiece Interfaces in Dry Machining of Aisi 4140 Steel, *International Journal of Material Forming*, 1 (2008) 511-514.

- [39] E.N. Lorenz, Deterministic Nonperiodic Flow, *Journal of the Atmospheric Sciences*, 20 (1963) 130-141.
- [40] T.C. Gao, Guanrong; Chen, Zengqiang; Cang, Shijian, The Generation and Circuit Implementation of a New Hyper-Chaos Based Upon Lorenz System, *Physics Letters A*, 361 (2007) 78-86.
- [41] D. Kim, P.H. Chang, A New Butterfly-Shaped Chaotic Attractor, *Results in Physics*, 3 (2013) 14-19.
- [42] M.U. Akhmet, M.O. Fen, Replication of Chaos, *Communications in Nonlinear Science and Numerical Simulation*, 18 (2013) 2626-2666.
- [43] G.P. Williams, *Chaos Theory Tamed*, Joseph Henry press Washington, D.C., Published by arrangement with Taylor & Francis Ltd., 1997, pp. 405.
- [44] F.H. Busse, An Exploration of Chaos, *Computer Methods in Applied Mechanics and Engineering*, 118 (1994) 413-414.
- [45] J.S. Lee, K.S. Chang, Applications of Chaos and Fractals in Process Systems Engineering, *Journal of Process Control*, 6 (1996) 71-87.
- [46] F. Moon, *Dynamics and Chaos in Manufacturing Processes*, John Wiley & Sons, 1997, 1997.
- [47] A.Y.-B. Abooe, H. A.; Jahed-Motlagh, M. R., Analysis and Circuitry Realization of a Novel Three-Dimensional Chaotic System, *Communications in Nonlinear Science and Numerical Simulation*, 18 (2013) 1235-1245.
- [48] I. Grabec, Chaotic Dynamics of the Cutting Process, *International Journal of Machine Tools and Manufacture*, 28 (1988) 19-32.

- [49] G. Licskó, G. Csernák, On the Chaotic Behaviour of a Simple Dry-Friction Oscillator, *Mathematics and Computers in Simulation*, 95 (2014) 55-62.
- [50] Y. Zhou, H. Zhu, X. Zuo, J. Yang, Chaotic Characteristics of Measured Temperatures During Sliding Friction, *Wear*, 317 (2014) 17-25.
- [51] G. Igor, Chaos Generated by the Cutting Process, *Physics Letters A*, 117 (1986) 384-386.
- [52] A.E. Gabriel FRUMUSANU, Chaotic Dynamics of Cutting Processes Applied to Reconfigurable Manufacturing Systems Control, Fascicle V (2007).
- [53] F.C. Moon, R.C. Hilborn, Chaotic and Fractal Dynamics: An Introduction for Applied Scientists and Engineers, *American Journal of Physics*, 61 (1993) 670-670.
- [54] M. Wiercigroch, A.H.D. Cheng, Chaotic and Stochastic Dynamics of Orthogonal Metal Cutting, *Chaos, Solitons & Fractals*, 8 (1997) 715-726.
- [55] S. Chatterjee, T.K. Singha, Controlling Chaotic Instability of Cutting Process by High-Frequency Excitation: A Numerical Investigation, *Journal of Sound and Vibration*, 267 (2003) 1184-1192.
- [56] G. Litak, Chaotic Vibrations in a Regenerative Cutting Process, *Chaos, Solitons & Fractals*, 13 (2002) 1531-1535.
- [57] M. Banihasan, F. Bakhtiari-Nejad, Chaotic Vibrations in High-Speed Milling, *Nonlinear Dynamics*, (2011) 1-18.
- [58] G.S. Litak, Asok K.; Syta, Arkadiusz, Intermittent and Chaotic Vibrations in a Regenerative Cutting Process, *Chaos, Solitons & Fractals*, 41 (2009) 2115-2122.
- [59] J. Sprott, Some Simple Chaotic Jerk Functions, *American Journal of Physics*, 65 (1997) 537-543.

- [60] T. Stachowiak, M. Szydlowski, A Differential Algorithm for the Lyapunov Spectrum, *Physica D: Nonlinear Phenomena*, 240 (2011) 1221-1227.
- [61] T.A. Burton, Fractional Differential Equations and Lyapunov Functionals, *Nonlinear Analysis: Theory, Methods & Applications*, 74 (2011) 5648-5662.
- [62] R. Caponetto, S. Fazzino, A Semi-Analytical Method for the Computation of the Lyapunov Exponents of Fractional-Order Systems, *Communications in Nonlinear Science and Numerical Simulation*, 18 (2013) 22-27.
- [63] J. Wu, H. Tian, Functionally-Fitted Block Methods for Ordinary Differential Equations, *Journal of Computational and Applied Mathematics*, 271 (2014) 356-368.
- [64] M.E. Davis, *Numerical Methods and Modeling for Chemical Engineers*, Courier Corporation, 2013.
- [65] J.C. Trigeassou, N. Maamri, J. Sabatier, A. Oustaloup, A Lyapunov Approach to the Stability of Fractional Differential Equations, *Signal Processing*, 91 (2011) 437-445.
- [66] N. Bajcinca, S. Hofmann, K. Sundmacher, Method of Moments over Orthogonal Polynomial Bases, *Chemical Engineering Science*, 119 (2014) 295-309.
- [67] H.M. Ahmed, Solutions of 2nd-Order Linear Differential Equations Subject to Dirichlet Boundary Conditions in a Bernstein Polynomial Basis, *Journal of the Egyptian Mathematical Society*, 22 (2014) 227-237.
- [68] R.C. Mittal, R. Bhatia, A Numerical Study of Two Dimensional Hyperbolic Telegraph Equation by Modified B-Spline Differential Quadrature Method, *Applied Mathematics and Computation*, 244 (2014) 976-997.

- [69] F. Mazzia, A. Sestini, D. Trigiante, The Continuous Extension of the B-Spline Linear Multistep Methods for Bvps on Non-Uniform Meshes, *Applied Numerical Mathematics*, 59 (2009) 723-738.
- [70] R.C. Mittal, R.K. Jain, Cubic B-Splines Collocation Method for Solving Nonlinear Parabolic Partial Differential Equations with Neumann Boundary Conditions, *Communications in Nonlinear Science and Numerical Simulation*, 17 (2012) 4616-4625.
- [71] B.B. Mandelbrot, *The Fractal Geometry of Nature*, W.H. Freeman ed., Freeman and San Francisco, 1982.
- [72] A. Wolf, J.B. Swift, H.L. Swinney, J.A. Vastano, Determining Lyapunov Exponents from a Time Series, *Physica D: Nonlinear Phenomena*, 16 (1985) 285-317.
- [73] H.-O. Peitgen, H. Jürgens, D. Saupe, *Length, Area and Dimension: Measuring Complexity and Scaling Properties*, *Chaos and Fractals*, Springer New York, 2004, pp. 173-214.
- [74] B.B. Mandelbrot, M. Frame, *Fractals*, in: A.M. Editor-in-Chief: Robert (Ed.) *Encyclopedia of Physical Science and Technology* (Third Edition), Academic Press, New York, 2003, pp. 185-207.
- [75] J. Lopez, G. Hansali, H. Zahouani, J.C. Le Bosse, T. Mathia, 3d Fractal-Based Characterisation for Engineered Surface Topography, *International Journal of Machine Tools and Manufacture*, 35 (1995) 211-217.
- [76] C.Q. Yuan, J. Li, X.P. Yan, Z. Peng, The Use of the Fractal Description to Characterize Engineering Surfaces and Wear Particles, *Wear*, 255 (2003) 315-326.
- [77] M. Chen, Q. Pang, J. Wang, K. Cheng, Analysis of 3d Microtopography in Machined Kdp Crystal Surfaces Based on Fractal and Wavelet Methods, *International Journal of Machine Tools and Manufacture*, 48 (2008) 905-913.

- [78] M. Hasegawa, J. Liu, K. Okuda, M. Nunobiki, Calculation of the Fractal Dimensions of Machined Surface Profiles, *Wear*, 192 (1996) 40-45.
- [79] M.C.K. Kang, Jeong Suk; Kim, Kwang Ho, Fractal Dimension Analysis of Machined Surface Depending on Coated Tool Wear, *Surface and Coatings Technology*, 193 (2005) 259-265.
- [80] S. Raman, A. Longstreet, D. Guha, A Fractal View of Tool-Chip Interfacial Friction in Machining, *Wear*, 253 (2002) 1111-1120.
- [81] X. Yin, K. Komvopoulos, An Adhesive Wear Model of Fractal Surfaces in Normal Contact, *International Journal of Solids and Structures*, 47 (2010) 912-921.
- [82] X. Yin, K. Komvopoulos, A Slip-Line Plasticity Analysis of Abrasive Wear of a Smooth and Soft Surface Sliding against a Rough (Fractal) and Hard Surface, *International Journal of Solids and Structures*, 49 (2012) 121-131.
- [83] X. Yin, K. Komvopoulos, A Slip-Line Plasticity Analysis of Sliding Friction of Rough Surfaces Exhibiting Self-Affine (Fractal) Behavior, *Journal of the Mechanics and Physics of Solids*, 60 (2012) 538-555.
- [84] M.V. Berry, and Lewis, Z. V., On the Weierstrass–Mandelbrot Fractal Function, *Proc. R. Soc. London, Ser. A* (1980) 459-484.
- [85] W.Y.a.K. Komvopoulos, Contact Analysis of Elastic-Plastic Fractal Surfaces, *Journal of Application Physics*, 84 (1998) 3617–3624.
- [86] Y. Sahin, G. Sur, The Effect of Al₂O₃, Tin and Ti (C,N) Based Cvd Coatings on Tool Wear in Machining Metal Matrix Composites, *Surface and Coatings Technology*, 179 (2004) 349-355.
- [87] P. Sahoo, S.K. Roy Chowdhury, A Fractal Analysis of Adhesive Wear at the Contact between Rough Solids, *Wear*, 253 (2002) 924-934.

- [88] J.M. Karandikar, A.E. Abbas, T.L. Schmitz, Tool Life Prediction Using Bayesian Updating. Part 2: Turning Tool Life Using a Markov Chain Monte Carlo Approach, *Precision Engineering*, 38 (2014) 18-27.
- [89] Z. Klim, Ennajimi, E., Balazinski, M., Fortin, C., Cutting Tool Reliability Analysis for Variable Feed Milling of 17-4ph Stainless Steel, *WEAR, International Journal on the Science and Technology of Friction and Wear*, Wear 195 (1996), (1996) pp. 206-213.
- [90] ISO3685, Tool-Life Testing with Single-Point Turning Tools, International Standard 1993.
- [91] M. Rahman, Z.-G. Wang, Y.-S. Wong, A Review on High-Speed Machining of Titanium Alloys, *JSME Int. J*, 49 (2006) 11-20.
- [92] M. Aramesh, B. Shi, A.O. Nassef, H. Attia, M. Balazinski, H.A. Kishawy, Meta-Modeling Optimization of the Cutting Process During Turning Titanium Metal Matrix Composites (Ti-Mmcs), *Procedia CIRP*, 8 (2013) 575-580.
- [93] D. Xuan-Truong, M. Balazinski, R. Mayer, Chaotic Tool Wear During Machining of Titanium Metal Matrix Composite (Timmcs), *ASME 2014 International Mechanical Engineering Congress and Exposition*, American Society of Mechanical Engineers, 2014, pp. V02BT02A018-V002BT002A018.
- [94] M.J. Bermingham, J. Kirsch, S. Sun, S. Palanisamy, M.S. Dargusch, New Observations on Tool Life, Cutting Forces and Chip Morphology in Cryogenic Machining Ti-6al-4v, *International Journal of Machine Tools and Manufacture*, 51 (2011) 500-511.
- [95] H.B. Abdelali, C. Courbon, J. Rech, W. Ben Salem, A. Dogui, P. Kapsa, Identification of a Friction Model at the Tool-Chip-Workpiece Interface in Dry Machining of a Aisi 1045 Steel with a Tin Coated Carbide Tool, *Journal of Tribology*, 133 (2011) 042201-042201.
- [96] U. Beste, S. Jacobson, A New View of the Deterioration and Wear of Wc/Co Cemented Carbide Rock Drill Buttons, *Wear*, 264 (2008) 1129-1141.

- [97] T. Kagnaya, C. Boher, L. Lambert, M. Lazard, T. Cutard, Microstructural Analysis of Wear Micromechanisms of Wc–6co Cutting Tools During High Speed Dry Machining, *International Journal of Refractory Metals and Hard Materials*, 42 (2014) 151-162.
- [98] D. Zhu, X. Zhang, H. Ding, Tool Wear Characteristics in Machining of Nickel-Based Superalloys, *International Journal of Machine Tools and Manufacture*, 64 (2013) 60-77.
- [99] R.C. Hilborn, *Chaos and Nonlinear Dynamics: An Introduction for Scientists and Engineers* in: S. Edition (Ed.), United states by Oxford University Press Inc., New York, 2000.
- [100] I.S. Durazo-Cardenas, P.; Luo, X.; Jacklin, T.; Impey, S. A.; Cox, A., 3d Characterisation of Tool Wear Whilst Diamond Turning Silicon, *Wear*, 262 (2007) 340-349.
- [101] H.A. Kishawy, P. Lei, M. Balazinski, Modeling of Tool Wear During Hard Turning with Self-Propelled Rotary Tools, *International Journal of Mechanical Sciences*, 53 (2011) 1015-1021.
- [102] H. Zahouani, R. Vargiolu, J.L. Loubet, Fractal Models of Surface Topography and Contact Mechanics, *Mathematical and Computer Modelling*, 28 (1998) 517-534.
- [103] S.-C. Hung, M.-F. Tu, Is Small Actually Big? The Chaos of Technological Change, *Research Policy*, (2014).
- [104] P.A. Viktor, Cutting Tool Wear, Tool Life and Cutting Tool Physical Resource, in: P.A. Viktor (Ed.) *Tribology and Interface Engineering Series*, Elsevier, 2006, pp. 220-275.
- [105] E. Kreyszig, *Advanced Engineering Mathematics*, John Wiley & Sons, 2010.
- [106] J. Goh, A. Abd. Majid, A.I. Md. Ismail, Numerical Method Using Cubic B-Spline for the Heat and Wave Equation, *Computers & Mathematics with Applications*, 62 (2011) 4492-4498.
- [107] S. Ye-zhi, H. Yong, H.U. Xiao-gong, L.I. Pei-jia, C.A.O. Jian-feng, Spacecraft Orbit Determination with the B-Spline Approximation Method, *Chinese Astronomy and Astrophysics*, 38 (2014) 172-185.

- [108] S. Rostami, S. Shojaee, H. Saffari, An Explicit Time Integration Method for Structural Dynamics Using Cubic -Spline Polynomial Functions, *Scientia Iranica*, 20 (2013) 23-33.
- [109] R.C. Mittal, R. Bhatia, Numerical Solution of Second Order One Dimensional Hyperbolic Telegraph Equation by Cubic B-Spline Collocation Method, *Applied Mathematics and Computation*, 220 (2013) 496-506.
- [110] D. Xuan-Truong, M. Balazinski, R. Mayer, Initial Tool Wear Behaviour During Machining of Titanium Metal Matrix Composite (Timmcs), Submitted journal paper, March 2015, *Machining science and technology*, REF: LMST-2015-0083 (2015).
- [111] D. Xuan-Truong, T. Minh-Duc, Effect of Cutting Condition on Tool Wear and Surface Roughness During Machining of Inconel 718, *International Journal of Advanced Engineering Technology/IV/III/July-Sept*, 108 (2013) 112.

APPENDIX

- REFEREED JOURNAL PAPERS

- D. Xuan-Truong, M. Balazinski, R. Mayer, *Initial Tool Wear Behaviour during Machining of Titanium Metal Matrix Composite (TiMMCs)*, Machining science and technology (2015), REF: LMST-2015-0083, *under review*;
- D. Xuan-Truong, M. Balazinski, R. Mayer, *A New Concept for Tool Wear during Machining Process Based on Characteristics of Chaos Theory*, International Journal of Machine Tools and Manufacture; May (2015); Ref. No.: IJMACTOOL-D-15-00438, *under review*.

- REFEREED CONFERENCE PAPERS

- D. Xuan-Truong, M. Balazinski, R. Mayer, *Chaotic Tool Wear During Machining of Titanium Metal Matrix Composite (TiMMCs)*, ASME 2014 International Mechanical Engineering Congress and Exposition, American Society of Mechanical Engineers, 2014, pp. V02BT02A018-V002BT002A018.
- D. Xuan-Truong, M. Balazinski, R. Mayer, *A Novel Method to Investigate Tool Wear and Tool Life during Machining Process Based on Characteristics of Chaos Theory*, accepted for presentation at the 4th International Conference on Virtual Machining Process Technology (VMPT 2015) UBC, Vancouver, BC; June 2-5, 2015.

- JOURNAL PAPERS IN PREPARATION

- D. Xuan-Truong, M. Balazinski, R. Mayer; *Optimization of Initial Cutting Parameters during Machining of Titanium Metal Matrix Composite (TiMMCs)*; to be submitted to the International Journal of Machine Tools and Manufacture; (2015);
- D. Xuan-Truong, M. Balazinski, R. Mayer; *Fractal Geometry Analysis of Tool Wear Based on Wear Volume Lost during a Machining Process*; to be submitted to the Journal of Chaos, Solutions & Fractals; (2015).

- DECLARE INVENTION / PATENT

- Based on part of the main results obtained from this PhD thesis, a declaration as an invention of originality contribution to the advancement of knowledge and the development of technologies (entitled “A Novel methodology to Investigate Tool Wear and Tool Life during Machining Process Based on Characteristics of Chaos Theory”) is now under preparation.